THE BEHAVIOUR OF SILVER AND ZINC OXIDE NANOPARTICLES IN AQUEOUS ENVIRONMENTS, AND THEIR INTERACTION WITH AQUATIC HIGHER PLANTS

Submitted In Fulfillment
for the Requirements for the Degree
Doctor of Philosophy In Zoology

In the Faculty of Science
At the
University of Johannesburg

---

by
Melusi Thwala

Accepted by:

Prof Victor Wepener, Supervisor
Dr Ndeke Musee, Co-Supervisor

JANUARY 2015

Acknowledgements

I greatly acknowledge the guidance and support given by my supervisors, Prof Wepener and Dr Musee through the highs and lows of this study.

I will forever be grateful to Dr Musee for having gone many extra miles to provide an enabling foundation to establish and grow my scientific profile. From his excellent mentorship I have gained insights to what it takes to be a good scientist and how to stimulate others around you to grow with you.

I received great support on aspects of nanoparticle characterisation from Drs Sikhwivhilu and Shumbula of MINTEK, as well as Dr Wesley-Smith of the DST/CSIR Nano Centre.

I have achieved one of my goals for joining the CSIR and I am grateful to the organisation for providing an opportunity and funding to further my studies. Too many individuals to mention within the CSIR and NRE have supported and motivated me towards completion of this study. However, undertaking of the study will not have been possible without the support and guidance received from Dr Paul Oberholster. My colleagues in the Nanotechnology Sustainability Research Group have been my pillars of strength, and I am eternally grateful.

The National Research Foundation supported this PhD work through its Thuthuka-PhD Track funding stream, and I am grateful for the support. Further support from the Department of Science and Technology through its Nano-HSE platform is highly appreciated.

I extend my gratitude to the UNESCO/Keizo Obuchi Fellowship Programme for a research fellowship which enabled completion of this study. I also thank the offices of the Minister and the Director-General; Department of Basic Education (South Africa) as well as the Secretary-General: South African National Commission for UNESCO for their support during the fellowship. I thank Prof S Klaine of Clemson University, USA (CU-ENTOX) for his mentorship and the support received from the members of his laboratory during the fellowship.

The Lord is my spiritual fountain and without his guidance and protection I would not be where I am.

Dedication

I dedicate this work to my mother Hlalile Sikhakhane who always supported my endeavours and encouraged me to further my studies. Over decades I have seen her obtain post graduate qualifications whilst working full time and raising three boys single handed; her never-say-die attitude strongly motivated me to pursue this PhD part-time whilst working. Ngiyabonga MaMboma amagalelo akho empilweni yami angenze umuntu ebantwini.

My wife Mmaphefo and son Langelihle kept me motivated and never discouraged even when giving up was easiest. I will forever be thankful to you for being strong when my studies took most of my time: I dedicate this achievement to you.

To my extended family and many friends across boarders who kept me motivated; I hope this achievement also serves as motivation for your own goals.

LIST OF JOURNAL ARTICLES FROM THIS STUDY

Thwala M, Musee N, Sikhwivhilu L, Wepener V. 2013. The oxidative toxicity of Ag and ZnO nanoparticles towards the aquatic plant *Spirodela punctuta* and the role of testing media parameters. *Environ. Sci.: Processes Impacts*, 15, 1830-1843. (Thesis Chapter 6).

Thwala *et al.* in preparation. Interactions of metal-based engineered nanoparticles with higher aquatic plants: a note on the state of current knowledge. (Thesis Chapter 2).

Thwala *et al.* in preparation. Interaction of silver nanoparticles with *Salvinia minima*: bioaccumulation and toxic effects as a factor of particle size and exposure water chemistry. (Thesis Chapter 5)**.**

LIST OF CONFERENCE PAPERS FROM THIS STUDY

Thwala M, Musee N, Wepener V, Oberholster P. 2010. The toxicity effects of Fe_2O_3, TiO_2, ZnO, and Ag engineered nanomaterials (ENMs) on the macro-algal *Spirodela* species. Southern African Society for Aquatic Scientists Conference, 13-16 June, Augrabies Falls National Park, South Africa.

Thwala M, Musee N, Wepener V. 2011. The influence of metal-based engineered nanoparticles on the activity of catalase and superoxide dismutase in *Spirodela* species. Southern African Society for Aquatic Scientists Conference, 26-30 June, Ithala Game Reserve, South Africa.

Thwala M, Musee N, Wepener V, Nota N. 2012. Evidence of free radical and antioxidant activity in *Spirodela* exposed to metalic and metal oxide nanoparticles. NANO Africa Conference, 1-4 April, University of Free State, Bloemfontein, South Africa.

Thwala M, Musee N, Sikhwivhilu L, Wepener V. 2012. Zinc oxide and silver nanoparticles influence the antioxidative status in a higher aquatic plant, *Spirodela punctata*. 7th International Conference on the Environmental Effects of Nanomaterials and Nanoparticles, 10-12 September, Banff Centre, Canada.

Thwala M, Musee N, Sikhwivhilu L, Wepener V. 2013. How water chemistry determines the risk of metallic engineered nanoparticles in aquatic ecosystems: nAg and nZnO case study. 6th SETAC AFRICA Conference, 2-3 Spetember, Lusaka, Zambia.

Thwala M, Radebe N, Tancu Y, Musee N. 2014. The interactive influence of water chemistry and nanoparticle characteristics in determining the environmental fate of metal-based nanoparticles: a case of nAg and nZnO. 8th International Conference on the Environmental Effects of Nanomaterials and Nanoparticles, 7-11 September, Columbia, USA.

Thwala M, Radebe N, Tancu Y, Musee N. 2014. Exposure assessment of metal-based nanoparticles in aquatic environments: interactive influence of water chemistry and nanoparticle characteristics. Society for Risk Analysis: nano. 15-16 September, Washington DC, USA.

TABLE OF CONTENTS

Page

LIST OF TABLES

LIST OF FIGURES

LIST OF ABBREVIATIONS

ANOVA	analysis of variance
BET	Brunauer Emmett Teller method
Chl *a*	chlorophyll *a*
Chl *b*	chlorophyll *b*
cit-	citrate coated
DI	deionised
DLS	dynamic light scattering
DOC	dissolved organic carbon
EDX	energy dispersive x-ray spectroscopy
ENMs	engineered nanomaterials
ENPs	engineered nanoparticles
HM	Hoagland's Medium
ICP-MS	inductively coupled plasma-mass spectroscopy
ICP-OES	inductively coupled plasma-optical emission spectroscopy
IS	ionic strength
MHW	moderately hard water
nAg	silver nanoparticles
nZnO	zinc oxide nanoparticles
NOM	natural organic matter
NTA	nanoparticle tracking analysis
PCA	principal component analysis
RNS	reactive nitrogen species
ROS	reactive oxygen species
SEM	scanning electron microscope
SOD	superoxide dismutase

STEM	scanning transmission electron microscopy
TAC	total antioxidant capacity
TEM	transmission electron microscope
XRD	X-ray diffraction
10-nAg	10 nm silver nanoparticles
40-nAg	40 nm silver nanoparticles

SUMMARY

Nanotechnology generally entails the synthesis, manipulation, and application of materials of any phase with nanoscale dimensions. Over the past two decades nanotechnology has experienced remarkable growth essentially driven by demand for products with unique and novel properties, for instance, whose performance in many respects supersedes that of conventional products. The exponential increasing interest in nanoscale materials in product development is ascribed on their special characteristics as this renders their chemical and physical behaviour remarkably different from bulk scale counterpart materials. As a result, there is a year-on-year increase in the number of nano-enabled consumer products being introduced in the markets globally. Associated with increasing production and use of nano-enabled products is release of engineered nanoparticles (ENPs) during different stages of product life cycle into the environmental systems. Yet, presently the environmental fate, behaviour, and effects of ENPs are poorly understood which have raised concerns with respect to their potential environmental health, safety, and implications.

Therefore, to address the data and knowledge of ENPs motivated undertaking of systematic study whose results are summarized in this thesis. Chiefly the study sought to gain insights on the fate and behaviour of ENPs in aqueous media as well as their plausible interactions with free floating aquatic higher plants. Amongst the mostly produced and applied ENPs are nano silver (nAg) and nano zinc oxide (nZnO), hence, they are likely to be released into the environmental systems in elevated quantities. Owing to the limited nanoecotoxicity data on the aquatic higher plants and their valuable role in energy processing within the aquatic systems; *Spirodela punctuta* and *Salvinia minima* were selected as suitable models for the purposes of this study.

To document the environmental fate and behavioural dynamics of ENPs in water bodies; nAg and nZnO were investigated under varying water chemistries, namely; deionised water (DI) water, Hoagland's Medium (HM) and modified natural water. Two types of nAg were studied; citrate coated and uncoated powder forms. The behaviour of 10 and 40 nm citrate coated nAg (10-nAg and 40-nAg) remarkably differed due to their size difference. In moderately hard water (MHW), calcium (Ca^{2+}), and natural organic matter (NOM) water regimes, 10-nAg exhibited higher agglomeration rates resulting in the formation of larger sizes compared to 40-nAg where the latter was found stable under the same experimental conditions. Also in modified river water filtered at 0.2 and 0.45 µm levels, 40-nAg remained highly stable whilst 10-nAg quickly agglomerated resulting to significantly larger secondary particles. Such findings were associated with higher reactivity of smaller sized 10-nAg and this was further supported by their higher drift velocity indicative of agglomeration potential compared to 40-nAg.

Furthermore, nAg dissolution as an indicator of chemical transformation was found to be size dependent. In Ca^{2+} and NOM water regimes the 10-nAg was found to be more soluble compared to 40-nAg whilst the latter was more soluble in MHW. Studies with DI and modified river water showed that 10-nAg was highly soluble in 0.2 µm filtered water but its dissolution remained relatively similar to that of 40-nAg in DI water and 0.45 µm filtered water. Notably the latter results had low statistical confidence because many samples were found to be below the detection limit.

Further evidence of size induced behavioural differences was observed on nAg interactions with *S. minima.* Across different water chemistries, higher Ag accumulation was found on plants exposed to 10-nAg, and lower in 40-nAg exposures. This was attributed to relatively higher adsorption to plant surface and solubility of 10-nAg. Due to higher agglomeration of 10-nAg, their small primary size was unlikely to have enhanced their internalisation through the cell wall pores. Analysis of roots cross sections using electron microscopy techniques could have indicated if internalisation occurred, and also the dynamics of the process.

Water chemistry was also observed to be highly influential on the dispersion and stability of ENPs. Studies with uncoated powder forms of nAg and nZnO revealed that higher ionic strength promoted formation of larger agglomerates compared to lower ionic strength. The nAg concentration in exposure suspension also varied between different ionic strengths, as it was at the highest at higher ionic strength. Such findings contradicted expectations where at higher ionic strength larger nAg agglomerates were expected to succumb to gravitational sedimentation at higher rates resulting in particle concentration loss, but this was not the case, and the cause for the contradiction could not be established.

Size transformation of citrate coated nAg was also highly dependent on water chemistry. Agglomeration rates of 10-nAg and 40-nAg were both highest in Ca^{2+}, lesser in MHW, and least in NOM water regime. This was attributed to weakened electrostatic repulsion where the Ca^{2+} was most effective in particle surface charge shielding, and the steric stabilisation of NOM effectively counteracted agglomeration especially for the less reactive 40-nAg which retained primary size throughout. The expected inverse relationship between particle size and concentration was well demonstrated with 40-nAg, where the concentrations decreased in descending version under the following exposure conditions: NOM > MHW> Ca^{2+}. Similarly, the surface charge shielding was attributed to the transformation of nAg (powder) under different ionic strengths where at higher ionic strength the charge screening occurred, and as a result, larger agglomerates compared to those at lower ionic strengths were formed.

Chemical transformation of the ENPs changed with changing exposure water chemistry. For instance, the solubility of nAg and nZnO (powder form) was significantly influenced by the ionic strength where high ionic strength inhibited dissolution. Similarly, the dissolution of 10-nAg and 40-nAg varied under different water chemistries, namely; the MHW, Ca^{2+} and NOM water regimes. This was also the case with the dissolution of 10-nAg and 40-nAg in DI and modified river water. Modified river water refers to river collected water that was 0.2 and 0.45 µm filtered, and its pH adjusted to 7. Solubility of metal-based ENPs is regulated by oxidation of available reactive surfaces, and this was well demonstrated in this study because chemistries with high adsorption potential resulted in reduced dissolution, for instance, as function of the ionic strength.

Oxidative stress was confirmed as one underlying mechanism for the induction of ENPs toxicity. Exposure of *S. punctuta* to powder forms of nAg and nZnO indicated elevated free radical activity measured as ROS/RNS and H_2O_2; stimulating activity of superoxide dismutase and change in total antioxidative capacity. Oxidative stress was dependent on ENPs concentration and exposure duration. Furthermore, the water hardness and ionic strength, as well as ENPs properties were also established as additional factors that caused the observed toxicity. Toxicity of powder nAg was mainly associated with particulate form due to poor dissolution; whilst that of nZnO was mainly associated with dissolved Zn due to elevated solubility. Toxicity of cit-nAg was elevated in *S. minima* specimens exposed to 10-nAg compared to 40-nAg mainly due to superior reactivity, accumulation and solubility of former particles. The toxicological effects of citrate coated nAg were markedly different between MHW, Ca^{2+}, and NOM exposure regimes.

Overall, this study has shown that the fate and behaviour of ENPs in aqueous environments as well as their interactions with higher aquatic plants are highly dynamic processes principally dependent on ENPs properties and water chemical characteristics. Detailed characterisation of ENPs and exposure media were valuable in establishing the interplay of physical and chemical processes that influences the ENPs stability and their resultant interactions with aquatic plants. Aquatic higher plants hold potential to accumulate, and in turn, aid trophic transfer of nano-pollutants in the aquatic ecosystems. Thus, the outcomes of this study point to the need for systematic monitoring and regulation of nano-pollutants in order to protect aquatic health.

CHAPTER 1
Introduction and background

1.1. Nanotechnology and engineered nanoparticles

Nanotechnology in general is the synthesis, manipulation and application of materials of any phase at nanoscale or with nanoscale dimensions. The building blocks of nanotechnology are regarded as nanomaterials. Presently there are numerous differing definitions of a nanomaterial (ASTM 2006; BSI 2007; SCENIHR 2007, EU 2011); the mostly widely accepted and adopted is by the European Commission (EU). The EU defines a nanomaterial *as any natural, incidental or manufactured material containing particles, in an unbound state or as an aggregate or as an agglomerate and where, for 50 % or more of the particles in the number size distribution, one or more external dimensions is in the size range 1 nm-100 nm* (EU 2011). Although nanomaterials have for a long time been-defined as substances with all dimensions less than 100 nm (Klaine *et al.* 2012), it was later realised and now widely accepted that the 100 nm cut-off point is not practical to exclude larger sizes, as recently outlined in the EU (2011) report. Primarily based on the chemical composition, nanomaterials are broadly classified as: (a) carbon-based materials (e.g. fullerenes, carbon nanotubes, etc.), (b) inorganic engineered nanoparticles (ENPs) fabricated from metal oxide (e.g. titanium dioxide, zinc oxide, iron oxide, etc.) and metals (e.g. gold. silver, copper, palladium, iron, etc.), (c) semiconductor nanocrystals known as quantum dots (e.g. cadmium selenide, indium phosphide, etc.), and (d) mixtures of different phases of nanomaterials fabricated at laboratory and industrial scales.

Importantly, nanoscale dimension particles or nanoparticles have always occurred naturally, for instance, from sources such as volcanoes and other geochemical processes (Lead and Wilkinson 2006). However, as a result of scientific and technological advances, the ability to synthesise, measure/characterise, manipulate and apply nanoscale materials has improved remarkably over the last two decades. Consequently, this has stimulated huge interest in research as well as commercial and industrial application of nanomaterials. For the purposes of this research only engineered nanoparticles (ENPs) will be considered. The attractiveness of ENPs for application in many products is ascribed to their special characteristics underpinned by their size (≈ 1-100 nm). At nanoscale, the chemical and physical behaviour of materials differ remarkably in relation to their bulk scale counterparts. Among the novel properties of ENPs include; exceptional material physical strength, solubility, reactivity, fluorescence, and conductivity (Wang and Herron 1990; Jolivet *et al.* 2004). For instance, the melting point of tin ENPs can be reduced by about 80°C due to size change from 100 to 10 nm (Lai 1996). Other changes at nanoscale can be ascribed to the inverse relationship between material size and surface area which render ENPs to exhibit high

ratio of surface atoms (Auffan *et al.* 2008). Generally, the ratio of surface to total atoms or molecules increases exponentially with decreasing size, hence ENPs are characterised by excess surface energy and high surface reactivity (Jolivet *et al.* 2004; Auffan *et al.* 2008). For instance, whilst surface energy of macroscale materials is very low (0.56 J/g); the size reduction to ≈ 1nm increases the surface energy by a thousand fold to 560 J/g (Auffan *et al.* 2010).

1.2. Trends on nanotechnology applications

The global nanotechnology market is estimated to grow to approximately $48.9 billion by 2017 underpinned by a compound annual growth rate (CAGR) of 18.7% from 2012, as summarized in Table 1.1 (BCC Research 2012). Other predictions forecasted a market value of $2.6 trillion by 2014 (Roco 2005), and $1 trillion by 2015 (NSF 2001). One key thread of these predictions among many is the indication of vast anticipated high economic growth through exploitation of nanotechnology-driven capabilities. Although it is challenging to provide actual figures on the global market value of nanotechnology-based products and industrial applications to date, as there is no requirement for companies to declare nano-enabled products as they are introduced into the market; however all indicators suggest a rapid growth rate. For example, according to PEN (2014) the number of nano-enabled products increased from 54 in 2005 to an impressive 1628 in August 2014 (Figure 1.1).

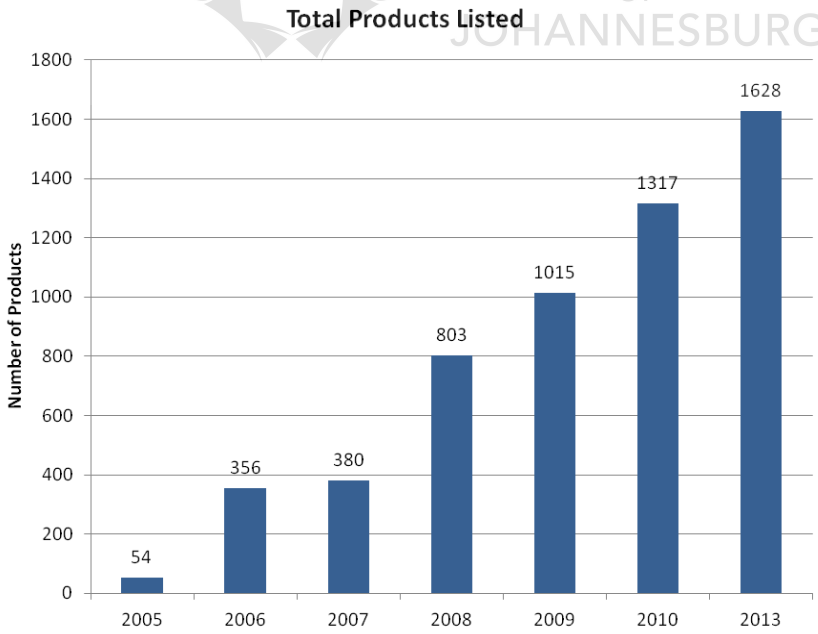

Figure 1.1: Graphical presentation of the number of nano-enabled products from 2005 to 2013. Image adopted from inventory of the Project on Emerging Nanotechnologies (PEN 2014).

Table 1.1: Summary of predicted global nanotechnology market value from 2011-2017 in US $ millions. Adapted from BCC Research (2012).

Technology	2011	2012	2017	CAGR%* 2012-2017
Nanomaterials	14 072.9	15 924.8	32 327.5	18.6
Nanotools	6 032.8	4 763.5	11 416.9	19.1
Nanodevices	39.5	45.3	176.2	31.2
Total	20 145.2	20 733.6	48 920.6	18.7

*CAGR; compound annual growth rate

Studies suggest that titanium dioxide, carbon nanotubes, silver, zinc oxide, and fullerenes are amongst the most produced types of nanomaterials (Nowack and Bucheli 2007; Muller and Nowack 2008; Musee 2010; Westerhoff *et al.* 2011; BCC Research 2012; Yang and Westerhoff 2014). The applications of ENPs crosscut numerous fields, and new ones are being realised continuously as scientific and technological capabilities improve. For instance, ENPs are applied in cosmetics, personal care products, antimicrobial dressings, catalysts, lubricants, fuel cells, water purification and treatment, bioremediation, nanoscale thin films, paints and coatings, food and food packaging, nanomedicines, agriculture, and drug delivery systems. In terms of current nano-enabled products in the market; most are in the health and fitness (605) category, followed by home and garden (152) whilst the food and beverage category account for 98 products, just to list top categories according to the PEN (2014).

Nanotechnology as an enabling technology holds potential for advances in numerous applications and economic sectors' and some of the benefits are already being realised as the development of nano-enabled products is in the increase (BCC Research 2012; Yang and Westerhoff 2014). It is expected that the number of nano-enabled products will increase remarkably as nanotechnology matures from a research and development phase to industrial production (Roco 2011). To take advantage of the nanotechnology capabilities public and private sectors globally have invested substantially in nanotechnology research and development chiefly to stimulate industrial growth enabled by nanotechnologies (Roco 2005; Musee *et al.* 2010; Roco 2011; Whiteley *et al.* 2013); and in turn accrue benefits to the society.

For example, South Africa has identified nanotechnology as one of key drivers of industrial and economic growth, and also to address social national challenges in pursuit of improving quality of life within the Republic (DST 2005; DST 2010). Thus, in South Africa since to 2005 to 2012, more than ZAR 2.622 billion has been invested to support the exploitation of nanotechnology in

business enterprise adventures as well as support research and development in science councils and higher educational institutions (DST 2012). These figures suggest remarkable awareness by South Africa on the beneficial impacts of nanotechnology. It is in this context that exploitation of nanotechnology should be sustainable; and this study seeks to support this goal through generation of data to support risk assessment of ENPs in the environmental systems.

1.3. Nanotechnology environmental concerns

Inevitably during manufacturing, transportation, usage, storage, and disposal of ENPs; they are continuously released into the environment. This trend is in the increase as more nano-enabled products are introduced in the market as nanotechnology market grows globally. Natural water resources and engineered waste water bodies are end-recipients of ENPs as contaminants with nanoscale dimensions from consumer products and industrial applications (Kaegi *et al.* 2010; Musee 2011; Musee *et al.* 2011; Gaiser *et al.* 2012; Coleman *et al.* 2013). On the other hand, wastewater treatment plants (WWTPs) are likely a major source of such pollutants to the receiving water bodies (Kaegi *et al.* 2010; Musee *et al.* 2014). Moreover, application of sludge from WWTPs on agricultural soils as a soil conditioner also contributes to the release nano-scale contaminants into water bodies during run-off conditions (Kaegi *et al.* 2010; Chaúque *et al.* 2014; Musee *et al.* 2014).

More than a decade ago, calls were raised concerning the need for nanotechnology risk assessment to protect human and environmental health owing to unknown effects of ENPs (Brumfiel 2003; Colvin 2003; Oberdörster *et al.* 2005). Many ENPs have been shown to be potentially toxic owing to their small size and large surface area to volume ratios (as discussed earlier), which renders them highly reactive and detrimental even at very low exposure concentrations (Oberdörster 2004; Nel *et al.* 2006; Handy *et al.* 2008a; 2008b; Klaine *et al.* 2008; 2012). Consequently, the same attractive properties that render ENPs valuable for a diversity of applications are the same cause for concern regarding the less understood potential adverse health and environmental effects. Therefore, taking into account the rapid growth rate of incorporation of ENPs into consumer products and nanotechnology in general; merits for systematic investigations to elucidate their potential risks to humans and environment.

The foregoing scenario based on available literature raises environmental concerns because: (1) the exponential growth on the production and application of ENPs suggests increasing environmental pollution potential; (2) exposure scenarios and environmental concentrations of nanoscale contaminants are yet to be determined under real world settings; (3) the fate, transformations and transport of ENPs in aqueous environments presently is a scientific

challenge and yet to be fully elucidated; and (3) the toxicological properties and effects of ENPs are also poorly understood.

1.4 Study motivation

Although lately there has been an increase in the generation of data on the potential mobility and effects of ENPs in aquatic environments, such information remains miniscule relative to the production and applications of ENPs (Schrurs and Lison 2012; Kahru and Ivask 2013). This implies that nanoecotoxicology information being produced is inadequate to support detailed and systematic hazard and risk assessment of ENPs in numerous products and applications. Although generally accepted that it is impossible and unnecessary to screen the toxicological effects and environmental implications of all of ENPs produced, however, the little amount of data available to date is inadequate to support systematic assessment in complex environmental systems. This is further compounded by shortage of real world data, for instance on: (a) usage patterns of nano-enabled products and applications, and (b) environmental exposure scenarios and concentrations of ENPs. Such information lag status suggests that one of rapidly growing technologies globally is being utilised without credible environmental risk assessment. Therefore, this study seeks to contribute in generating data useful to support environmental sustainability of nanotechnology.

Previous studies on nano-ecotoxicology suggest that: (i) limited attention has been given on ENPs environmental fate and transport to obtain information on bioavailability, (ii) exposure and uptake pathways are poorly known, (iii) the data availability is skewed towards certain trophic levels, and to others bare minimal, and (iv) there are little nanotoxicity data obtained from consumer nano-enabled products during life cycle assessments (Ostrowski *et al.* 2009; Kahru and Dubourgier 2010; Kahru and Ivaski 2013). For instance, a nano-ecotoxicological review by Kahru and Dubourgier (2010) indicated that the distribution of literature with respect to trophic levels (as test organisms) were as follows: crustaceans (33%), bacteria (27%), algae (14%), fish (13%), ciliates (6%), yeast (4%), and nematodes (3%). Data on algae was for handful micro-algal species but with no data on higher or vascular aquatic plants. These findings pointed to a research gap towards higher or vascular aquatic plants, and the current study aims to generate information as part of addressing this gap.

Only after 2010 were reports screening the toxicological effects of ENPs on higher aquatic plants published (Gubbins *et al.* 2011; Kim *et al.* 2011; Glenn *et al.* 2012; Song *et al.* 2012; Bian *et al.* 2013; Glenn *et al.* 2012; Hu *et al.* 2013; Li *et al.* 2013; Oukarroum *et al.* 2013; Thwala *et al.* 2013; Hu *et al.* 2014). Because ENPs are now being considered as emerging environmental contaminants (Colvin 2003; Park *et al.* 2014); motivates the need to generate information on their

potential fate, transformation, transportation, and ecological effects in water resources. Such information has the merit of supporting regulatory initiatives to mitigate possible ecological health impacts that if unattended may be highly costly to remediate (Musee 2011). For example, according to the National Water Act 36 of 1998 (RSA 1998) of South Africa, the Department of Water and Sanitation (DWAS) is tasked to monitor and manage water quality; and in addition to generate information and report on emerging water quality issues.

Silver (nAg) and zinc oxide (nZnO) were selected as ENPs of focus in this study as they are among the highest produced and widely applied in nano-enabled products for domestic and industrial purposes (BCC Research 2012; Yang and Westerhoff 2014). Silver nanoparticles are widely favoured for their antimicrobial properties in medicine, fabrics treatment, disinfectants, vacuum cleaners and washing machines. On the other hand, nZnO is applied in paints, beauty care products, sunscreens and coatings as a result of UV blocking ability and transparency at nano scale (Odzak *et al.* 2014; Yang and Westerhoff 2014). Owing to high production and application; these two ENPs are ideal candidates as they are suspect of higher rates for environmental release into water resources.

The choice of study organism was hinged on limited nanoecotoxicity data on higher aquatic plants and the overall skewness as earlier discussed. For the purposes of this study *Spirodela punctuta* and *Salvinia minima* were selected as test species. Higher aquatic plants, such as duckweeds have been ideal surface water candidates in ecotoxicological evaluation of bulk scale chemicals for several reasons: (i) these plants are generally easy to culture; (ii) are characterized by rapid growth rates relative to other vascular plants; (iii) the homogeneity of its populations is favourable for ecotoxicology; and (iv) as producers they hold a valuable trophic position in energy metabolism within the aquatic food web (OECD 2002; USEPA 1996; Brain and Solomon 2007; Jiang *et al.* 2014) .

1.5 Study aims and approach

1.5.1 Hypothesis

The interaction of nAg and nZnO with aquatic higher plants is interactively influenced by the physical and chemical characteristics of the ENPs and those of the exposure aqueous media.

1.5.2 Aims

This study is hinged on the following two aims:

- Investigate the influence of exposure water quality on the physical and chemical transformations of nAg and nZnO, in order to gain insights on their interaction, bioavailability as well as toxicity to free floating higher aquatic plants.
- Investigate the toxicological effects of nAg and nZnO towards free floating aquatic higher plants.

1.5.3 Objectives

The objectives of the study were identified and addressed as follows:

- Review the current state of knowledge on the interaction of ENPs with higher aquatic plants**.** This is addressed in Chapter 2.
- Investigate the physical and chemical transformations of nAg and nZnO in aqueous media so as to gain insights into environmental fate and behaviour dynamics of the ENPs in water bodies. This aspect is addressed in investigations covered in Chapters 3 and 4 which focus on ENPs fate in reconstituted fresh water and environmental water respectively.
- Investigate the role of ENPs size and aqueous media characteristics on uptake, accumulation and effects of nAg and nZnO towards free floating higher aquatic plant specimen; *Salvinia minima* and *Spirodela punctuta*. This objective is addressed in Chapters 5 and 6.

1.5.4 Thesis layout

To accomplish the aims of the study, the research was approached by dividing into inter-linked components reported in different chapters as follows:

- **Chapter 1** provides background information on nanotechnology and environmental implications as rational for the project. The chapter also gives aims and objectives of the study and closes by providing thesis outlay.
- **Chapter 2** undertakes a literature review to give knowledge status on the interaction of metal-based nanoparticles with higher aquatic plants.
- **Chapter 3** investigates the stability of nAg and nZnO in a standard toxicity testing medium, Hoagland's medium by studying agglomeration and dissolution dynamics of the ENPs and how aqueous properties influence their physical and chemical behaviour.
- **Chapter 4** focuses on the fate and behaviour of nAg in environmental water as a factor of ENPs size. Thus citrate capped nAg of average sizes 10 and 40 nm are used to investigate physical and chemical transformations in environmental water.
- **Chapter 5** investigates uptake, accumulation and toxicity of nAg towards *Salvinia natans* and the role of ENPs size and water quality variables.
- **Chapter 6** investigates the oxidative toxicity of nAg and nZnO towards a higher aquatic plant, *Spirodela punctuta.*
- **Chapter 7** highlights the major findings and provides concluding remarks of the study, whilst further makes recommendations for future investigations in the research domain.
- **Chapter 8** provides a full reference list of the study.

CHAPTER 2

Interactions of metal-based engineered nanoparticles with higher aquatic plants: a note on the state of current knowledge

2.1 Introduction

Initial concerns on the environmental effects of engineered nanomaterials (ENMs) emerged approximately in 2000s based on scientific findings related to increased toxicity potential associated with nanoscale-driven characteristics – and uncertainties on mechanistic biological interactions (Colvin 2003; Oberdörster 2004; Oberdörster *et al.* 2005; Nel *et al.* 2006). The unique and novel physicochemical properties of ENMs relative to bulk scale counterparts suggested that traditional toxicological assessment tools may be inadequate to assess risks of ENMs in environmental systems. For example, the distinctive large surface area to mass ratio exhibited at nanoscale challenges previously established common approaches for risk assessment which are founded mainly on concentration level factors. Until now notable research effort has been expended towards gaining further insights on the environmental implications of nanotechnology, for example; toxicological effects, fate, transportation, etc., – but still lacks behind aspects of production and application of ENMs (Kahru and Ivask 2013). Thus, the rapidly growing production and incorporation of ENMs in nano-enabled products has triggered the need to generate information on potential unintended environmental effects of nano-enabled products as likelihood of nanoscale pollutants environmental exposure consequently increases.

The drive to generate information on the effects of ENMs fostered the birth of a scientific field concentrating on the effects of ENMs towards living organisms generically regarded as nanotoxicology (Oberdörster *et al.* 2005). Notably, initial efforts in nanotoxicology were primarily to establish the harmful effects of ENMs towards humans (Oberdörster *et al.* 2005; Kreyling *et al.* 2006; Nel *et al.* 2006; Baun *et al.* 2008; Xia *et al.* 2009), and latter similar concerns were raised on potential environmental effects (Oberdörster 2004; Oberdörster *et al.* 2006; Handy and Shaw 2007; Moore 2006). Nanoecotoxicology later emerged as a branch of nanotoxicology focusing on ecological health aspects associated with exposure to ENMs (Behra and Krug 2008; Handy *et al.* 2008a; 2008b; Kahru and Dubourgier 2010).

The purpose of this review is to present an overview of the literature concerning nanoecotoxicology of metal-based engineered nanoparticles (ENPs) in aquatic higher plants, from which future recommendations are made on areas that merit further knowledge development in the context of aquatic higher plants interaction with metal-based ENPs. In the current study, metal-based ENPs refer to metal and metal oxide. The review exclusively focuses

on metal-based ENPs as result of their unique characteristics which differ markedly from other ENMs forms (e.g. fullerenes, carbon nanotubes, quantum dots), for instance, dissolution potential being one key discriminant trait. Metal-based ENPs are among highly produced ENM forms for consumer products development and industrial applications as a result of their unique magnetic, catalytic capacity, and optoelectronic properties that render them attractive for a broad range of applications (BCC Research 2012; PEN 2014). The high production accompanied by increasing application of metal-based ENPs heightens their potential for environmental release and in turn, motivates the need to establish their environmental consequence(s).

Aquatic higher or vascular plants, mostly those of the Lemnnoideae family are widely used as test candidates in aquatic ecotoxicology (Park *et al.* 2013). These plant types are preferred test candidates in ecotoxicology because they are: (i) relatively easy to culture under laboratory conditions, (ii) have rapid growth rates, (iii) accumulate surrounding chemicals (especially metals), and are (iv) sensitive to a wide range of pollutants (USEPA 1996; OECD 2002; ISO 2005). In addition, they provide sufficient tissue biomass essential to undertake diverse biochemical toxicity assessments (Song *et al.* 2012; Oukarroum *et al.* 2013). Aquatic higher plants occupy an important position in energy metabolism within ecosystems as producers, as food source and shelter for a variety of invertebrates (Lahive *et al.* 2014). Many studies concur that there is a shortage of nanoecotoxicity information on aquatic higher plants as opposed to effects expended towards micro-algal species, and terrestrial, or agricultural vascular plants (Kahru and Dubourgier 2010; Peralta-Videa *et al.* 2011; Miralles *et al.* 2012; Glenn and Klaine 2013; Ma *et al.* 2013).

Such an information gap impedes the assessment of ENMs potential risks to aquatic environments, since information at all trophic levels is essential for effective risk assessment (Holden *et al.* 2013). Overall this review on the interaction of aquatic higher plants with ENMs focuses on the following aspects: (i) bioavailability, (ii) uptake, translocation and accumulation and (iii) toxicity effects. The aim of the review is to generate an information portfolio on what presently has been done in studying the interactions of metal-based ENMs and aquatic higher plants and also present recommendations for future research. It is envisaged that the study aim will be addressed following a targeted literature breakdown as already mentioned.

2.2 Bioavailability

Behaviour, fate and transport of ENPs in aquatic systems are partly influenced by their physical and chemical traits such as size, shape, crystal structure, composition and surface coating. In the aqueous media, ENPs undergo transformation as a result of abiotic and biotic factors –which

consequentially determine firstly their stability in suspension and thus “phase distribution”, then bioavailability, uptake and toxicity potential upon interactions with aquatic biota (Delay and Frimmel 2012; Unrine *et al.* 2012). Therefore, the biota in the water phase encounters or interacts with ENPs whose physicochemical properties differ compared primary state (during manufacturing and application), or as released into aquatic environments (Stone *et al.* 2010; Nowack *et al.* 2012). Examples of transformations that metal-based ENPs undergo in aqueous media are illustrated in Figure 2.1. It is not the intention of this review to discuss the ENPs transformations but merely to highlight their relevance to interaction with aquatic plants as the subject has been addressed elsewhere (Auffan *et al.* 2009; Stone *et al.* 2010; Bone *et al.* 2012; Unrine *et al.* 2012; von Moos *et al.* 2014).

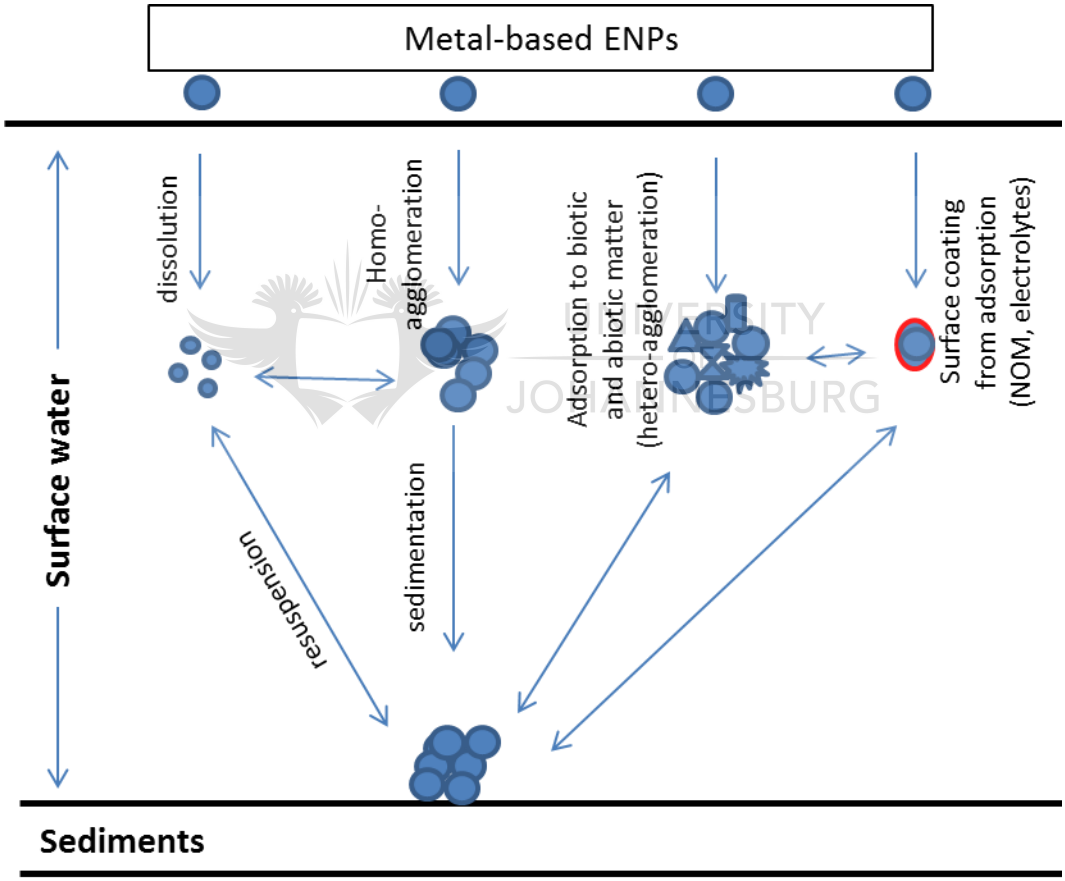

Figure 2.1: Schematic presentation of transformations that metal-based engineered nanoparticles (ENPs) undergo in aqueous environments. These are key processes that determine behaviour (chemical and physical) and bioavailability of metal-based ENPs in aquatic ecosystems.

For metal-based ENPs, dissolution is highly influential in determining their environmental fate. The release of ions by metal-based ENPs is a chemical trait highly enhanced at nanoscale, and in turn increases their reactivity (Auffan *et al.* 2009). Dissolution is also regarded as aging effect because ENPs chips off, and as a result release soluble ionic forms. Therefore; metal-based ENPs interact with biota in the following forms: (i) dissolved metals, (ii) new chemical substances formed after interacting with aqueous media components, and, (iii) particulates (Ma *et al.* 2013). Thus every study needs to pay attention on the bioavailable fractions of metal-based ENPs as a result of associated implications for uptake and toxicity. For instance, Yin *et al.* (2011) and Bone *et al.* (2012) have proposed that the toxicological potency of nAg in a microcosm is dependent on the bioavailable fraction of nAg.

Moreover, environmental factors such as pH, ionic strength, dissolved and natural organic matter amongst others play key roles in determining the transformation of ENPs (Peralta-Videa *et al.* 2011; Bone *et al.* 2012; Unrine *et al.* 2012) either by altering bioavailable size, surface chemistry, or influencing dissolution rate. For example, the surface chemistry of nAu influences accumulation of Au by tobacco plants (Judy *et al.* 2012) thus further stressing the role of ENPs characteristics to what is bioavailable to biota. On the other hand, generally the dissolution rate of metal-based ENPs increases at acidic pH range regime relative to neutral and basic conditions; although other abiotic factors like NOM may exert influence on the pH effect. Whether in particulate or dissolved form, ENPs interact with higher plants through process such as adsorption, deposition, and uptake – and the fate and toxicity implications of this aspect have been discussed elsewhere (Reed *et al.* 2012; Turner *et al.* 2012; Unrine *et al.* 2012; Chernousova and Epple 2013; Luyts *et al.* 2013; Odzak *et al.* 2014).

In suspension, metal-based ENMs generally undergo agglomeration where the gravitational forces may overcome buoyancy forces. This effect can result in sedimentation and loss of particles in suspension, thereby effectively reducing exposure concentration (von Moos *et al.* 2014). However, often overlooked is the opposite effect of de-agglomeration as ENPs transformation is dynamic and not one-dimensional. Furthermore; chemical processes such as reduction of metal cations (e.g. Ag^{+}) can also result in the formation of smaller secondary particles in suspension (Stebounova *et al.* 2011); introducing new bioaccessible size state. Both ENPs' size reduction and growth processes play an important role in determining the exposure size as well as persistence in aqueous systems. Therefore, the interplay of agglomeration, de-agglomeration, sedimentation and re-suspension of ENPs carries implications for both free floating and rooted aquatic plants – and each process exhibit both temporal and spatial variations. It has been suggested that settling of ENPs onto sediments effectively purifies aquatic

systems (Remedios *et al.* 2012); however, such arguments overlook the fact that aquatic systems are not one-dimensional, for instance, during re-suspension ENPs can dissolve or de-agglomerate. As mentioned earlier, water properties (pH, dissolved oxygen, temperature) and constituents (organic matter; electrolytes) significantly influence the properties of ENPs in aqueous systems.

For instance, electrolytes and organic matter control the stability of ENPs as they interact with ENP surfaces; thereby altering surface characteristics such as surface charge potential, and coating. Glenn and Klaine (2013) investigated the interplay of nano gold (nAu) size (4, 18 and 30 nm) and dissolved organic carbon (DOC) as a water quality parameter. Dissolved organic carbon treatment was found to reduce nAu bioavailability as a result of steric stabilisation; however, the nAu/DOC complexes formed reduced bioavailability as a result of nAu size growth. The authors concluded that the bioavailability of nAu to aquatic higher plants is underpinned by complex interplay of ENPs and test media characteristics as evidenced by varying rates of Au accumulation between treatments.

In light of summary given, there is value in integrating ENP characteristics and aqueous properties when investigating environmental behaviour of ENPs, rather than treating each component singularly as none is superior but are strongly interactively linked. Ultimately the bioavailability of ENPs in environmental aquatic systems is determined by the complex interplay of processes highlighted earlier in this section, which by nature are dynamic and dependent on spatial and temporal scales as well as chemical and physical characteristics of ENPs and exposure media. It is in this context that such a system is difficult to predict or replicate especially under natural conditions.

2.3 Uptake, translocation and accumulation

2.3.1 Uptake

Metal-based ENPs in aqueous systems occur either as dissolved ions, dissolved metallic complexes, or particulate forms, and the uptake by aquatic vascular plants is determined by numerous processes as depicted in Figure 2.1. It can be expected that there us variability on ENPs uptake mechanisms due to physiological and anatomical/morphological diversity amongst aquatic higher plants. For instance, differing uptake kinetics can result from differing root (Glenn *et al.* 2012) and xylem morphology (Ma *et al.* 2010) between plant species. Herein, the term uptake broadly refers to association of plants with ENPs from exposure medium through different pathways, be it absorption and adsorption to plant surfaces or internalisation into plant cells and

tissues. Although generally uptake mechanisms and kinetics of ENPs by plant cells are poorly understood (Bian *et al.* 2013; Judy *et al.* 2012); a few have been postulated are briefly summarized in this section, and listed in Table 2.1.

Physical structural forms and various forms of exudates (amino acids, enzymes, sugars) lining plant cell walls present a layer capable of further transforming ENPs (on interaction), and in turn facilitate ENPs uptake, or even rejection (Dietz and Herth 2011; Sabo-Attwood *et al.* 2011). In addition, for internalisation to occur, ENPs should pass through cell wall pores which can reject or allow entry dependent ENPs size encountered (Lin and Xing 2008). Reports indicate plant pore sizes vary and their maximum diameter has been estimated as 20-50 nm (Adani *et al.* 2011; Judy *et al.* 2012). Yet small ENPs size alone does not effectively guarantee uptake as shown with 10, 30 and 50 nm nAu where internalisation by tobacco plants did not occur irrespective of nAu sizes (Judy *et al.* 2012). This is because in addition; plant characteristics such as physiology and phenotype influence ENPs internalisation (Glenn *et al.* 2012). Others suggest endocytosis (Liu *et al.* 2009a), cell wall penetration (Chen *et al.* 2010), and even passive internalisation by damaged plant tissues (Judy *et al.* 2012) as uptake mechanisms of ENPs by plants.

In the work of Glenn and colleagues (2012) using three plant species, the uptake of nAu was found to be both ENP size and plant species dependent. No nAu internalisation was observed with *Egeria densa*; however, traces of Au were measured in tissues, and suggested to be adsorbed onto plant surfaces as no internalisation was observed using electron microscopy techniques (TEM, STEM and SEM), and EDX scan. A study by Judy *et al.* (2012) also revealed that even without nAu internalisation, Au, was detected in plant tissue as a result of nAu adsorbed onto tobacco plant surfaces. Similarly, Li *et al.* (2013) could not establish evidence of $nTiO_2$ internalisation by *Lemna minor* using electron microscopy as aggregates of $nTiO_2$ were observed on cell surfaces but none inside the cells. The observation was attributed to the fine sieving nature of the cell wall and adsorption of ENPs to cell surface exudates which are known to promote agglomeration. This argument was supported by images of agglomerates on the surfaces indicating interactions occurred, however, without internalisation. In the works of Hu *et al.* (2014), adsorption was suggested as uptake mechanism after *Salvinia natans* was exposed to nZnO.

Table 2.1: Reports of uptake of metal-based ENPs by aquatic higher plants

Uptake pathway	ENP type	Uptake detection	ENPs characterisation	Exposure water	Plant	Reference
Internalisation (tissue)	nAu	TEM, STEM and SEM, and EDX	4 nm; spherical; -14.1 mV; 250 g/L	Well/borehole water, pH 7.1, TOC=8.56 mg/L, C_aCO_3=107 mg/L; conductivity=210 µs/cm^3	*M. simulans*	Glenn *et al.* 2012
Internalisation (cellular)	nAu	TEM, STEM and SEM, and EDX	4; 18 nm; spherical; -14.1 mV; -9.73 mV	Well/borehole water, pH 7.1, TOC=8.56 mg/L, $CaCO_3$=107 mg/L; conductivity=210 µs/cm^3	*A. caroliniana*	Glenn *et al.* 2012
Adsorption (no internalisation)	nAu	TEM, STEM and SEM, and EDX	4; 18 nm; spherical; -14.1 mV; -9.73 mV	Well/borehole water, pH 7.1, TOC=8.56 mg/L, $CaCO_3$=107 mg/L; conductivity=210 µs/cm^3	*E. densa*	Glenn *et al.* 2012
Adsorption (no internalisation)	$nTiO_2$	SEM, TEM	275 - 2398 nm; SSA=50±15 m^2/gA; 0.005-1.59 mg/L	Steinburg growth medium, pH 5.5, CaCO3 = 166 mg/L	*L. minor*	Li *et al.* 2013
Adsorption	nZnO	ICP-OES	25 nm; uncoated; SSA=90 m^2/g; 1-10 mg/L	OECD growth medium; pH 6.5±0.2	*S. natans*	Hu *et al.* 2014

TOC-total organic carbon; SSA-specific surface area; QDs-quantum dots

For the case of *Myriophyllum simulans* and *Azolla caroliniana*; presence of nAu in all root cross section images was confirmed using electron microscopy and EDX. The 4 nm nAu was detected in higher numbers relative to the larger 18 nm counterparts, more so with *A. caroliniana* which accumulated higher Au concentrations from both 4 nm and 18 nm nAg exposures (Glenn *et al.* 2012). The relative high uptake of nAu by *A. caroliniana* was attributed to the presence of stomata roots on both sides of fronds as well as root hairs which increased the surface area for uptake unlike the other two species which generally do not have roots.

The exclusion of 18 nm Au by *M. simulans* confirmed size dependent effect on ENPs uptake possibly as a result of discrimination by cell wall pores sized approximately 3-50 nm, and varies between species. In addition, physiological adaptation of *E. densa* and *M. simulans* with respect to high salt tolerance was related to their ability to exclude or control uptake of nAu compared to the salt intolerant *A. caroliniana* which had higher Au accumulation. Overall, Glenn *et al.* (2012) findings suggested several mechanisms for ENPs uptake, singularly or synergistically, namely: (a) size regulation by cell wall pores; (b) species physiology, and (c) phenotypic or structural regulation. Because of poor dissolution of Au it is likely that the observed accumulation of Au was predominantly from the particulate Au forms.

Glenn and Klaine (2013) studied the uptake dynamics of nAu using the same aquatic macrophytes as in Glenn *et al.* (2012), they found that DOC treatment did not influence nAu uptake by *E. densa*; thus, further confirming total nAu exclusion as reported previously (Glenn *et al.* 2012). Addition of DOC in the test suspension inhibited Au uptake by *M. simulans*, and the roots were found to be the main route of nAu uptake as earlier reported (Glenn *et al.* 2012). Treatment with DOC inhibited nAu uptake by *A. caroliniana*, however; the trend was not uniform for all size treatments. For *A. caroliniana*; significant uptake was again attributed to the roots as reported earlier by Glenn *et al.* (2012). The association of nAu with DOC was observed to decrease with increasing ENPs size whereby 30 nm nAu was least associated with DOC. The findings indicate size-driven reactivity variations of ENPs where smaller sizes are highly reactive as opposed to larger ones. For instance, highest accumulation of nAu in *A. caroliniana* was recorded from 4 nm nAu exposure indicative of high uptake for smallest-sized ENPs. The results also revealed that whilst DOC induced steric stabilisation of nAu (agglomeration minimisation) however, the resultant nAu/DOC complexes were large enough to induce a size exclusion effect even for the smallest nAu (Glenn and Klaine 2013). This was evident by distinctive accumulation differences observed under the DOC treatment regimes of similar nAg size compared to those without DOC treatment.

The findings provided insights on the interplay of ENPs characteristics and abiotic factors in determining resultant bioavailability and uptake of ENPs by aquatic plants. In addition, the findings suggest plausible high variability of ENPs risk towards aquatic plants and aquatic biota in general, whereby the degree of risk is dependent on ENP-environment-biota interactions. Despite actual environmental scenario being highly complex; however, the results (Glenn *et al.* 2012; Glenn and Klaine 2013) provide evidence of key determinants of ENPs uptake by vascular plants, and how ENPs uptake should be estimated or interpreted taking into account ambient conditions.

2.3.2 Translocation

Translocation of metal-based ENPs in aquatic vascular plants is poorly understood, and the same is true for terrestrial counterparts (Rico *et al.* 2011; Sabo-Attwood *et al.* 2011; Glenn *et al.* 2012). Using an estuarine macrophyte, *Spartina alterniflora*, Burns *et al.* (2013) reported high distribution of Au in the roots (117 µg/kg), then aerial parts (11.3 µg/kg), and least in the stem (4.42 µg/kg). These results suggested active transportation of nAu from the site of uptake (roots) through stems (least deposition) to the aerial parts where deposition increased. *Spartina alterniflora* as a member of the Poaceae family uses roots for nutrient uptake, has thick cuticle on stems and leaves to avoid water loss but also to reduce substance uptake from these parts (Glenn *et al.* 2012). Terrestrial members of the same family, *Lolium multiflorum and Lolium perenne* exhibited low translocation capability of Ag and Zn from roots to shoots after exposure to nAg and nZnO, respectively (Lin and Xing 2008; Yin *et al.* 2011).

Contrary to findings of Glenn *et al.* (2012), the shoot system of another Poaceae family the water dropwort *Oenanthe javanica* was reported to have accumulated 8% and 15% Ti in roots following exposure to nanotube-TiO_2 and nanoparticle-TiO_2, respectively, after 17 days (Yeo and Nam 2013). These results again suggest relatively low transfer of $nTiO_2$ to the shoot system from the roots. The difference Glenn *et al.* (2012) and Yeo and Nam (2013) can be attributed to ENPs size because the nanotubes used in the latter study were likely limited in translocation capability as size is known to influence vascular plants internal distribution of ENPs (Lin *et al.* 2009; Ma *et al.* 2010; Miralles *et al.* 2012). Hu *et al.* (2013) observed higher accumulation of Zn in the fronds relative to the roots by *Salvinia natans* after exposure to nZnO (1-50 mg/L) for 7 days. However, this may not necessarily be attributed to active translocation as the root systems itself is a modified leaf elongation in *S. natans*, and therefore, even in absence of roots or root loss these plant-type are capable of nutrient uptake via leaves (Smith *et al.* 2006).

Overall, published data suggest that translocation of internalised ENPs is predominantly determined by plant type as well as associated physiological and phenotypic traits, and is similar

for both aquatic and terrestrial vascular forms. Secondly, even for closely related species, differences may occur between different ENP types possible as a result of internalised size as illustrated by findings of Glenn *et al.* (2012) and Yeo and Nam (2013), and finally, ENPs size play an important role in rate of translocation. Although until now, no study assessed the influence of ENPs size on translocation; it is likely that the trend on particle size influence on observed uptake and accumulation also correlates to translocation rate within a single species and ENPs exhibiting similar characteristics.

2.3.3 Accumulation

In this report accumulation refers to whole tissue metal bioaccumulation, without discriminating between internalised and internalised quantities. Accumulation of metal-based ENPs by aquatic higher plants has been reported for nAu (Ferry *et al.* 2009; Glenn *et al.* 2012; Burns *et al.* 2013; Glenn and Klaine 2013), nAg (Jiang *et al.* 2012), nZnO (Hu *et al.* 2013); $nTiO_2$ (Yeo and Nam 2013; Li *et al.* 2013), and nCuO (Nekrasova *et al.* 2011; Perreault *et al.* 2014). The most salient findings for each of the specific metal-based ENPs are listed in Table 2.2, and further summarized in the following sub-sections.

2.3.3.1 Zinc oxide nanoparticles (nZnO)

Accumulation of Zn by the duckweed *Spirodela polyrhiza* exposed to nZnO (1, 10 and 50 mg/L) for 96 hours increased with increasing exposure concentration up to about 4.5 mg/g dry weight (Hu *et al.* 2013). It was reported that nZnO was predominantly available for uptake in dissolved form (Zn^{2+}) based on the measured nZnO in the assay medium. The nZnO went up to *ca* 4 µm (average 130 nm) and hence it was argued the particulate form of nZnO was deemed too large for plausible cellular uptake. In the works of Hu et al (2014); there was not much variation in Zn accumulation between leaves and roots of *S. natans*. Accumulation of Zn was dependent on exposure concentration, varying between 0.015-3.65 mg/g (leaves) and 0.018-2.97 mg/g (rinsed roots) after exposure to 1-50 mg/L nZnO. However, unrinsed roots accumulated relatively more Zn compared to rinsed roots, pointing towards notably adsorption of nZnO onto root surfaces.

2.3.3.2 Titanium dioxide nanoparticles ($nTiO_2$)

Lemna minor exposed to 0.01-5 mg.$nTiO_2$/L accumulated in excess of 80 mg/kg Ti at the highest concentration after 7 days exposure, and accumulation was $nTiO_2$ concentration dependent (Li *et al.* 2013). The Ti quantified was attributed to adsorbed fractions as no internalisation was detected using electron microscopy-based techniques. The large sized agglomerates in the testing media mainly accounted for a lack of cell pore uptake by the duckweed.

Table 2.2: Summary findings on accumulation of metal based ENPs by aquatic higher plants

ENPs	ENPs characteristics	Exposure concentration	Exposure water	Exosure duration	Bioconcentration	Plant	Reference
nZnO	25 nm; SSA = 90 m^2/g	1-50 mg/L	Hoagland's medium, pH 6.5	96 hrs	~2-4.5 mg/g (whole plants)	*S. polyrhiza*	Hu *et al.* 2013
nZnO	25 nm; SSA= 90 m^2/g	1-50 mg/L	Hoagland's medium, pH 6.5	7 days	3.65 mg/g (leaves) 2.97 mg/g (roots rinsed) 8.18 mg/g (roots unrinsed)	*S. natans*	Hu *et al.* 2014
$nTiO_2$	275 - 2398 nm; SSA = 50±15 m^2/gA; *~-20 to -25 mV*	0.005-1.59 mg/L	Steinburg growth medium, pH 5.5, $CaCO_3$ = 166 mg/L	7 days	~ <1-70< mg/kg (whole plants)	*L. minor*	Li *et al.* 2013
$nTiO_2$	5-10 nm; rhombic and spherical; -33.83 mV	1.8 mg/L	mesocosm	17 days	489.1 µg/g (whole plant) 54.5 µg/g (whole plant)	*O. javanica* *I. japonica*	Yeo and Nam 2013
$nTiO_2$ (nanotube)	7-9 nm (width); 2 nm (thick); 6 nm (diameter); tubular; -41.5 mV	1.8 mg/L	Freshwater mesocosm	17 days	79.5 µg/g (whole plant) 155.2 µg/g (whole plant)	*O. javanica* *I. japonica*	Yeo and Nam 2013
nCuO	30 nm	0.025-5 mg/L		3 days	20946-521 (*BAC) (whole plant)	*E. densa*	Nekrasova *et al.* 2011
nCuO	523 nm; -40 mV	0.7-4.5 g/L	Freshwater culture medium ;pH 6.5; IS=0.0127 M	48 hours	~<0.006-<0.018 mg/mg (whole plant)	*L. gibba*	Perreault *et al.* 2014
nCuO	97 nm; Poly(styrene-co-butyl acrylate) coating; -40 mV	0.3-1.2 g/L	Freshwater culture medium ;pH 6.5; IS=0.0127 M	48 hours	~<0.005-<0.025 mg/mg (whole plant)	*L. gibba*	Perreault *et al.* 2014
nCuO	38±7 nm; SSA = 12.84 m^2/g; -2.8±0.41 mV	0.5-50 mg/L	Hoagland's medium	21 days	14-4057 µg/g (roots) 0.8-17.7 µg/g (shoots)	*S. tabernaemontani*	Zhang *et al.* 2014
CdS	4.3±0.3 nm; -9.8±0.3 mV	0.5-50 mg/L	Hoagland's medium	21 days	9-1518 µg/g (roots) 0.8-8.7 µg/g (shoots)	*S. tabernaemontani*	Zhang *et al.* 2014
nAu	65X15 nm; rods	7.08 *10^8 particles/mL	Estuarine mesocosm; pH ~7.7-8.5; salinity=~16.5-18 ppt; DO=~5-12 mg/L	12 days	3.45 µg/kg (whole plant)	*S. alterniflora*	Ferry *et al.* 2009
nAu	48.3X9.8 nm; rods; -53.5± mV	3.42* 10^7 particles/mL	Estuarine mesocosm; salinity =20 ppt; pH ~8	11 days	117 (roots), 4.42 (shoots), 1.17 µg/kg (stems)	*S. alterniflora*	Burns *et al.* 2013
nAu (4, 18 nm)	4 nm; 18 nm; spherical; -14.1 mV; -9.73 mV	250 µg/L	Well/borehole water, pH 7.1, TOC=8.56 mg/L, $CaCO_3$=107 mg/L; conductivity=210 µs/cm^3	24 hours	~100, ~<60 mg/kg (whole plant)	*M. simulans*	Glenn *et al.* 2012
nAu (4, 18 nm)	4 nm; 18 nm; spherical; -14.1 mV; -9.73 mV	250 µg/L	Well/borehole water, pH 7.1, TOC=8.56 mg/L,	24 hours	~120, ~<60 mg/kg (whole plant)	*A. caroliniana*	Glenn *et al.* 2012

			$CaCO_3$=107 mg/L; conductivity=210 µs/cm^3					
nAu (4, 18 nm)	4 nm; 18 nm; spherical; -14.1 mV; -9.73 mV	250 µg/L	Well/borehole water, pH 7.1, TOC=8.56 mg/L, $CaCO_3$=107 mg/L; conductivity=210 µs/cm^3	24 hours	~40, ~<60 mg/kg (whole plant)	*E. densa*	Glenn *et al.* 2012	
nAu (4, 18, 30 nm)	8±6; 17.5±2; 25±7; -16.7±2 mV; -17.8±3 mV; -23.7±4 mV	250 µg/L	Well/borehole water, pH 6.8, DOC=0.1±0.02 mg/L, $CaCO_3$=107 mg/L; conductivity=210 µs/cm^3	24 hours	~<50-150 mg/kg (whole plant); <50 mg/kg (shoots)	*A. caroliniana*	Glenn and Klaine 2013	
nAu (4, 18, 30 nm)	8±6; 17.5±2; 25±7; -16.7±2 mV; -17.8±3 mV; -23.7±4 mV	250 µg/L	Well/borehole water+DOC, pH 6.8, DOC=2±0.4 mg/L, $CaCO_3$=107 mg/L; conductivity=210 µs/cm^3	24 hours	<50 mg/kg (whole plant: 4 nm); ~50 mg/kg (whole plant: 18, 30 nm); <50 mg/kg (shoots)	*A. caroliniana*	Glenn and Klaine 2013	
nAu (4, 18, 30 nm)	8±6; 17.5±2; 25±7; -16.7±2 mV; -17.8±3 mV; -23.7±4 mV	250 µg/L	Well/borehole water, pH 6.8, DOC=2±0.4 mg/L, $CaCO_3$=107 mg/L; conductivity=210 µs/cm^3	24 hours	<50 mg/kg (whole plant); <50 mg/kg (shoots)	*E. densa*	Glenn and Klaine 2013	
nAu (4, 18, 30 nm)	8±6; 17.5±2; 25±7; -16.7±2 mV; -17.8±3 mV; -23.7±4 mV	250 µg/L	Well/borehole water+DOC, pH 6.8, DOC=2±0.4 mg/L, $CaCO_3$=107 mg/L; conductivity=210 µs/cm^3	24 hours	<50 mg/kg (whole plant); <50 mg/kg (shoots)	*E. densa*	Glenn and Klaine 2013	
nAu (4, 18, 30 nm)	8±6; 17.5±2; 25±7; -16.7±2 mV; -17.8±3 mV; -23.7±4 mV	250 µg/L	Well/borehole water, pH 6.8, TOC=2±0.4 mg/L, $CaCO_3$=107 mg/L; conductivity=210 µs/cm^3	24 hours	<50 mg/kg (whole plant); <50 mg/kg (shoots)	*M. simulans*	Glenn and Klaine 2013	
nAu (4, 18, 30 nm)	8±6; 17.5±2; 25±7; -16.7±2 mV; -17.8±3 mV; -23.7±4 mV	250 µg/L	Well/borehole water+DOC, pH 6.8, DOC=2±0.4 mg/L, $CaCO_3$=107 mg/L; conductivity=210 µs/cm^3	24 hours	<50 mg/kg (whole plant); <50 mg/kg (shoots)	*M. simulans*	Glenn and Klaine 2013	
nAg	7.8±2.6 nm; gum-arabic coating; SSA=100±25 m^2/g; -49 to -44 mV	0.5-10 mg/L	10% Hoagland's medium	72 hours	2.81 mg/g (whole plant)	*S. polyrhiza*	Jiang *et al.* 2012	

BAC-biological accumulation coefficient; DOC-dissolved organic carbon; IS-ionic strength; SSA-specific surface area

Studies of Yeo and Nam (2013) with *O. javanica* and *Isoetes japonica* exposed to 1.8 mg/L nanoparticle (TiO_2-NP) and nanotube (TiO_2-NT) TiO_2 forms over 17 days; resulted to whole plant accumulation of Ti in both plant species. The total accumulated TiO_2-NP and TiO_2-NT in both species were 489.1 µg/g and 155.2 µg/g, respectively. The study did not account for the variations observed; however, it is likely that the longitudinal–symmetry of TiO_2-NT rendered them large and were not easily assimilated compared to uptake sites e.g. cell wall pores thereby effectively limiting any probable internalisation. Accumulation of Ti in *O. javanica* after 17 days was higher at the roots compared to the shoot system with accumulated 424.4 µg/g and 64.7 µg/g, respectively (Yeo and Nam 2013). The study also highlighted remarkable bioconcentration and bioaccumulation of Ti within the mesocosm, which pointed towards potential trophic transfer of nano pollutants in aquatic ecosystems.

2.3.3.3 Copper oxide nanoparticles (nCuO)

Nekrasova *et al.* (2011) investigated accumulation of Cu by leaves of *Elodea densa* after 3 days exposure to 0.025-5 mg/L of nCuO and $CuSO_4$ salt. Copper accumulation decreased with increasing exposure concentration and generally more significant for nCuO than $CuSO_4$. The large nCuO agglomerates which adsorbed onto cell walls were too big for internalisation – effectively blocking cell wall pores. This is suggested to have caused the inverse relationship between Cu accumulation and nCuO concentration. Agglomerates size increased with increasing exposure concentration of nCuO. On the other hand, accumulation of Cu increased with increasing dose concentration in *Lemna gibba* exposed to $CuSO_4$, and two forms of nCuO (non-coated and styrene-co-butyl acrylate coated) for 48 hours (Perreault *et al.* 2014). Exposure of *L. gibba* to $CuSO_4$ and nCuO led to accumulation 0.05 mgCu/mg and 0.025 mgCu/mg biomass, respectively, after 48 hours.

Higher accumulation of Cu was observed from polymer coated nCuO exposures compared to bare counterparts (Perreault *et al.* 2012), suggesting polymer coating stabilised nCuO and were more bioavailable. Although the coating effect on accumulation to the aquatic vascular plants remains unexplored, previously ENPs coating has been shown to improve nCuO uptake and accumulation in micro-algal specimen largely because of size retention capability of coated nanoparticles relative to the bare forms where the latter undergoes remarkable size growth effects (Perreault *et al.* 2012). Higher uptake of smaller nAu by aquatic higher plants following steric stabilisation with NOM has been reported (Glenn *et al.* 2012), and further supports this viewpoint.

2.3.3.4 Gold nanoparticles (nAu)

In an estuarine mesocosm, *S. alterniflora* accumulated 3.45 µg/kg Au after 12 days exposure to nAu nanorods (Ferry *et al.* 2009). *S. alterniflora* had the lowest concentration factor suggested to be as a result of limited leaching of nAu through sediments to reach the roots, and/or the agglomerates were too large; thus consequently hindered uptake. However, findings of Burns *et al.* (2013) showed *S. alterniflora* had highest Au accumulation after 11 days in the roots (117 µg/kg) compared to aerial parts (4.42 µg/kg) and stems (1.17 µg/kg). The investigators conceded that sediments adhered to the roots may have contributed to Au quantified in the roots, although efforts were made to wash off sediment particles. Glenn *et al.* (2012) in a comparative study reported higher Au uptake from 4 nm exposed plants relative to 18 nm exposures. These results further suggest ENP size plays an important factor in influencing their environmental fate and behaviour as well as potential for trophic system transfer. The observations were attributed to relatively higher internalisation of 4 nm nAu compared to the larger size of 18 nm. In addition, it was reported that Au accumulation varied between plant species where higher accumulation rates were observed in *M. simulans* and *A. caroliniana* in comparison to *E. densa*. The morphological and physiological adaptations accounted for the accumulation differences between the three species as discussed in earlier under the uptake section.

Glenn and Klaine (2013) reported a blocking effect on *M. simulans, A. caroliniana,* and *E. densa* exposed to 4, 18 and 30 nm nAu dosed with DOC for 24 hours. The authors argued that the resultant nAu/DOC complexes were larger than original particles and the cell pores thereby effectively reducing the potential for nAu uptake.

2.3.3.5 Silver nanoparticles (nAg)

Spirodela polyrhiza exposed to 0.5-10 mg/L nAg and $AgNO_3$ were observed to accumulate Ag in a concentration dependent manner (Jiang *et al.* 2012). For instance, samples exposed to 5 mg/L of either nAg or $AgNO_3$ accumulated significantly higher concentrations in comparison to lower concentrations. According to Jiang and colleagues (2012), accumulation of Ag from the silver salt was always higher relative to plants exposed to nAg at any given exposure concentration. The average size of nAg in suspension (7.8 nm) was suggested as small enough to enable internalisation, however, the cause for favourable Ag accumulation from $AgNO_3$ was not investigated, and the authors recommended further work to gain insights aimed to elucidate ENPs uptake mechanisms. In this instance, one approach to elucidate underlying mechanism for accumulation could be through dissolution analysis of Ag in test media in order to differentiate uptake rates between nAg and $AgNO_3$. Although nAg in the test had small-sized particles

plausible for cell pore uptake, however possibly underwent severe agglomeration and lower dissolution relative to $AgNO_3$, and hence preferable Ag accumulation from $AgNO_3$ exposures. This hypothesis appears plausible as a recent study of Jiang *et al.* (2014) showed significantly higher dissolution for 1 µm Ag relative to 6 and 20 nm nAg. Dissolution analysis by Jiang *et al.* (2012) would have provided more insights into bioavailability dynamics of nAg to be able to explain higher Ag internalisation from $AgNO_3$ exposures.

2.4 Toxicity effects

Most studies have evaluated the toxicity of metal-based ENPs on aquatic vascular plants in comparison to uptake and accumulation, and are summarized in Tables 2.3, 2.4 and 2.5 for the subcellular, photosynthetic and growth effects respectively.

2.4.1 Subcellular effects

2.4.1.1 Copper oxide nanoparticles (nCuO)

Oxidative stress was induced on *E. densa* exposed to nCuO (0.025-5 mg/L) and was quantified by assessing the activities of peroxidase activity (POD), superoxide dismutase (SOD) and catalase (CAT), as well as lipid peroxidation and thiobarbituric acid reactive substances (TBARS) quantification as indicators of oxidative damage (Nekrasova *et al.* 2011). Nano CuO induced higher oxidative stress at low exposure concentrations unlike $CuSO_4$, and this was associated to higher nCuO uptake at lower concentrations as a result of smaller-sized particles compared to agglomerates formed at higher concentrations which were not easily internalised. After 48 hours exposure of *L. gibba* to nCuO (bare and polymer coated), the activity of esterase was inhibited by increasing nCuO exposure concentration whilst the generation of reactive oxygen species (ROS) increased with increasing nCuO concentration (Perreault *et al.* 2014). The production of ROS was in the order of: highest with polymer coated-nCuO, then bare-nCuO, and lesser with $CuSO_4$. These findings were attributed to higher dissolution rate of polymer-coated nCuO as corroborated by higher toxicity at nanoscale than bulk counterparts ($CuSO_4$).

Table 2.3: Summary of the subcellular effects of metal-based ENPs to higher aquatic plants.

ENPs	ENPs characteristics	Exposure water	Exposure concentration	Duration	Endpoint	Effect/response	Plant	Reference
nCuO			0.025-5 mg/L		POD SOD CAT TBARS	Inhibition Activation Inhibition Decreased	*E. densa*	Nekrasova *et al.* 2011
nCuO	523 nm; -40 mV	Freshwater culture medium ;pH 6.5; IS=0.0127 M	0.7-4.5 g/L	48 hours	Esterase ROS	Decreased Increased	*L. gibba*	Perreault *et al.* 2014
nCuO	97 nm; Poly(styrene-co-butyl acrylate) coating; -40 mV	Freshwater culture medium ;pH 6.5; IS=0.0127 M	0.3-1.2 g/L	48 hours	Esterase ROS	Decreased Increased	*L. gibba*	Perreault *et al.* 2014
$nTiO_2$	10 nm; ~ -15 to 25 mV; SSA = 120 m^2/g	10% Steinberg medium	1-2000 mg/L	7 days	POD CAT SOD MDA	activation activation activation then inhibition Increased	*L. minor*	Song *et al.* 2012
nZnO	25 nm; uncoated; 90 m^2/g; spherical	Hoagland's medium; pH 6.5	1-50 mg/L	96 hours	CAT POD SOD Na^+K^+ATPase	Activation Inhibition Activation No effects	*S. polyrhiza*	Hu *et al.* 2013
nZnO	326-1350 nm; -4.9 to 11 mV; SSA = 11.4 m2/g; spheres; polydispersed morphology	Hoagland's medium;	0.01-1000 mg/L	14 days	ROS/RNS H_2O_2 TAC SOD	Increase then stabilised (4 days), increase (14 days) Uniform, increased at highest exposure concentration (14 days) Increase at lowest exposure concentration (4 days), uniform Mostly inhibited (4 days), only activated at highest exposure conc. (14 days)	*S. punctuta*	Thwala *et al.* 2013
nZnO	25 nm; uncoated; 90 m^2/g; 1-10 mg/L	OECD growth medium; pH 6.5±0.	1-50 mg/L	7 days	SOD CAT POD	Increased by 50 mg/L Increased by 50 mg/L Inhibited by 50 mg/L	*S. natans*	Hu *et al.* 2014
nAg	352-1313 nm; -3.6 to 11.6 mV; SSA = 3.4	Hoagland's medium;	0.01-1000 mg/L	14 days	ROS/RNS H_2O_2 TAC	No effects (4-14 days) Increased No effects	*S. punctuta*	Thwala *et al.* 2013

	m2/g; polydispersed morphology				SOD	Inhibition and activation (4 days), inhibition (14 days)		
nAg	7.8±2.6 nm; gum-arabic coating; SSA=100±25 m^2/g; -49 to -44 mV	10% Hoagland's medium	0.5-10 mg/L	72 hours	Nitrate-nitrogen	Reduction	*S. polyrhiza*	Jiang *et al.* 2012
					Phosphate-phosphorus	Reduction		
					Carbohydrate	No effects		
					Proline	Increased		
nAg	7.8±2.6 nm; gum-arabic coating; SSA=100±25 m^2/g; -49 to -44 mV; spherical	10% Hoagland's medium	0.5-10 mg/L	72 hours	ROS content	Increased (≤ 1 mg/L)	*S. polyrhiza*	Jiang *et al.* 2014
					SOD	Activated		
					POD	Activated (≤ 5 mg/L)		
					CAT	Activated (≤ 5 mg/L)		
					Protein content	Increased (1,5 mg/L)		
					MDA	Increased (5 mg/L)		
					GSH	Increased (5, 10 mg/L)		
nAg	22.9±6 nm; PVP coating; spherical	10% Hoagland's medium	10 mg/L	72 hours	ROS content	Increase of ROS, SOD, POD, GSH and protein content.	*S. polyrhiza*	Jiang *et al.* 2014
					SOD, POD, CAT, Protein content, MDA GSH	No significant effect on CAT and MDA		

2.4.1.2 Zinc oxide nanoparticles (nZnO)

The activities of CAT, POD, SOD and Na^+K^+ATPase in *S. polyrhiza* were measured after exposure to nZnO (1-50 mg/L) and $ZnSO_4$ (3.5 mg/L) for 96 hours (Hu *et al.* 2013). The activities of SOD and CAT were stimulated by 10, 50 mg/L and 50 mg/L nZnO, as well as exposure to $ZnSO_4$. On the other hand, POD and Na^+K^+ATPase were inhibited by $ZnSO_4$ whilst 50 mg/L nZnO was only inhibitive to POD activity. When *Salvinia natans* was exposed to nZnO (1-50 mg/L) and $ZnSO_4$ (44 mg/L); $ZnSO_4$ and only 50 mg/L nZnO stimulated SOD and CAT whilst these exposures inhibited POD activity (Hu *et al.* 2014). The two studies suggested that toxicity of nZnO under test conditions was dependent on dissolution to release dissolved Zn which were bioavailable and capable of internalisation.

2.4.1.3 Silver nanoparticles (nAg)

Jiang *et al.* (2012) reported that *S. punctuta* experienced significant reduction of total nitrate-nitrogen, phosphate-phosphorus, and carbohydrate after exposure to nAg and $AgNO_3$ where the effect was more severe with the latter. Proline production as an indicator of stress increased with increasing exposure concentration, and was more pronounced with $AgNO_3$ compared to the nano forms. In contrast Jiang *et al.* (2014) found the micron-Ag did not enhance free radical production or induce antioxidative capacity (CAT, POD, CAT) and oxidative damage (MDA) except for glutathione (GSH) activity compared to nano counterparts which exhibited toxic effects in a concentration dependent manner. Moreover protein content was not influenced by micron sized Ag. The toxicity of nAg was attributed to the particulate form of nAg as a result of low dissolution quantified (20 µg/L), a concentration found not to induce ROS production or antioxidative activity (Jiang *et al.* 2014). The cause for the contradiction between the two studies by the same investigators remains unclear as similar forms of nAg and testing media characteristics were used. However, the studies did not assay for similar variables but the differing toxicity of micron Ag form between the two studies is unclear and difficult to account especially taking into account the relatively high dissolution of bulk Ag compared to nAg.

2.4.2 Photosynthetic effects

2.4.2.1 Copper oxide nanoparticles (nCuO)

Following an initial increase of photosynthetic activity in *E. densa* (mg CO_2/g/h and chlorophyll pigments) at 0.025 mg/L nCuO, photosynthetic inhibition increased with increasing exposure ENP concentration (Nekrasova *et al.* 2011). In excess, copper is known to be inhibitive on photosynthesis and its effect on the photosystem II (PSII) well described (Maksymiec 1997), and

has been reported by other investigators with nCu. Perreault and co-workers (2014) observed the PSII inhibition in *L. gibba* exposed to variants of nCu and a copper salt, where effect was more pronounced with polymer coated-nCuO, followed by $CuSO_4$ and lesser with bare-nCuO after 48 hours. However, Shi *et al.* (2011) reported bulk CuO as less inhibiting to photosynthesis after *Landoltia punctata* was exposed to nCuO and bulk CuO.

2.4.2.2 Titanium dioxide ($nTiO_2$)

Chlorophyll *a* content on TiO_2 exposed *L. minor* remained similar to the control but increased at higher exposure concentrations of $nTiO_2$ (200-2000 mg/L) (Song *et al.* 2012). Song *et al.* (2012) findings revealed no chlorophyll *a* content changes in *L. minor* exposed to $nTiO_2$ (0.01-5 mg/L) for 14 days, and was attributed to lack of $nTiO_2$ uptake (Li *et al.* 2013). A study on *L. minor* reported increased photosynthetic efficiency after 7 days exposure to nAl_2O_3 (Juhel *et al.* 2011). Similar observations for spinach have been reported after exposure to $nTiO_2$ and was attributed to enhanced activity of Rubisco activase (Gao *et al.* 2008), a parameter not studied by Juhel and colleagues (2011).

2.4.2.3 Zinc oxide nanoparticles (nZnO)

Hu *et al.* (2013) after exposing *S. polyrhiza* to 50 mg/L nZnO and 3.5 mg/L $ZnSO_4$ observed induction of photosynthetic effects measured as a ratio of chlorophyll *a* (Chl *a*) to phaeophytin. Similarly, findings of Hu *et al.* (2014) after exposure of 50 mg/L nZnO and 44 mg/l $ZnSO_4$ induced photosynthetic effects in *S. natans*.

2.4.2.4 Silver nanoparticles (nAg)

Spirodela polyrhiza exposed to nAg and $AgNO_3$ (0.5-10 mg/L) showed a reduction of Chl *a*, Chl *a*/Chl *b* ratio, and photochemical efficiency in a concentration dependent manner following exposure (Jiang *et al.* 2012). The $AgNO_3$ had higher inhibiting effect relative to nAg on Chl *a*/Chl *b* and photochemical efficiency, but not always with Chl *a*. However following further comparison, the authors concluded that $AgNO_3$ was not always the most toxic form and that the toxicity of the two forms was generally similar but sensitivity to $AgNO_3$ and nAg varies between toxicity endpoints. Following low accumulation of Ag in nAg exposures (Jiang *et al.* 2012), it can be hypothesized that if uptake/internalisation of nAg was increased likewise the toxicity of nAg would likely be higher than $AgNO_3$ based on mass/volume exposure concentrations. This case further indicates the need for more detailed information on ENPs uptake by aquatic vascular plants. For instance, future studies need to consider whether linkages between the toxicity effects and accumulation of ENPs exist.

Table 2.4: Reports of photosynthetic effects in aquatic plants exposed to metal-based ENPs.

ENPs	ENPs characteristics	Exposure water	Exposure concentration	Duration	Endpoint	Effect/response	Plant	Reference
nCuO	30 nm		0.025-5 mg/L	3 days	Photosynthetic rate Chl *a* Chl *b* Carotenoids	Initial activation then inhibition Decreased Uniform then increased Decreased	*E. densa*	Nekrasova *et al.* 2011
nCuO	523 nm; -40 mV	Freshwater culture medium ;pH 6.5; IS=0.0127 M	0.7-4.5 g/L	48 hours	PSII yield PSII index	Inhibition (4.5 g/L) Inhibition (1-4.5 g/L	*L. gibba*	Perreault *et al.* 2014
nCuO	97 nm; Poly(styrene-co-butyl acrylate) coating; -40 mV	Freshwater culture medium ;pH 6.5; IS=0.0127 M	0.3-1.2 g/L	48 hours	PSII yield PSII index	Inhibition Inhibition	*L. gibba*	Perreault *et al.* 2014
nCuO	10-15 nm (TEM); 43 nm (SMPS); 6.7 nm (BET); 9 (7 days)- 80 nm; SSA = 141 ±m^2/g	Hoagland's medium, pH 6	1 mg/L	14 days	Chl *a* Chl *b* Chl *a*+Chl*b*	Decreased Decreased Decreased	*L. punctuta*	Shi *et al.* 2011
$nTiO_2$	10 nm; ~-15 to -25 mV	10% Steinberg medium, pH 6.5	10-2000 mg/L	7 days	Chl content	Increased (≤200 mg/L)	*L. minor*	Song *et al.* 2012
$nTiO_2$	275 - 2398 nm; SSA = 50±15 m^2/gA	Steinburg growth medium, pH 5.5, $CaCO_3$ = 166 mg/L	0.005-1.59 mg/L	7 days	Chl *a*	No significant effects	*L. minor*	Li *et al.* 2013
nAl_2O_3	9.01±3 nm (TEM); 165-189 nm (NTA); SSA = 200 m^2/g; spherical to void; 5.3±1.4 mV	50% Hutner's medium; pH 5.3	10-1000 mg/L	7 days	PSII yield Photochemical quench Non-photo quench	Increased (100 mg/L) Increased (100 mg/L) No significant effects	*L. minor*	Juhel *et al.* 2011
nZnO	25 nm; SSA = 90 m^2/g	Hoagland's medium, pH 6.5	1-50 mg/L	96 hours	Chl:pheophytin	Significant reduction (50 mg/L)	*S. polyrhiza*	Hu *et al.* 2013
nZnO	25 nm; SSA = 90 m^2/g	Hoagland's medium, pH 6.5	1-50 mg/L	7 days	Chl *a* Chl *b* Carotenoid	Increased (50 mg/L) No effects Increased (50 mg/L)	*S. natans*	Hu *et al.* 2014
nAg	7.8±2.6 nm; gum-arabic coating; SSA=100±25 m^2/g; -49 to -44 mV	10% Hoagland's medium	0.5-10 mg/L	72 hours	Chl *a* Chl *a*/*b* Chl total Photochemical efficiency	Decreased Decreased (≥5 mg/L) Decreased Decreased	*S. polyrhiza*	Jiang *et al.* 2012

PSII-photosynthetic system II, SMPS-scanning mobility particle sizer; NTA-nanoparticle tracking analysis

Table 2.5: Reports of growth effects in aquatic plants exposed to metal-based ENPs.

ENPs	ENPs characteristics	Exposure water	Exposure concentration	Duration	Endpoint	Effect/response	Plant	Reference
nCuO	38±7 nm; SSA = 12.84 m^2/g; -2.8±0.41 mV	Hoagland's medium	0.5-50 mg/L	21 days	Biomass	No significant effects	*S. tabernaemontani*	Zhang *et al.* 2014
nCdS QDs	4.3±0.3 nm; -9.8±0.3 mV	Hoagland's medium	0.5-50 mg/L	21 days	Biomass	Reduction ≥5 mg/L	*S. tabernaemontani*	Zhang *et al.* 2014
nCuO	97 nm; Poly(styrene-co-butyl acrylate) coating; -40 mV	Freshwater culture medium; pH 6.5; IS=0.0127 M	0.3-1.2 g/L	48 hours	Growth rate	growth reduction from 0.4 g/L	*L. gibba*	Perreault *et al.* 2014
nCuO	109-523 nm (0-48 hrs)	Freshwater culture medium; pH 6.5; IS=0.0127 M	0.4-4.5 g/L	48 hrs	Growth rate	growth reduction >0.1 Log Cu g/L	*L. gibba*	Perreault *et al.* 2014
nCuO	10-15 nm (TEM); 43 nm (SMPS); 6.7 nm (BET); 9 (7 days) -80 nm; SSA = 141 ±m^2/g	Hoagland's medium; pH 6	0.0158-4 mg/L	96 hrs	Growth	Substantial growth inhibition (EC50 = 0.8 mg/L)	*L. punctuta*	Shi *et al.* 2011
			1 mg/L	14 days	Frond number	>50% inhibition	*L. punctuta*	Shi *et al.* 2011
nAg	700 nm, citrate coating; -7.87 mV	OECD 221 medium; pH 5.5±1.4	5-160 µg/L	14 days	Frond number	Decreased (≥20 µg/L)	*L. minor*	Gubbins *et al.* 2011
					Growth rate	Decreased (≥10 µg/L)		
					Dry weight	Decreased (≥10 µg/L)		
					Growth inhibition	Increased		
nAg	130 nm, citrate coating; -7.87 mV	OECD 221 medium; pH 5.5±1.4	5-160 µg/L	14 days	Frond number	Decreased (≥80 µg/L)	*L. minor*	Gubbins *et al.* 2011
					Growth rate	Decreased (≥20 µg/L)		
					Dry weight	Decreased (≥20 µg/L)		
					Growth inhibition	Increased		
nAg	7.8±2.6 nm; gum-arabic coating; SSA=100±25 m^2/g; -49 to -44 mV	10% Hoagland's medium	0.5-10 mg/L	72 hours	Fresh weight	Decreased (≥5 µg/L)	*S. polyrhiza*	Jiang *et al.* 2012
					Dry weight	Decreased (≥5 µg/L)		

nAg	5-2 nm (TEM); 84.97 nm (DLS); spherical; -34.9 mV	Greenhouse water	8-128 µg/L	7 days	Frond number Growth rate Total weight Total fronds Growth inhibition	Decreased Decreased Decreased Decreased Increased	*L. minor*	Ucuncu *et al.* 2014
nAg	50 nm	Algal assay procedure medium; pH 7.5	0.1-200 ppm	7 days	Growth rate	Decreased (≥1 ppm)	*L. pausicostata*	Kim *et al.* 2011
$nTiO_2$	2-3 nm	Algal assay procedure medium; pH 7.5	31.25-500 ppm	7 days	Growth rate	Decreased (≥250 ppm)	*L. pausicostata*	Kim *et al.* 2011
$nTiO_2$	*275 - 2398 nm; SSA = 50±15 m2/gA; ~-20 to -25 mV*	*Steinburg growth medium, pH 5.5, CaCO3 = 166 mg/L*	*0.005-1.59 mg/L*	*7 days*	Frond number Growth rate	No effects No effects	*L minor*	Li *et al.* 2013
nZnO	25 nm; SSA = 90 m^2/g	Hoagland's medium, pH 6.5	1-50 mg/L	7 days	Growth rate	No effects	*S. natans*	Hu *et al.* 2014

TEM-transmission electron microscopy; DLS-dynamic light scattering

2.4.3 Growth effects

2.4.3.1 Copper oxide nanoparticles (nCuO)

Lemna gibba exposed to bare- and polymer coated-nCuO exhibited higher growth inhibition compared to samples exposed to $CuSO_4$ (Perreault *et al.* 2014). Notably, polymer coated-nCuO caused elevated toxicity accounted by their higher dissolution and stabilisation; which in turn improved internalisation. Overall the study not only offered a compelling case of size driven toxicity, but also indicated the ENPs' surface characteristics influence on their environmental behaviour and effects (Perreault *et al.* 2014). Earlier work alluded the dissolved Cu as a driver of toxicity where $CuCl_2$ yielded higher inhibition to *L. punctuta* relative to bare-nCuO and bulk CuO (Shi *et al.* 2011). Findings from both studies suggested Cu ions as more toxic than nCuO based on differences arising from limited nCuO uptake compared to Cu salts where latter were more bioavailable as ionic species.

2.4.3.2 Silver nanoparticles (nAg)

Dissolved silver ($AgNO_3$) was found more toxic (on inhibitory) to *L. minor* compared to 29 and 93 nm nAg, when frond number, dry weight, and growth rate were assayed (Gubbins *et al.* 2011). The dissolution for both nAg sizes was less than 1%, thus rendering ionic-driven toxicity insignificant but effects were rather driven by particulate nAg forms. Although $AgNO_3$ was more toxic due to ease of Ag^+ internalisation, the study findings pointed to nAg internalisation – at lower rate than Ag^+ – and induced toxicity effects. Jiang *et al.* (2012) showed $AgNO_3$ exerted higher growth inhibition to *S. polyrhiza* compared to nAg after 72 hours exposure. The higher toxicity of $AgNO_3$ was postulated to be due to higher Ag accumulation in the plants relative to nAg exposures. Lower concentrations (8-32 µg/L) of nAg were reported to exert elevated growth retardation to *L. minor* exposed to higher concentrations of nAg (32-128 µg/L) (Ucuncu *et al.* 2014). As mentioned earlier, increasing exposure concentration tends to induce remarkable agglomeration of ENPs, and in turn, renders larger agglomerates improbable for internalisation whilst smaller particles at low exposure concentrations are easily internalised.

2.4.3.3 Titanium dioxide nanoparticles ($nTiO_2$)

A study by Kim *et al.* (2011) showed nAg being highly inhibitive to *Lemna paucicostata* growth rate compared to $nTiO_2$, and the effect was hypothesized as particulate-driven linked to low dissolution quantified after 7 days. Notably, although nAg (50 nm) was about 17-fold larger than $nTiO_2$ (3 nm), it was still more toxic than the later. The results point to the significant role of chemical behaviour differences besides the rod-shaped nAg may have induced a darting effect

on cells as opposed to spherical TiO_2 (Kim *et al.* 2011). In a study with *L.* minor, $nTiO_2$ increased plant growth at low exposure concentrations relative to bulk form, however, by 1000 mg/L, the trend reversed with $nTiO_2$ being highly inhibitive whilst plant growth increased with bulk TiO_2 concentration (Song *et al.* 2012). The relatively high toxicity of $nTiO_2$ at higher concentrations was attributed to the nano form higher uptake rate than the bulk form; although unexpected, $nTiO_2$ size decreased with increasing exposure concentration. It is commonly accepted that ENPs tend to undergo remarkable size growth with increasing concentration, in some instances even sedimenting out as agglomerates experience gravitational effect – for instance, reported by Ucuncu *et al.* (2014), however, the findings of Song *et al.* (2012) contrasted the known trends.

No growth effects were observed after *L. minor* was exposed to 0.1-5 mg/L $nTiO_2$ (Li *et al.* 2013). This may have emanated from size reduction with increasing concentration such that the agglomerates continuously settled out of suspension, thereby the remaining $nTiO_2$ were of insignificant quantities to cause any detectable effects. The authors (Li *et al.* 2013) suggested the lack of toxicity effects (photosynthetic and growth related) were as a result of poor $nTiO_2$ uptake as evidenced by electron microscopy-based results. *Lemna minor* exposed to nAl_2O_3 for 7 days experienced growth stimulation (Juhel *et al.* 2011), and the growth enhancement was associated with poor internalisation of ENPs whilst Al from bulk forms was internalised and hence inhibited photosynthesis and growth.

2.4.3.4 Zinc oxide nanoparticles (nZnO)

Similarly, growth rate and biomass retardation were reported for *S. polyrhiza* exposed to nZnO and $ZnSO_4$ (50 mg/L), and $ZnSO_4$ was more toxic than nZnO (Hu *et al.* 2013). The nZnO underwent severe agglomeration which in turn reduced in its bioavailability. Therefore, lower toxicity of nZnO was attributed to low bioavailability whilst $ZnSO_4$ was more bioavailable as dissolved Zn, and hence the latter was more toxic. At comparable exposure concentrations of *S. natans* to 50 and 44 mg/L for nZnO and $ZnSO_4$, to; $ZnSO_4$ caused growth inhibition whereas no effects were observed for nZnO (Hu *et al.* 2014). Similar to Hu *et al.* (2013) findings the higher dissolution of $ZnSO_4$ translated to more bioavailable Zn forms compared to nZnO.

2.5 Concluding remarks and future perspectives

Literature reviewed here can be regarded as representing the latest body of information on the interaction of metal-based ENPs and aquatic higher plants. It is therefore pertinent to summarise key information extracted as to identify those aspects that require future investigations.

- It is clear that highly diverse experimental protocols were adopted between the studies accessed in the current literature survey. This then raises important questions with respect to data quality on aspects of comparability, uniformity, and usability. Therefore, adoption standardized testing protocols for aquatic higher plants might need to be adopted as already done for other organisms, for instance the OECD guidelines. This can enhance the quality and application of data generated across the scientific community in order to make meaningful contribution on the risk assessment of nanotechnologies.

- There appears to be reasonable justification to approach ENPs risk evaluation towards aquatic plants differently from terrestrial counterparts, based on differences in exposure pathways and ENPs' bioavailability between the two environmental matrices. The interaction of aquatic plants and ENPs' is highly dynamic as a result of the numerous chemical and physical processes that determine final interaction, in the root-soil environment the situation might not be as highly variable (temporal and spatial) as the aquatic scenario in Figure 2.1.

- Overall, this literature review obtained information further supporting the importance of the interplay between ENPs and water and physico-chemical characteristics of exposure media in determining environmental implications of ENPs in aquatic environments. For instance, limited ENPs uptake was in some studies suggested to be as a result of severe ENPs agglomeration which effectively render the agglomerates too large for cell wall uptake. It is widely known that water chemistry highly influences the rate of agglomeration as well as dissolution of metal-based ENPs. Hence exposure water characteristics highly influential of ENPs bioavailability. The stabilisation effect by water variables can induce higher uptake and accumulation rates as reported by Glenn and Klaine (2013).

- Cell wall pores appear to be the key sites for internalisation of any bioavailable ENPs fraction by aquatic higher plants. Numerous studies indicated or suggested that uptake of ENPs' was regulated by the cell wall pores, for instance the lack of uptake is often related to the size of ENPs in suspension. Studies by Glenn and colleagues (Glenn *et al.* 2012; Glenn and Klaine 2013) gave solid evidence on ENPs uptake rate as factor of nAu size, and because of limited dissolution observed, we can be confident that only the particulate/nano fraction of Au was bioavailable in these two studies. However, not only the small ENP bioavailable size ensures effective uptake, but the physiological and phenotypic characteristics of aquatic plants appear to play a major role as well. Such a

suggestion is based on the differences observed between species with respect to uptake and translocation. For instance the high proportion of root hairs was reported to be one of the key resultant of high uptake of nAu in *A. caroliniana* compared to the other species which did not possess such a feature. Therefore any modeling approaches to estimate the interaction of metal-based ENPs with aquatic higher plants need not only regard the ENPs characteristics but also the plant's phenotypic and physiological features.

- Translocation of ENPs fractions also appears to vary between plant species. However there are indications that bioavailable size also plays a key role, however this aspect is yet to be investigated in detail. In this instance, a species with a high translocation rate could be selected and exposed to different sizes of a highly stable ENP such as nAu.

- The induction of nanotoxicity effects in aquatic higher plants is directly linked to ENPs uptake rate and this is supported by the numerous reports indicating a direct relationship between ENPs uptake (in any bioavailable form) and toxicity. In many instances toxicity effects were related to bioavailable dissolved metal ions, and there is still limited evidence of the "nano" induced toxicity. The bias to translate toxicity effects based on dissolution could be influenced by the current limited analytical ability to detect, characterise and quantify ENPs in complex environmental matrices; this can be supported by the extremely high exposure concentrations which are mostly environmentally irrelevant, used in many studies reviewed here.

- Future studies need to pay particular attention on the uptake dynamics of ENPs by aquatic vascular plants as this aspect remains poorly studied. These types of investigations need to take into account the characteristics of bioavailable ENPs forms, as it will help us gain better insights regarding exposure scenarios.

- Information obtained by this review indicates that aquatic higher plants are capable of internalising ENP forms and that has implications for bioaccumulation and trophic transfer. Even adsorbed ENPs are candidates for trophic transfer within aquatic ecosystems as the process does not discriminate between adsorbed and internalised ENPs.

CHAPTER 3

The role of solution chemistry on agglomeration and dissolution of silver and zinc oxide nanoparticles

3.1 Introduction

The pursuit of products with improved and novel performance in the past decade has resulted in rapid increase of nano-enabled products; dominated by products in the health and fitness category followed in descending order by home and garden, automotive, and lastly food and beverage, just to list the top four categories (Wijnhoven *et al.* 2010; PEN 2011). Such trends have led to increased potential for environmental release of nano-pollutants at various life cycle stages of nano-enabled products; more so from mostly produced and applied nanomaterials which are expected to be major sources of nanoscale pollutants into engineered and natural water bodies (Muller and Nowack 2008; Musee *et al.* 2014; Yang and Westerhoff 2014). Therefore, more comprehensive investigations are warranted to understand potential risks towards the environment from usage of nano-enabled products, especially considering nanotechnology applications have penetrated different facets of society.

Metal-based ENPs such as nAg and nZnO are among the highest produced and applied in nano-enabled consumer products and industrial applications (BCC Research 2012; Yang and Westerhoff 2014). Silver nanoparticles are widely favoured for their antimicrobial properties in medicine, fabrics treatment, disinfectants, vacuum cleaners and washing machines and nZnO are applied in paints, beauty care products, sunscreens and coatings as a result of their UV blocking ability and transparency at nano-scale (Odzak *et al.* 2014; Yang and Westerhoff 2014). As Class B soft metals; nAg and nZnO mainly induce toxicity through the release of soluble Ag and Zn forms (Lowry *et al.* 2012). Silver nanoparticles have been shown to induce toxic effects mainly through their dissolition (Navarro *et al.* 2008; Miao *et al.* 2009; Turner *et al.* 2012). The same is true nZnO dissolution (Franklin *et al.* 2007; Xia *et al.* 2008). In addition, nanoparticulate forms have also been reported to induce toxicity effects (Jassby *et al.* 2012; Oukarroum *et al.* 2013; Laban *et al.* 2010; Griffitt *et al.* 2008; Moos *et al.* 2010).

As a result of concerns fuelled by suggestions of increased toxicological potential (Oberdorster *et al.* 2005; Nel *et al.* 2006) and highly dynamic environmental behaviour at nanoscale (Auffan *et al.* 2009; 2010); a remarkable effort has been dedicated on investigating fate, behaviour and toxic effects of ENPs in aquatic environments. Numerous reports have been dedicated towards shedding more light on environmental fate, behaviour and toxicity of nZnO and nAg in aqueous settings (Nowack 2009; Johnston *et al.* 2010a; Chang *et al.* 2012; Jassby *et al.* 2012; Jiang *et al.*

2012; Reed *et al.* 2012; Wang *et al.* 2012; Yin *et al.* 2012; Oukarroum *et al.* 2013; Yu *et al.* 2013). In spite of these research efforts there still remains high uncertainty surrounding fate and behaviour ENPs in aquatic environments.

For instance, there is no common understanding underpinning drivers of physical and chemical transformations of nAg and nZnO in aqueous environments, which eventually determine bioavailability and toxicity of ENPs to aquatic biota. Partly this has been ascribed to varying experimental procedures between investigations and data inconsistency and conflicts (Schrurs and Lison 2012). For instance, data inconsistency and conflicts may arise from inappropriate and insufficient reporting of dispersion conditions as well as characterisation of ENPs under test conditions (Handy *et al.* 2012; Schrurs and Lison 2012; Bondarenko *et al.* 2013). Whereas detailed ENPs characterisation under test conditions can lead to a better understanding bioaccessibility state and mechanistic drivers of toxicity (Bondarenko *et al.* 2013). For instance, both nAg and nZnO are soluble to some extent in aqueous media, a parameter that can influence their toxicity (Gao *et al.* 2009; Pasquet *et al.* 2014) and key to environmental risk assessment of metal-based ENPs. In addition, solubility as key determinant of environmental fate and behaviour is highly influenced by water quality conditions (Auffan *et al.* 2009; 2010; Behra *et al.* 2013). Amongst the key determinants of ENPs dispersion is agglomeration state, which can be dependent on ENPs size (Liu *et al.* 2009b), surface charge and coating (Coleman *et al.* 2013), and characteristics of exposure medium (Casals *et al.* 2010), just to mention a few. Agglomeration state can for instance alter ENPs reactivity and solubility (Liu *et al.* 2009b; Ma *et al.* 2012; Hamilton *et al.* 2014), and exposure concentration (Gallego-Urrea *et al.* 2011; Baalousha *et al.* 2013), thus directly influencing bioavailability and toxicity potential. This summary information indicates that poor characterisation of both ENPs and exposure media conditions can mislead interpretation of findings, and risk estimation.

In light of the key role of water chemistry in determining environmental fate and behaviour of metal-based ENPs, as well as conflicting findings with respect to toxicity basis of metal-based ENPs; the mechanisms of ionic strength in governing physical (size dynamics) and chemical (dissolution) transformation of nAg and nZnO in aqueous environments were investigated. Specifically; the investigation focused on the influence of exposure water ionic strength variation on the stability of nAg and nZnO, where hydrodynamic size, zeta potential, particle concentration and dissolution were analysed. In this instance, uncoated dry powder nAg and nZnO forms were utilised. The study was undertaken to generate knowledge that aids hazard and exposure assessments of nAg and nZnO in aquatic systems, specifically towards pelagic biota. Better

insights are warranted in order to generate information that supports development of water quality guidelines for nano-pollutants to aid risk assessment framework for nano-enabled products.

3.2 Materials and methods

3.2.1 Nanoparticles characterisation

Powder forms of nAg (product code: 576832-5G) and nZnO (product code: 544906-5G) were purchased from Sigma Aldrich® (USA) with size of <100 nm according to the manufacturer's supplied information. Prior to testing, the ENPs were characterised for the following: (a) size and morphology using transmission electron microscopy (TEM) (JEOL JEM-2100®), (b) zeta potential measured in pure water (15 MΩ/cm) with a zetasizer (Nano-ZS, Malvern), (c) particle surface area measured following the Brunauer–Emmett–Teller theory (BET) (Brunauer *et al.* 1938) and (d) XRD (PAN Analytical X'Pert PRO PW 3040/60) was used for particle surface analysis. The BET method quantifies particle surface area under vacuum by introduction of known amount of nitrogen gas on the sample, then determine surface are from amount of free nitrogen. The method is highly suitable for solid phase samples.

During testing, ENP size was measured using the TEM and Nanoparticle Tracking Analysis (NTA, NS500, NanoSight). The NTA was further used to determine particle concentration per volume. For NTA analysis, a test volume of 1.5 mL was pipetted from each exposure beaker, transferred into a 1.5 mL microtube and vortexed for 30 seconds before analysis. Following homogenisation (vortex), the samples were immediately injected into the NTA and analysed in triplicate (each replicate analysed 3 times, each run 60 s video), where in between runs, the sample was advanced to introduce a fresh sample aliquot for measurement. The TEM samples were prepared by dipping the copper grid using forceps in a sample, after which the grid was left to air dry at room temperature on weighing paper before inspection.

3.2.2 Testing medium

Hoagland's Medium (HM) of different strengths was used as the testing medium, and was prepared by dissolving Hoagland's No. 2 Basal Mixture (product code: H2395-10L) obtained from Sigma Aldrich® in deionised water (DI). The chemical composition of HM is: $(NH_3)PO_4$, H_3BO_3, $Ca(NO_3)_2$, $Cu_2SO_4.5H_2O$, $Fe_2(C_4H_4O_6)_3.2H_2O$, $MgSO_4$, $MnCl_2.2H_2O$, MoO_3, KNO_3 and $ZnSO_4.7H_2O$. Full strength (100HM) medium was prepared by dissolving 1.6 g Hoagland's No. 2 Basal Mixture in a litre of DI water, whilst 0.8 g similarly was used to prepare half strength Hoagland's medium (50HM). During testing HM was characterised through triplicate measurements of Ca, Mg and water hardness as $CaCO_3$. The average values for Ca, Mg and

$CaCO_3$ in 50HM were 74, 20, 269 mg/L respectively, and 150, 43, 550 mg/L correspondingly for 100HM.

3.2.3 Experimental conditions

The ENPs stock solutions prepared were 1 mg/L in 50HM and 100HM, and were immediately diluted with respective HM strength to achieve the 100 µg/L experimental nominal concentration at pH 6 in Schott® bottles. Each exposure condition was triplicated and contained 200 mL of the test solution (nAg/nZnO + HM) in a 250 mL acid washed glass beaker. During testing, beakers were covered with pierced parafilm (5 holes) to minimise evaporation and shaken at 100 RPM in a Labcon® incubator to homogenise test solutions. The test temperature was set at 22^{o}C over 15 days, with pH and dissolved oxygen monitored continuously over this period using a pH meter (Jenway, 3510 Model, UK).

3.2.4 Sample preparation and dissolution analysis

Dissolution analysis was undertaken after 2, 24, 72, 144, 240 and 360 hours (hrs) intervals following ultracentrifugation an efficient technique for separation of particulate and dissolved metallic forms (Ma *et al.* 2012; Odzak *et al.* 2014). A volume of 25 mL from each test vessel was centrifuged (HermLe Labortechnic GmbH, Z236K, Germany) at 6000 RPM, 22^{o}C for 2 hrs in 3 kDa membrane (*ca*. 1-2 nm) Amicon® Ultra Centrifugal Filter units. The filtrate was then transferred into 50 mL conical tubes, acidified to achieve a 5% (v/v) HNO_3 concentration, and stored at frozen until analysis. The 3 kDa filters are suitable for the efficient separation of nAg from Ag ions (Ma *et al.* 2012; Merdzan *et al.* 2014). The dissolved metallic fraction was measured by ICP-MS (Agilent, 7500 Series, Japan) with a detection limit of 1 µg/L.

3.2.5 Data analysis

JMP Pro version 10 was used for statistical comparison between treatments. Comparison between HM strengths at a given time point were undertaken with a Students t-test at $\alpha = 0.05$ significance level, following normality test with Shapiro-Wilk W Test. The data is presented as the mean of triplicates within a treatment.

3.3 Results and discussion

3.3.1 Nanoparticle characterisation

Characteristics of the ENPs prior testing are summarised in Table 3.1 and Figure 3.1. The TEM results confirmed the presence of nanoscale particles, and also agglomerates larger than 100 nm

in both samples (Figure 3.1a,b). Notably, the morphology of both ENPs forms varied widely, where nAg was mainly spherical and semi-spherical, whilst nZnO was polydispersed consisting of spherical, cuboidal, rods and hexagonal plates (Figure 3.1b). Plausibly due to multi-morphological states, inter- and intra-particle porosity, presence of curvatures and smaller particles (< 30 nm) resulted to nZnO exhibiting larger surface area and wide size distribution compared to nAg. The XRD pattern of nAg (Figure 3.1c) confirmed the spherical morphology that is characteristic of nAg with limited crystallinity. The XRD pattern of nZnO (Figure 3.1d) indicated poly-crystallinity supporting suggestion of curvatures. All peaks were clearly identified, evidence that the material was pure phase. Thus, no characteristic peaks were observed for impurities (e.g., Zn or $Zn(OH)_2$).

Detailed characterisation of ENPs before introduction is essential in order to generate reference conditions and obtain a basis to interpret transformations observed in-test, as outlined elsewhere (Warheit 2008; Pettitt and Lead 2013). The zeta potentials for nZnO and nAg were positive and negative, respectively (Table 3.1) in DI water, and were in agreement with reports for similar uncoated ENP types (Li *et al.* 2011; Li and Lenhart 2012).

Table 3.1: Characteristics of nAg and nZnO prior testing; the measurements for size were obtained with TEM, zeta potential with zetasizer, surface area and pore volume calculated following BET theory (Brunauer–Emmett–Teller theory (BET).

ENPs	Manufacturer size (nm)	TEM size (nm)	Zeta potential (mV)	SA_{BET} (m^2/g)	Pore volume (cm^3/g)
nAg	< 100	40.3 - 153.5	-29.3	3.83	0.019
nZnO	< 100	10.1 – 130.8	24.6	16.37	0.037

Introduction of ENPs into the testing medium induced various forms of transformations for both nAg forms, for instance, alteration of zeta potentials. In the case of nAg, there was a reduction of zeta potential from -29.3 mV to -7.20 mV and -9.23 mV in 50HM and 100HM respectively. On the other hand, nZnO zeta potential was altered from 24.6 mV to -8.17 mV and -11.3 mV in 50HM and 100HM respectively. Even though the extent of alteration was dissimilar between the two ENPs, however, overall reflects the important role of water quality on environmental fate and behaviour of ENPs or nano-pollutants in aquatic systems. The reduction and reversal of zeta potential observed was plausibly as a result of electrolytes adsorbing to ENPs surfaces and shielding original surface charge observed in DI water.

For instance, highly effective action of divalent cations on neutralisation of nAg zeta potential has been reported (Cumberland and Lead 2009; Delay *et al.* 2011; Baalousha *et al.* 2013), and species such as Mg^{2+} and Ca^{2+} are components of HM used in this study. Similar effect has also been observed with negatively charged electrolytes (Li *et al.* 2013), as species such as Cl^- are assumed to cause complete reversal of nZnO surface charge. Quantification of water hardness as $CaCO_3$ as well as Ca^{2+} and Mg^{2+} in 50HM and 100HM revealed almost a 2-fold increase in concentration between the two HM strengths, where in 50HM $CaCO_3$, Ca^{2+} and Mg^{2+} were 256, 71 and 19 mg/L respectively whilst in 100HM they were 536, 147 and 41 mg/L. Such evidence points to the electrolytic effect because 100HM was more agglomeration promoting than 50HM probably as a result of higher electrolytic concentration in the former.

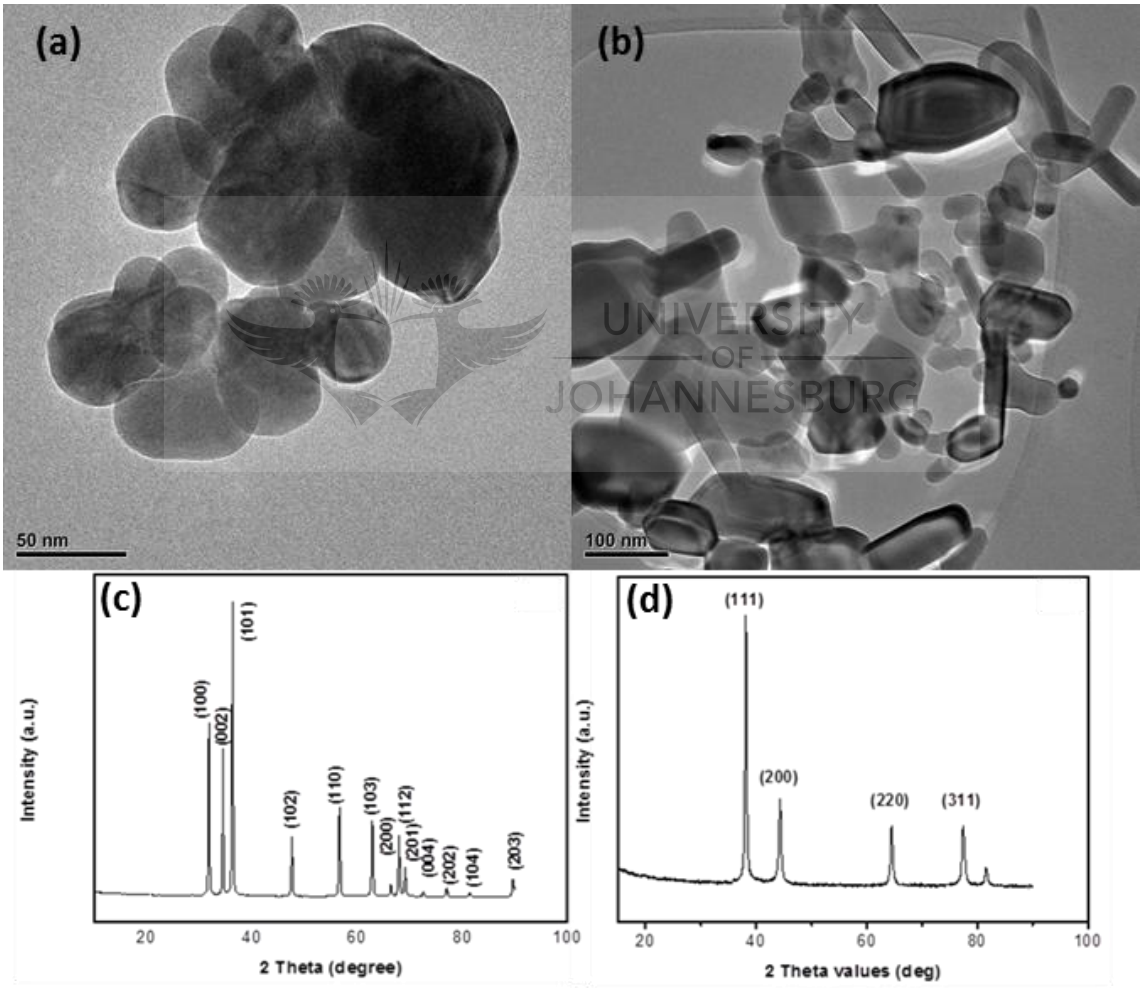

Figure 3.1: Characteristics of the ENPs before being added to the test medium (HM): TEM images of (a) nAg and (b) nZnO, and their respective XRD patterns (c) nAg and (d) nZnO.

As a secondary effect, the alteration of ENPs surface charge can result to a reduction of inter-particle repulsion which in turn leads to agglomeration (Cumberland and Lead 2009; Delay *et al.* 2011; Baalousha *et al.* 2013). Size related changes were investigated using NTA collaborated with TEM. While NTA analysis for nAg was successful, repeated attempts for nZnO analysis were unsuccessful, even attempts to improve stabilisation using citrate also failed. No NTA analysis was undertaken in DI water, as the intention was so to investigate influence of ionic strength variation between 50HM and 100HM. Dry powder ENP-types are generally poorly dispersed in aqueous media; hence posing a challenge for accurate in-test characterisation and exposure estimation as they are prone to high agglomeration and sedimentation rates (Liu and Hurt 2010; Lee *et al.* 2012). The formation of large agglomerates was evident during preparation of stock suspensions. This was addressed through elongated vortexing during preparation of exposure concentrations (Figure 3.2a); but still high sedimentation persisted and was observed after a few minutes after vortexing (Figure 3.2b). The severe agglomeration of nZnO resulted to large sized particles being stuck on sides of the NTA optical plate, hence making analysis unsuccessful.

Conversely, dilution resulted in poor detection of particles, hence no meaningful analysis of nZnO. The difficulty in nZnO quantification using NTA was likely partly a result of its numerous morphologies, as the instrument is more suitable for mono-dispersed spherical particles and limited for analysis of high aspect-ration ENPs (Gallego-Urrea *et al.* 2011). Although NTA analysis for nAg was undertaken, challenges linked to large agglomerates fouling the optical plate were encountered and the plate had to be dismantled more frequently for cleaning. Therefore only nAg NTA results are presented as vortexing of nZnO was ineffective in stabilising them. The experience in this aspect also supports suggestions of poor dispersion of powder ENPs in aqueous media, and NTA analysis of such forms is discouraged unless the samples have been shown to be highly stable. Already it appears the NTA has mostly been favoured for characterisation of liquid suspended ENPs (as received/synthesized) rather than dry powder, as summarised in Gallego-Urrea *et al.* (2011).

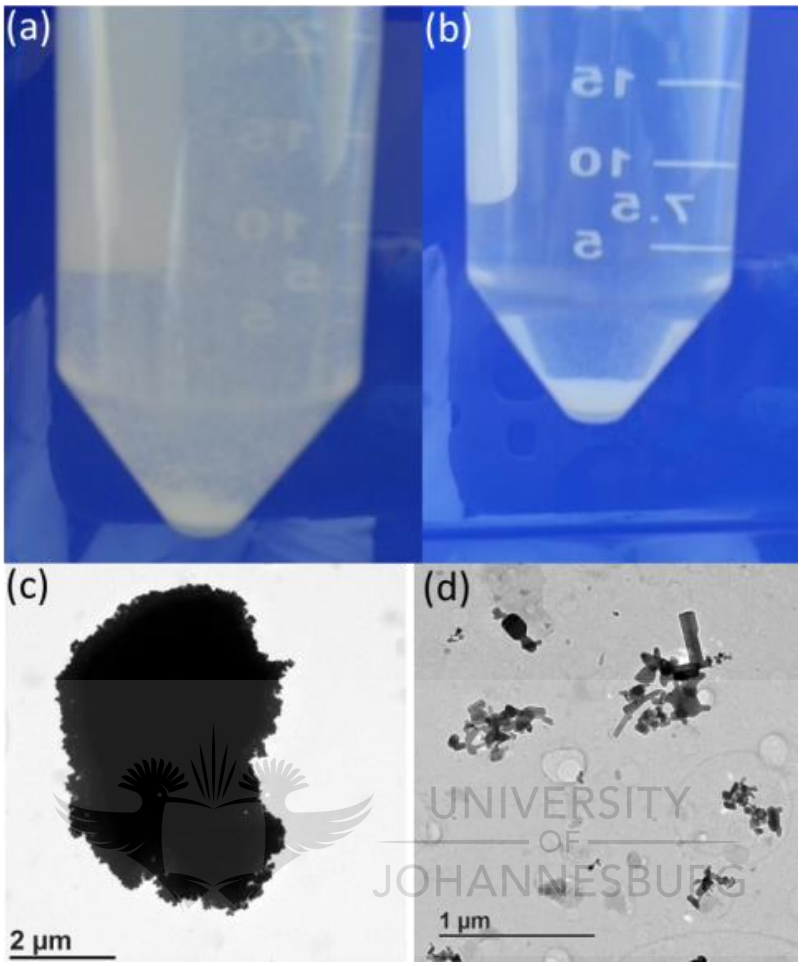

Figure 3.2: Illustration representing the poor dispersion of nAg and nZnO in powdered form. (a) Visible nZnO particles suspended and, (b) ZnO particles sedimenting out of suspension after a few minutes. Representative TEM images of: (c) nAg and (d) nZnO obtained under test conditions indicating severe ENPs agglomeration.

As suggested earlier the modification of zeta potential induced conditions that were favourable for agglomeration as illustrated by nAg size growth up to 96 hrs (Figure 3.3a). Immediately after introduction of nAg into testing medium (0 hrs); modal size of nAg in 100HM was significantly smaller than in the 50HM exposure. This was unexpected given on 100HM relatively higher ionic strength shielding effect on the zeta potential. However, as the experiment progressed nAg agglomeration rate in 100HM remained slightly higher than in 50HM until the experiment ended, but no significant statistical difference was observed. Since hydrodynamic size remained larger in 100HM (2-96 hrs) seems to suggests that higher destabilisation of nAg in 100HM was a result of high ionic strength expected to be more agglomeration-enhancing compared to 50HM. Whilst the

influence of HM strength on nAg size may not be great, the 100HM resulted in greater agglomeration. However, these results should be viewed with caution due to wide data distribution (mostly in 100HM) as a result of poor dispersion of the ENPs and limited ability of the NTA to accurately quantify the powder form ENPs. Notably, 50HM appeared to effectively stabilise nAg as size remained relatively similar between 0-48 hrs, with a slight size growth in after 48 hrs.

Based on agglomeration of 50HM and 100HM, one would expect fewer particles in 100HM compared to 50HM from 2 hrs onwards as larger agglomerates are more prone to gravitational sedimentation (Brownian motion). However in most instances higher average particle concentration was recorded in 100HM (Figure 3.3b), but the underlying cause for such results was unclear. Therefore, there is low confidence in these data due to the large variation; further indicating poor dispersion and difficulty in obtaining accurate results when analysing powder ENPs with the NTA technique. The average particle concentration increased from 0 hrs to 2 hrs in both HMs, which raises further suspicion on data accuracy from NTA measurements. Such an increase is not justified by physical or chemical transformation of nAg under test conditions.

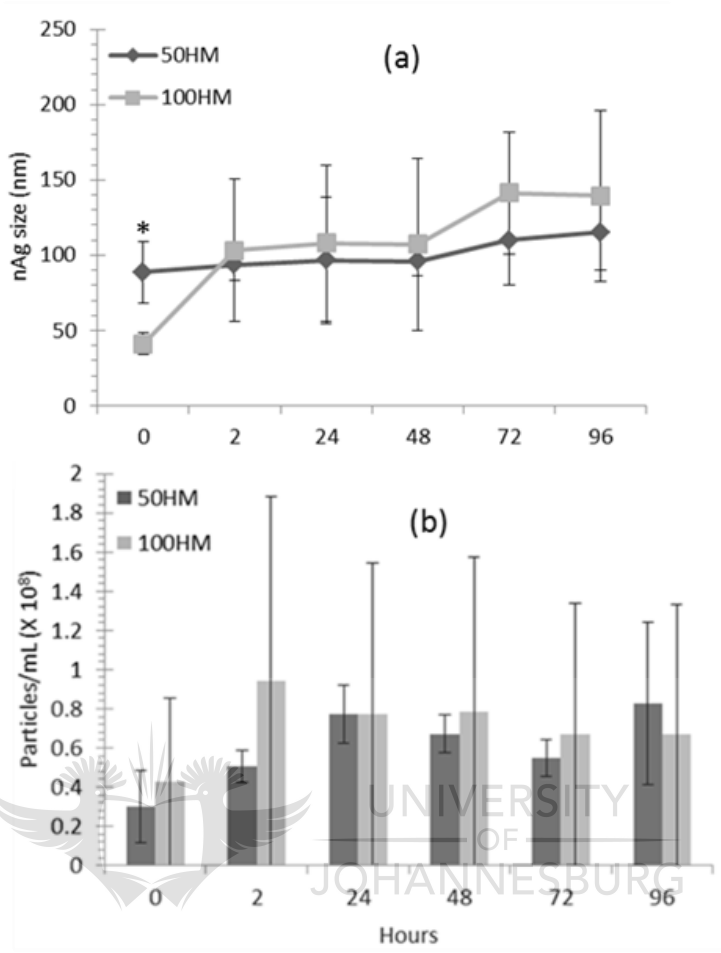

Figure 3.3: Illustration of nAg characterisation data obtained using NTA for: (a) hydrodynamic size and (b) particle per mL under test conditions for 96 hrs. Statistical difference (α = 0.05) between the two HM strengths is denoted by * where *n*=3.

3.3.2 Dissolution

Variation of test media strength altered dissolution of both ENPs as shown in Figure 3.4. For the nZnO, there was significant reduction in dissolution in higher ionic strength 100HM throughout the exposure period. A rapid initial increase of dissolution was observed after 24 hrs in each HM strength, followed by a relatively steady state until the end of the test with significant variation after 24 hrs, suggesting equilibrium state. Other studies have reported dissolution equilibrium in under 10 hrs (Majedi *et al.* 2014; Odzak *et al.* 2014) and as long as 5 days to 19 days (Odzak *et al.* 2014). Also evident was the high dissolution rate of nZnO compared to nAg where dissolution of the former was > 80% of the dosing concentration after 24 hrs and remained so until test end. In general, nZnO are highly soluble (Auffan *et al.* 2009) and high dissolution of bare nZnO forms

exhibited similar features to this study, even complete dissolution has been reported previously (Mudunkotuwa *et al.* 2012; Merdzan *et al.* 2014). Therefore findings of this study are in agreement with previous works.

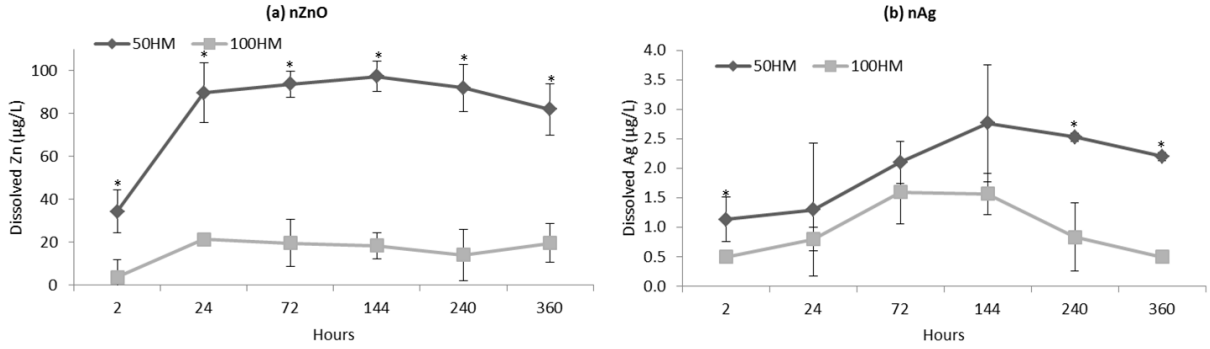

Figure 3.4: Dissolution of (a) nZnO and (b) nAg in half strength (50HM) and full strength (100HM) Hoagland's Medium as a function of time under static conditions (*n*=3). Statistical difference is denoted by * indicate a significant difference (α = 0.05) between the two HM strengths.

Similar to nZnO, dissolution of nAg was dependent on the testing medium strength where 100HM was highly inhibitive of dissolution. Dissolution of nAg was almost negligible (< 4%) compared to the dosing concentration. Such low dissolution has been reported by others (Cumberland and Lead 2009; Lee *et al.* 2012; Li and Lenhart 2012; Unrine *et al.* 2012; Chernousova and Epple 2013; Oukarroum *et al.* 2013; Yu *et al.* 2013) and is generally typical of nAg forms (Navarro *et al.* 2008; Fabrega *et al.* 2009). The poor dissolution of nAg may have resulted partly from the formation of highly stable silver complexes (particulate and dissolved) where different silver forms (Ag^0 solids, dissolved Ag^+/Ag*x*/Ag^+adsorbed) readily complexed with a variety of water constituents (dissolved and insoluble).

Examples of dissolved Ag complexes include: AgCl, $AgNO_3$, Ag_2SO_4 and Ag_2S. Furthermore, Ag solubility is highly dependent on oxidation by dissolved oxygen (Li and Lenhart 2012) and access to reactive nAg surface is necessary to initiate dissolution. Thus, higher particle surface availability can directly translate to high dissolution under oxic conditions. Similarly, oxygen is necessary to facilitate Zn solubility in aqueous media (Majedi *et al.* 2013; Omar *et al.* 2014).

The composition of HM (Section 3.2.2) indicates complex electrolytic activity. Furthermore analysis of Mg^{2+}, Ca^{2+}, $CaCO_3$ confirmed the two fold increase of media constituents from 50HM to 100HM. Thus, it is proposed that such physico-chemical difference between 50HM and 100HM accounted for the influence of testing media on nAg and nZnO dissolution observed. The

dissolution inhibition effect by 100HM compared to 50HM is explained by higher ionic strength in the former, which translates to higher ENPs coating effect (adsorption) and also higher potential for formation of silver complexes, such processes effectively reduced available ENP surface reactive sites and hence reduced dissolution (El Badawy *et al.* 2010; Jin *et al.* 2010; Li *et al.* 2010; Delay *et al.* 2011; Huynh and Chen 2011; Li and Lenhart 2012; Li *et al.* 2013).

Inhibition of nAg dissolution by higher ionic strength has been reported by comparing dissolution in deionised water and Elendt's M4 medium, where Ag^{+} release was slow in complex Elendt's M4 (Lee *et al.* 2012). Also the inhibition of nAg dissolution has been attributed to a reduction of surface area available for oxidation in complex aqueous media (Sal'nikov *et al.* 2009; Liu and Hurt 2010). Divalent species such as Mg^{2+} and Ca^{2+} have high affinity for nAg (Baalousha *et al.* 2013)- which in turn enhances coating kinetics. Similarly, dissolution inhibition for nZnO owing to testing media conditions has been reported by other investigators (Li *et al.* 2011; Reed *et al.* 2012; Majedi *et al.* 2014; Park *et al.* 2014) but with conflicting and inconsistent results at times. For instance, similar to current observations, nZnO dissolution is known to be inhibited by increasing ionic strength (Reed *et al.* 2012; Park *et al.* 2014). Yet low ionic strength medium did not yield elevated nZnO dissolution in comparison to higher ionic strength medium (Li *et al.* 2011) and in other reports nZnO dissolution was enhanced by increasing salt content (Majedi *et al.* 2014). Despite these conflicting findings, the influence of aqueous chemistry on the chemical transformation and fate of nZnO is well established.

The opposing information is probably due to differences in nZnO forms (coating, size, morphology, etc) and water quality regimes (NOM, pH, IS, etc.) used in different studies. Based on current findings and on knowledge that Class B metals possess high affinity for organic and inorganic components in the media (Lowry *et al.* 2012)- it is concluded that water quality influences dissolution of both nAg and nZnO, and increasing ionic strength inhibited dissolution of the two forms mainly as a result of electrolytes adsorbing to nAg surfaces and reducing oxidation sites. Given the test suspension pH range (6 - 6.35) and dissolved oxygen (average of 7.03 mg/L with 97.7% saturation) was constant; it is evident that the variation of ionic strength is the only influence on dissolution differences between 50HM and 100HM reported in this study.

3.4 Concluding remarks

- Uncoated powder ENPs are poorly dispersed in aqueous medium as a result of dramatic agglomeration and sedimentation, posing challenges for analytical detection and quantification. Such a situation implies that exposure estimation of this type of ENP will be highly inaccurate as dosing and actual exposure concentrations remain highly

unrelated. Therefore, it is recommended that uncoated powder ENPs are not a suitable model for investigating fate and behaviour of ENPs in aqueous environments.

- The effect increased from lower ionic strength 50HM to 100HM on nAg size was not observed by NTA analysis due to poor dispersion of the ENPs. It was expected that increasing electrolyte concentration would result in ENPs size increase, as a result of inter-particle repulsion reduction. Furthermore solubility of both ENPs was influenced by water quality alteration, where high ionic strength inhibited dissolution. Such findings confirm the high influence of ambient chemistry in fate and transport of ENPs in aqueous environments, and further illustrate that nano-pollutants' fate and effects in actual environments is highly dependent on local water regimes. Therefore severity of their implications will vary spatially. Hence it is suggested that risk assessment of nano-pollutants in aquatic resources need to be approached with consideration of site specificity.

- Based on dissolution findings; nZnO is expected to exist mostly in dissolved form and hence its interaction and toxicity will mainly be resultant from dissolved and ionic Zn forms. On the other hand, nAg is poorly soluble and is expected to mainly remain in transformed particulate form whilst dissolved components will mainly be Ag salt complexes and likely less as free Ag^{+}; hence its effects will be the result of particulate exposure.

CHAPTER 4

Fate and behaviour of nAg in deionised water and modified river water

4.1 Introduction

There is currently limited data on the bioavailability and toxicology of engineered nanoparticles (ENPs) in aquatic ecosystems (Lowry *et al.* 2012; Nowack *et al.* 2012). This is largely because there has been limited attempts to determine ENPs' fate and their movements under environmentally relevant conditions (Cumberland and Lead 2009; El Badawy *et al.* 2010; Mwaanga *et al.* 2014; Omar *et al.* 2014). This is essential because fate and implications of nano-pollutants are controlled by physical and chemical transformations of ENPs, which are partly determined by environmental conditions. For instance; ENPs' physical transformation such as size growth highly influence nanoparticle interaction with biota (Glenn *et al.* 2012; Wang and Wang 2014), and are dependent on water chemistry. For example physicochemical properties will vary between de-ionised and environmental water because of the presence of dynamic biotic and abiotic factors in the latter (Keller *et al.* 2010; Lowry *et al.* 2012; Collin *et al.* 2014).

The information gaps hamper systematic risk assessment and regulation of emerging nano-pollutants (da Silva *et al.* 2011), and also present both short and long term threats to nanotechnology sustainability. This is further compounded by challenges in detection and quantification of ENPs in environmental matrices (da Silva *et al.* 2011; Levard *et al.* 2012) whilst additional burden comes arises from the requirement of highly specialised (often costly) expertise from diverse disciplines (material sciences, chemistry, environmental science), which are often not readily available, especially in aquatic ecotoxicology (Baalousha *et al.* 2012). Notably, investigators have raised calls (Lowry *et al.* 2012) and also initiated steps towards improving environmental relevance of data generated in the field of nanotoxicology (Bone *et al.* 2012; Li and Lenhart 2012; Unrine *et al.* 2012; Xiao-hong *et al.* 2015).

Silver nanoparticles (nAg) are amongst some of the highly produced ENPs and are increasingly incorporated into commercial products (Hendren *et al.* 2011; BCC Research 2012; Yang and Westerhoff 2014). The attractiveness of nAg is attributed mainly to its highly effective antibacterial properties, and hence used in products for fabrics sterilisation, anti-odor treatments, soaps, inks, and medical imaging (Luoma 2008; Fabrega *et al.* 2011). Increasing production and use of nAg (and other ENPs) in products raises its potential for environmental release as a nano-pollutant during product use, disposal and aging (Gottschalk *et al.* 2009; 2011). For instance, ENPs can be released into environmental water resources from waste handling systems receiving from poorly treated effluents of waste water treatment plants (Musee *et al.* 2011; Chaúque *et al.* 2013) and

run-off conditions on sludge treated agricultural soils (Nowack 2009; Westerhoff *et al.* 2013; Musee *et al.* 2014).

Numerous studies have highlighted on the fate and toxicity of nAg to aquatic biota (Benn and Westerhoff 2008; Chae *et al.* 2009; Allen *et al.* 2010; Laban *et al.* 2010; Tolaymat *et al.* 2010; Fabrega *et al.* 2011; Jiang *et al.* 2012; Chernousova and Epple 2013; Oukarroum *et al.* 2013; Whiteley *et al.* 2013). However there are still persistent debates on the mechanisms of nAg toxicity in aquatic environments, where the release of Ag^{+} and other soluble forms are often postulated as basis for nAg toxicity effects. Yet a combination of ionic and nano particulate toxicity mechanism has also been suggested (Chae *et al.* 2009; Allen *et al.* 2010; Bondarenko *et al.* 2013; Chernousova and Epple 2013) and argued to be highly dependent on ENPs characteristics and aqueous media chemistry (Dasari and Hwang 2010; El Badawy *et al.* 2010; Li *et al.* 2010; Fabrega *et al.* 2011). Because natural aquatic environments are dynamic across spatial and temporal dimensions, it is suggested that in such systems ENPs undergo dynamic chemical and physical transformations. However, such conditions are not considered in investigations using simple or clean laboratory synthesized water.

Behaviour and fate of nAg in environmental waters has been investigated by very few studies. In the one study (Metrevelli *et al.* 2014), aggregation of nAg in Rhine River water was relatively similar between filtered and unfiltered water, but initial aggregation was slightly faster in unfiltered and 0.45 um filtered water compared to lower filtration levels. This suggested the influence of nAg heteroaggregation with river adsorbants. The investigators futher raised that nAg behaviour in actual environmental water is highly influenced by water properties, and the behaviour (and probably risk) is expected to vary seasonally as water composition changes. In another case (Velzeboer *et al.* 2014), sedimentation rate of nAg with different polymer coatings was studied in sediment-water systems replicating fresh, estuarine and marine environments. The rate of sedimentation was not significantly influenced by water types; however sediment flocks (suspended solids) were suggested to be the dominant fctor determining removal of nAg in suspension. Additionally; resuspension of sediment was not observed in substantial release of nAg into suspension, indicating high adsorption to sediment particles.

Therefore from the two case studies highlighted (Metrevelli *et al.* 2014; Velzeboer *et al.* 2014), the dissolution (chemical transformation) of nAg in natural water systems is yet to be investigated. Furthemore, the physical transformations have not been investigated using multi-parametric analysis, for instance not only to investigate size changes but also if such alters nAg

concentration in suspenstion. In the current study, chemical and physical transformations of citrate-coated nAg in manipulated natural river water under static conditions were investigated for 48 hours. To factor in size driven differences; 10 nm (10-nAg) and 40 nm nAg (40-nAg) were tested in modified natural river water. Modification of river water by 0.45 and 0.2 µm filtration (2-stage filtering) was done in order to minimise interference of water suspended matter during NTA analysis, and compared with deionized water. It was assumed that suspended organic particulates would probably influence the light scattering of the NTA, resulting in inaccurate readings. Furthermore, the 2-stage filtering approach was adopted to investigate if reduction of particulates influences nAg behaviour. Dissolution, particle size, and concentration of nAg were monitored over the exposure period by adopting a complementary multi-parametric approach to gain more detailed information on physical-chemical nAg transformation. In particular, the study was undertaken to probe potential fate and behaviour of nAg likely to occur in natural aquatic environments. It should be pointed out that even though environmental conditions and processes can never be fully replicated in laboratory systems, however; the study generated valuable insights on the potential state of nAg pollutants in water resources. Furthermore, the study is amongst few investigations utilising natural river water as opposed to highly simplified and clean laboratory reconstituted water as exposure media.

4.2 Materials and methods

4.2.1 Nanoparticles and characterisation

Citrate coated nAg suspensions averaged 10 nm (10-nAg) and 40 nm (40-nAg) were obtained from Sigma-Aldrich, USA (catalog 730785-25 mL and 730807-25 mL) and were stored in accordance to manufacture instructions. Prior to testing the morphology and sizes of nAg were characterised using transmission electron microscopy (TEM; JEM 2100, JEOL), whilst particle zeta potentials were measured with a zetasizer (NanoZS, Malvern). Samples for TEM were prepared by pipetting 5 µL of sample on copper grids and allowing the sample to dry at room temperature. The absorbance spectra of both particles in DI water (600 µg/L) were obtained with a UV-vis spectrophotometer (Hach DR 3900) on a 5 nm path over 320-700 nm wavelength range.

Under test conditions the Nanoparticle Tracking Analysis (NTA; NS500, NanoSight) was utilised to monitor nAg modal size during test. For the NTA analysis; a test volume of 1.5 mL was pipetted from each exposure beaker, transferred into a 1.5 mL microtube and vortexed for no less than 30 seconds before analysis. After homogenisation (vortex), the samples were immediately injected into the NTA and analysed in triplicate (each replicate analysed 3 times, each run 60 s video), where in between runs, the sample was advanced to introduce a fresh sample aliquot for

measurement. The NTA and zetasizer were further used to quantify nanoparticle concentration and zeta potentials, respectively. Total dissolved Ag as a measure of dissolution was quantified using inductively coupled plasma mass spectroscopy (ICP-MS; Agilent 7500 Series) after sample 6000 RPM ultracentrifugation with 3 kDa Amicon® filter units and 5% acidification with HNO_3.

4.2.2 Water collection and test suspension preparation

River water samples were collected from the Tweedespruit, a tributary of the Elands River situated North-East of Pretoria, South Africa (25°32'55.89" S 28°33'55.58" E). On arrival in laboratory the water was stored at 4^0C for at least one day to allow large debris to settle. The water was then filtered under pressure using 47 mm microfiber filter followed by 0.45 and 0.2 µm cellulose filters. The pH of water was then adjusted to 7 with DI water in order to avoid pH driven differences between exposures with river water and DI water, since solubility of nAg is pH driven (Fabrega *et al.* 2011). Background river water quality parameters suspected to be highly influential of ENPs behaviour, were quantified with ICP-OES and are reported in Table 4.1.

Test suspensions were made in de-ionised water (18 MΩ, DI), as well as 0.45 and 0.2 µm filtered river water dosed with 10-nAg and 40-nAg to achieve a nominal 600 µg/L nAg concentration. The approach of filtering of river water at different levels in order to investigate influence of particulate matter has been adopted previously (Metrevelli *et al.* 2014). All glassware used in experiments were pre-washed with phosphate free soap, followed by rinsing with DI water, thereafter soaked in 10% (v/v) HNO_3 for 24 hours, and then rinsed with DI water before drying. The tests were run in triplicate in 100 mL volumetric flasks for 48 hours under static non-renewal conditions. Samples for size and concentration analysis were collected every 12 hours, whereas UV-Vis samples every 24 hours whilst dissolution samples were taken only at 48 hours.

4.2.3 Data analysis

All tests were done in triplicate and data are presented as means with their corresponding standard errors. Differences between treatments were undertaken using JMP Pro version 10, α = 0.05 with the Tukey-Kramer HSD test, following normality testing with Shapiro-Wilk W Test.

4.3 Results and discussion

4.3.1 Nanoparticles and characterisation

The nAg as received were both semi- and spherical with average sizes of 9.4 nm (8.74-11.09) and 40.5 nm (36.9-42.5) for 10-nAg and 40-nAg respectively (Figure 4.1a-b); this was consistent

with manufacture information. Both nAg sizes revealed a strong surface plasmon resonance peaks at 405 and 415 nm for 10-nAg and 40-nAg respectively (Figure 4.1c). The peaks were comparable to 392 nm earlier reported for citrate-coated nAg (cit-nAg) (Baalousha *et al.* 2015), however; the loss of absorbance for 10-nAg was likely due to immediate agglomeration in DI water whilst 40-nAg remained highly stable (Figure 4.1d-e). Both nAg samples carried a negative charge of -47.93 and –40.03 mV (Figure 4.2) indicative of the citrate ions influence- an observation previously made on cit-nAg (Liu *et al.* 2010; Baalousha *et al.* 2013).

Table 4.1: Background parameters of natural river water before filtration.

Parameter	Value (stdev.)
pH	7.05-7.54 (0.15)
DOC	3.20-3.77 (0.17) mg/L
Ag	<0.005 mg/L
Na^{+}	13 mg/L
Ca^{2+}	10.67 (0.47) mg/L
Mg^{2+}	7.93 (0.05) mg/L
SO_4^{2-}	7.97 (0.17) mg/L
Cl^{-}	0.02 (0.005) mg/L

Under test conditions nAg underwent transformations, which were both nAg size and water quality dependent. For instance, it was observed that 10-nAg immediately agglomerated following introduction into DI water, but remained highly stable for the next 48 hours (Figure 4.3a). On the other hand, 10-nAg in 0.2 and 0.45 µm filtered water exposures underwent severe agglomeration resulting in sizes significantly larger than in DI water (Figure 4.3a). The agglomerated 10-nAg sizes in 0.2 and 0.45 µm filtered water remained closely related. The results clearly demonstrate a water quality influence, where agglomeration was enhanced in natural freshwater. Size analysis for 40-nAg revealed that these particles were generally stable in all water types, but original size retention was greater in DI while in freshwater they increased gradually over 24 hrs exposure and remained uniform afterwards (Figure 4.3b). Similar to 10-nAg, the results suggested the influence of water quality on 40-nAg stability. Overall, the results illustrated clear nAg size driven behaviour differences across water quality treatments (Figure 4.3c). Whilst 40-nAg sizes were closely related between different water quality regimes and with 10-nAg in DI water, however; the sizes of 10-nAg in natural freshwater were significantly larger than in all other treatments.

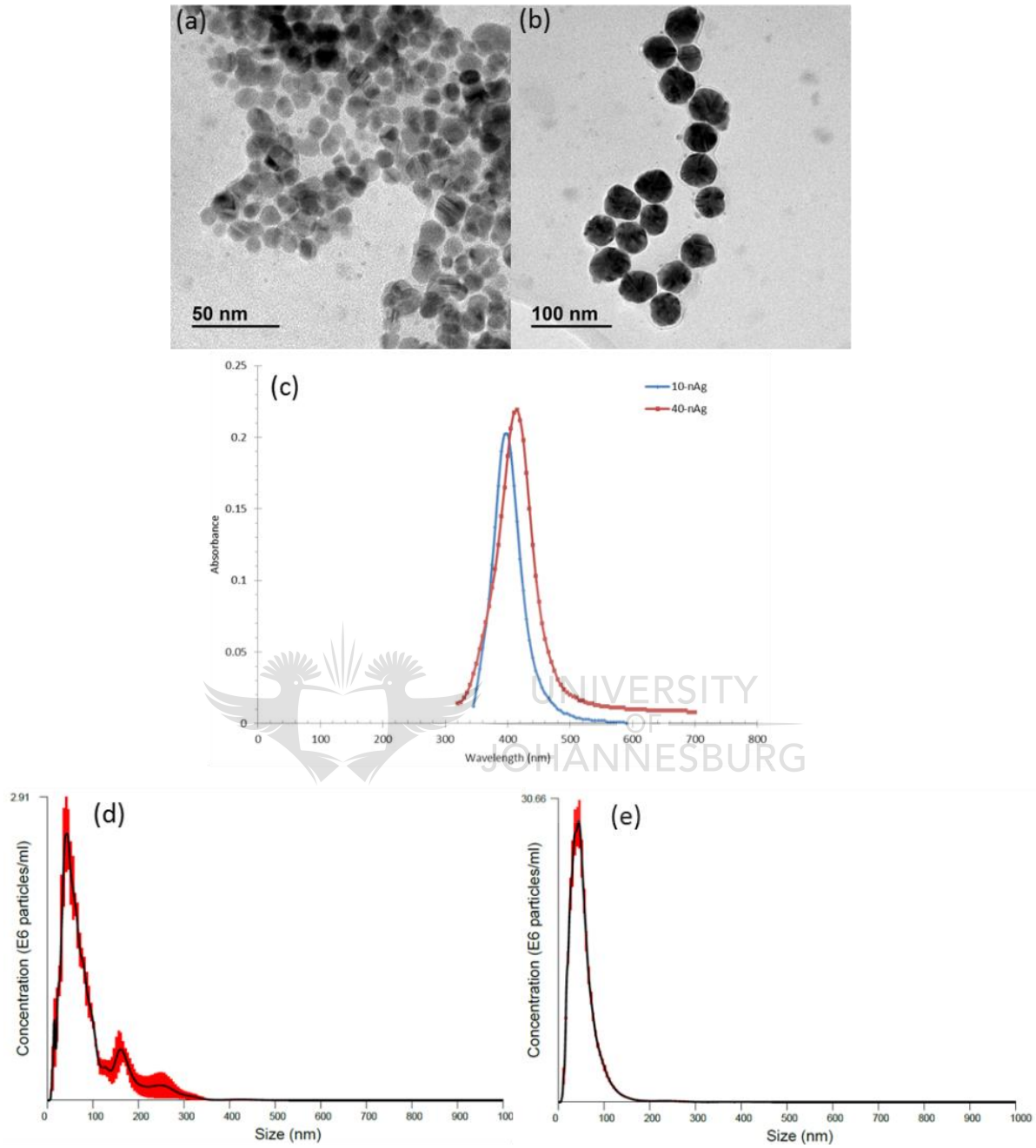

Figure 4.1: Illustrations of nAg characterisation prior testing: TEM images of (a) 10-nAg and (b) 40-nAg, (c) absorbance spectra of 10-nAg and 40-nAg as well as NTA modal sizes for (d) 10-nAg and (e) 40-nAg where red bars indicate standard error, (*n*=3).

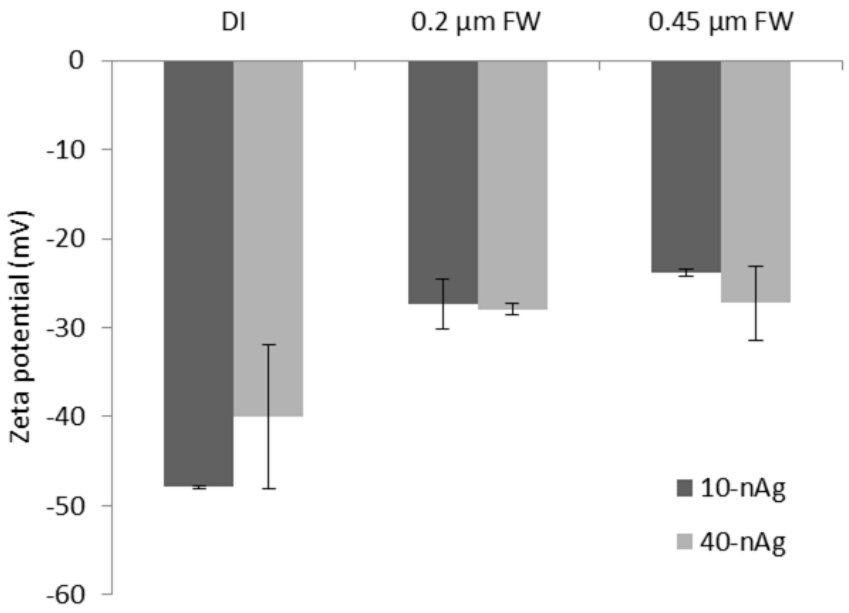

Figure 4.2: Zeta potentials of 10-nAg and 40-nAg measured in de-ionised water (DI) at 0 hours and in DI water, 0.2 and 0.45 µm filtered river water after 48 hours. Bars denote standard error (*n*=3).

Further evidence of relatively high instability of 10-nAg compared to 40-nAg was demonstrated by hydrodynamic size distribution results (Figures 4.4 and 4.5), where up to 48 hrs the 40-nAg maintained uniform and narrow size distributions across water filtration regimes unlike 10-nAg which exhibited non-uniform size growth under similar conditions. Overall, size induced differences showed that 10-nAg were more susceptible to size growth in all water regimes relative to 40-nAg. Furthermore, natural river water enhanced agglomeration (indicated by widening size distribution; Figure 4.4), more so for 10-nAg, but between different levels of filtration, the influence was not always observable (Figure 4.3, 4.4, 4.5).

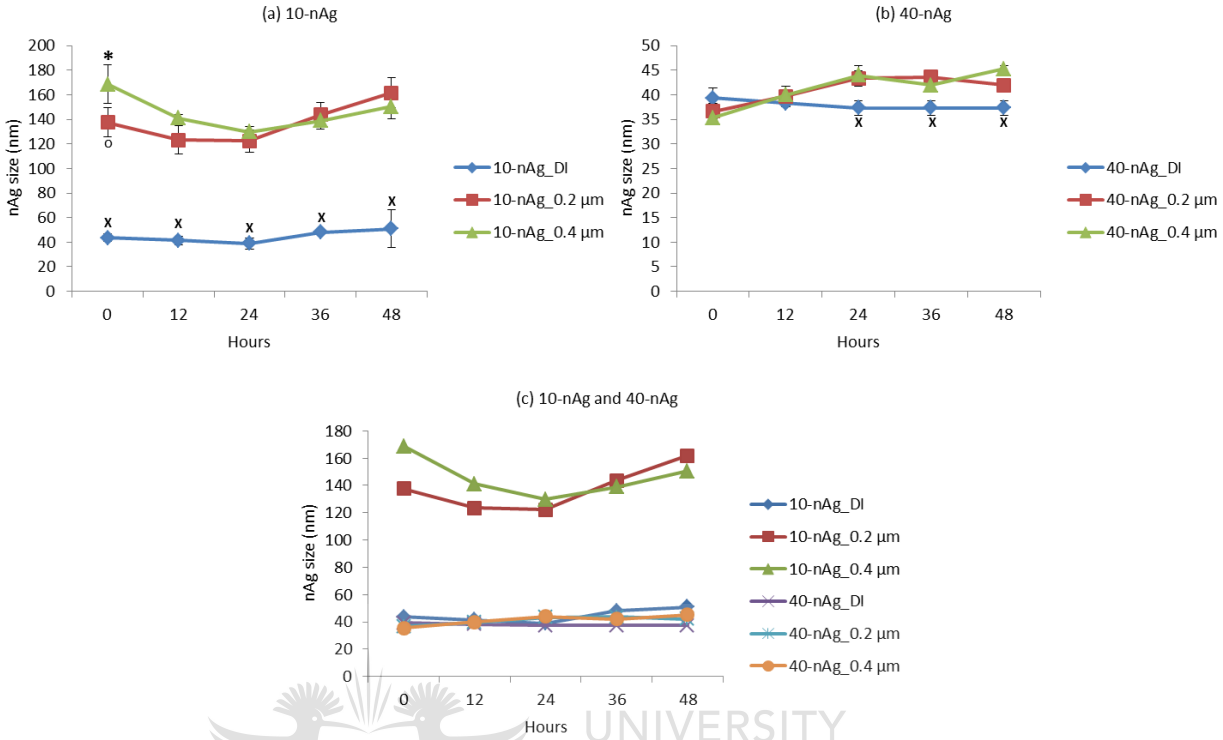

Figure 4.3: The NTA modal hydrodynamic sizes for (a) 10-nAg, (b) 40-nAg and (c) 10-nAg vs 40-nAg in DI water, 0.2 and 0.45 µm filtered river water. Bars denote standard error (*n*=3) and statistical difference between treatments is represented by differing symbols on top/below of error bars.

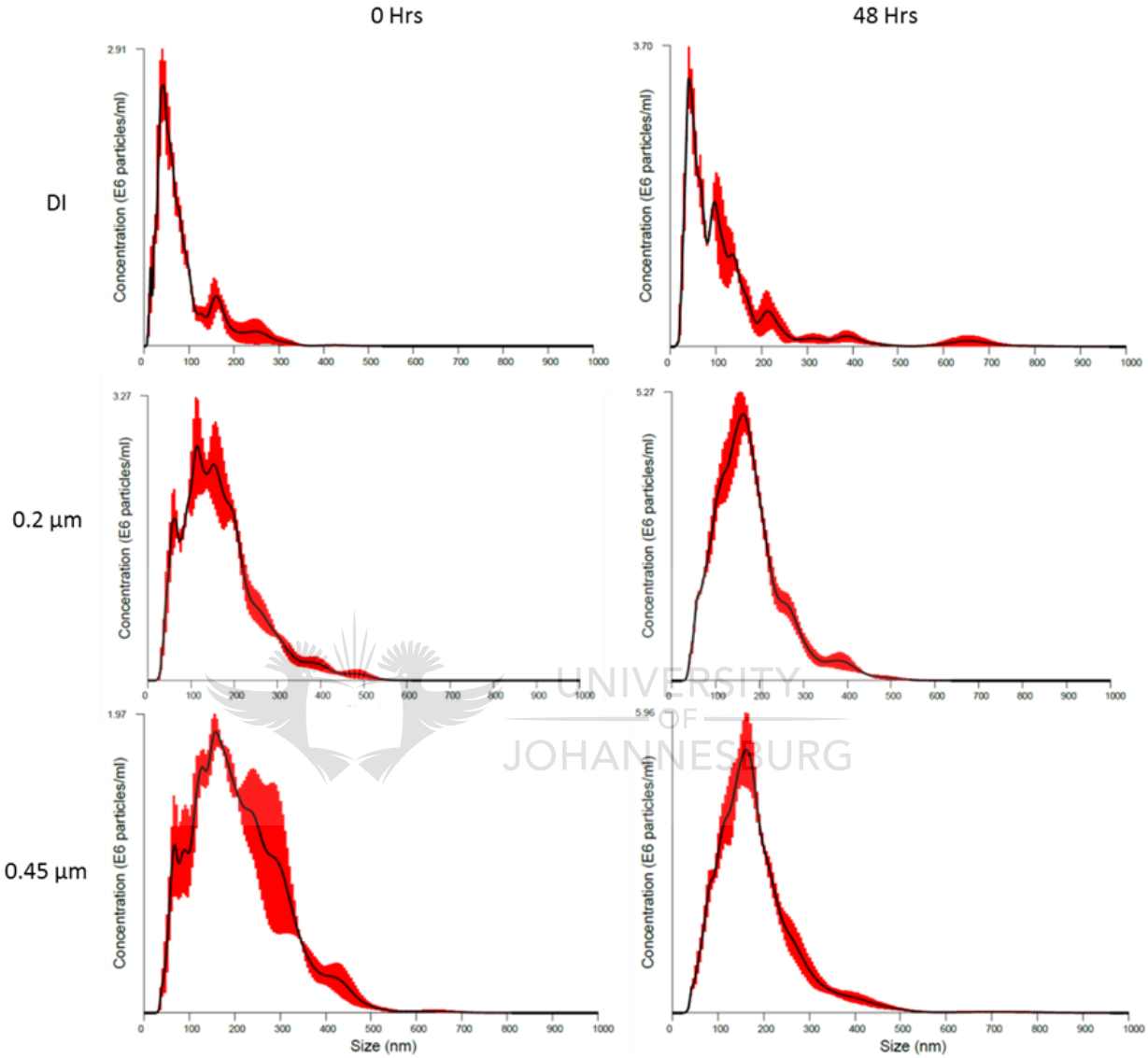

Figure 4.4: The 10-nAg size distributions obtained with NTA at 0 and 48 hours in DI water, as well as 0.2 and 0.45 µm filtered river water. Red bars indicate standard error, *n*=3.

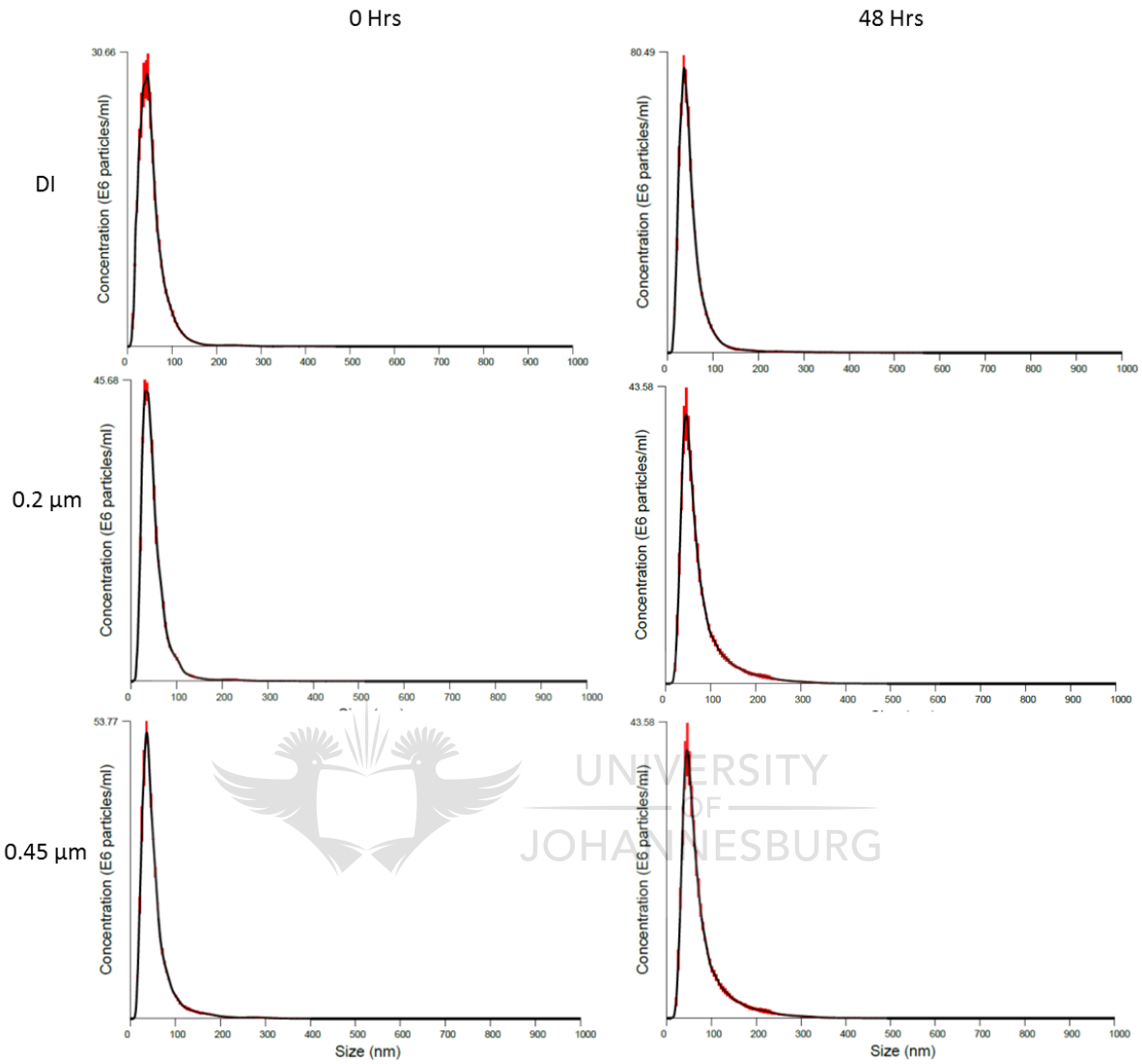

Figure 4.5: The 40-nAg size distributions obtained with NTA at 0 and 48 hours in DI water, as well as 0.2 and 0.45 µm filtered river water. Red bars indicate standard error, *n*=3.

Results suggested 10-nAg to be more reactive than 40-nAg as indicated by higher agglomeration rates for the former. Thus, the results are in agreement with widely known phenomena that smaller sized nAg (general ENPs) are more reactive than larger counterparts as a result of large surface areas and high surface atom composition which in turn translates to higher reactivity (Jolivet *et al.* 2004; Park *et al.* 2011; Zhang *et al.* 2011). Further evidence of higher reactivity and hence higher agglomeration rates of 10-nAg was observed on particle drift velocity (Figure 4.6). Average drift velocity for 10-nAg was mostly higher than for 40-nAg, except in DI water after 48 hours. The results are in agreement with Brownian motion theory and indicate 10-nAg possessed higher potential for particle collision and agglomeration compared to bigger 40-nAg. On the other hand, slow drift velocity of 40-nAg partly accounted for its higher stability across water regimes compared to 10-nAg (Figure 4.5).

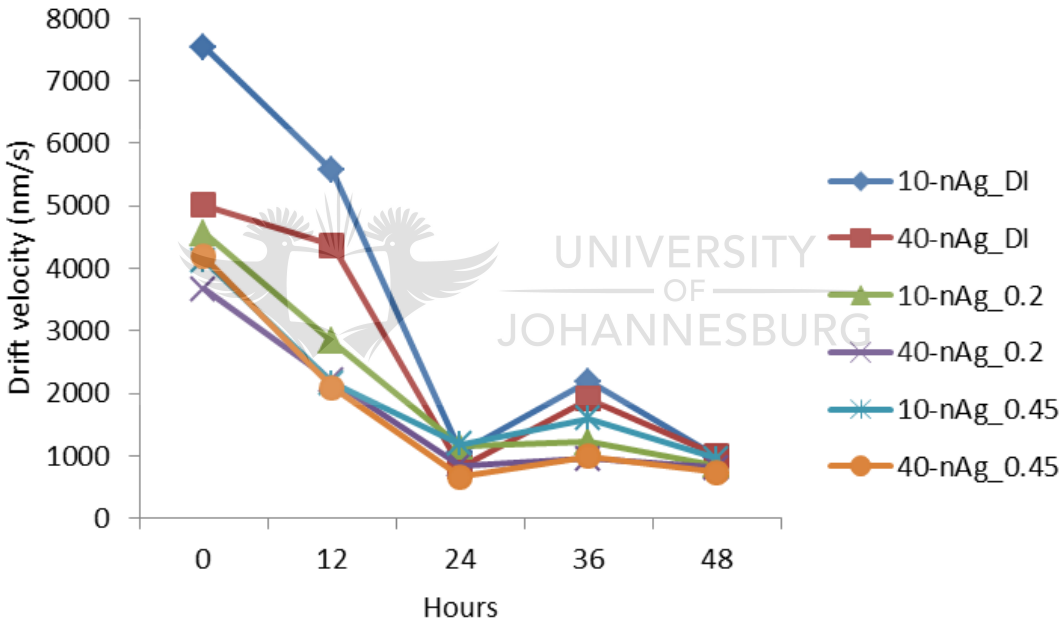

Figure 4.6: Average drift velocity of 10-nAg and 40-nAg in DI water, as well as 0.2 and 0.45 µm filtered river water, *n*=3.

As previously mentioned, the behaviour of nAg was influenced by variation of water quality, which led to size growth. In this study, size growth was postulated to be partly as a result of reduction of electrolytic inter-particle repulsion, as evidenced by difference of zeta potentials in DI and natural river water (Figure 4.2). The high negative charge of both nAg sizes in DI water was effectively reduced in river water, although after 48 hours the zeta potentials were relatively similar for the

0.2 and 0.45 µm filtered waters. The higher ionic strength of filtered water compared to DI water induced agglomeration by neutralising nAg surface charge through adsorption of various organic and inorganic composition of river water (Luoma 2008; Yu *et al.* 2013). The presence of potential adsorbents in natural river water is supported by findings reported in Table 4.1, Figure 4.7 and confirmed by TEM analysis (Figure 4.8). The presence of various electrolytes and organic matter (Table 4.1), points towards potential of river water to alter physico-chemical properties of nAg.

After 48 hours, both nAg sizes had absorbance peaks in DI water differing considerably from that of natural river water (Figure 4.7), giving further credence on the role of surface adsorbents in river water. Cations such as Ca^{2+} and Mg^{2+} greatly enhanced agglomeration through reduction of electric double layer and weakening electrostatic repulsion (Jin *et al.* 2010; Delay *et al.* 2011; Baalousha *et al.* 2013; Yu *et al.* 2013). Organic matter is also an additional factor coating nAg surfaces reducing the negative charge and inter-particle repulsion, but also improves steric stabilisation of ENPs (Cumberland and Lead 2009; Liu and Hurt 2010; Delay *et al.* 2011). Furthermore, the release of Ag^{+} (dissolution) can enhance neutralisation of nAg surface charge (Henglein 1998), however; this is unlikely at the beginning of the test as nAg dissolution is relatively slow (Zhang *et al.* 2011).

The fact that the hydrodynamic sizes of both nAg remained relatively similar in 0.2 and 0.45 µm filtration, suggested that the transformation was mainly accounted for by dissolved constituents rather than particulate matter. Further agglomeration enhancement in water was evidenced by effective reduction of drift velocity for both nAg sizes following introduction into freshwater (Figure 4.6). Overall, the observed transformations of nAg, which varied markedly between DI and natural river water illustrate the critical influence of testing water quality on ENPs fate and transport, as well as the significance of deriving such information under environmentally relevant conditions.

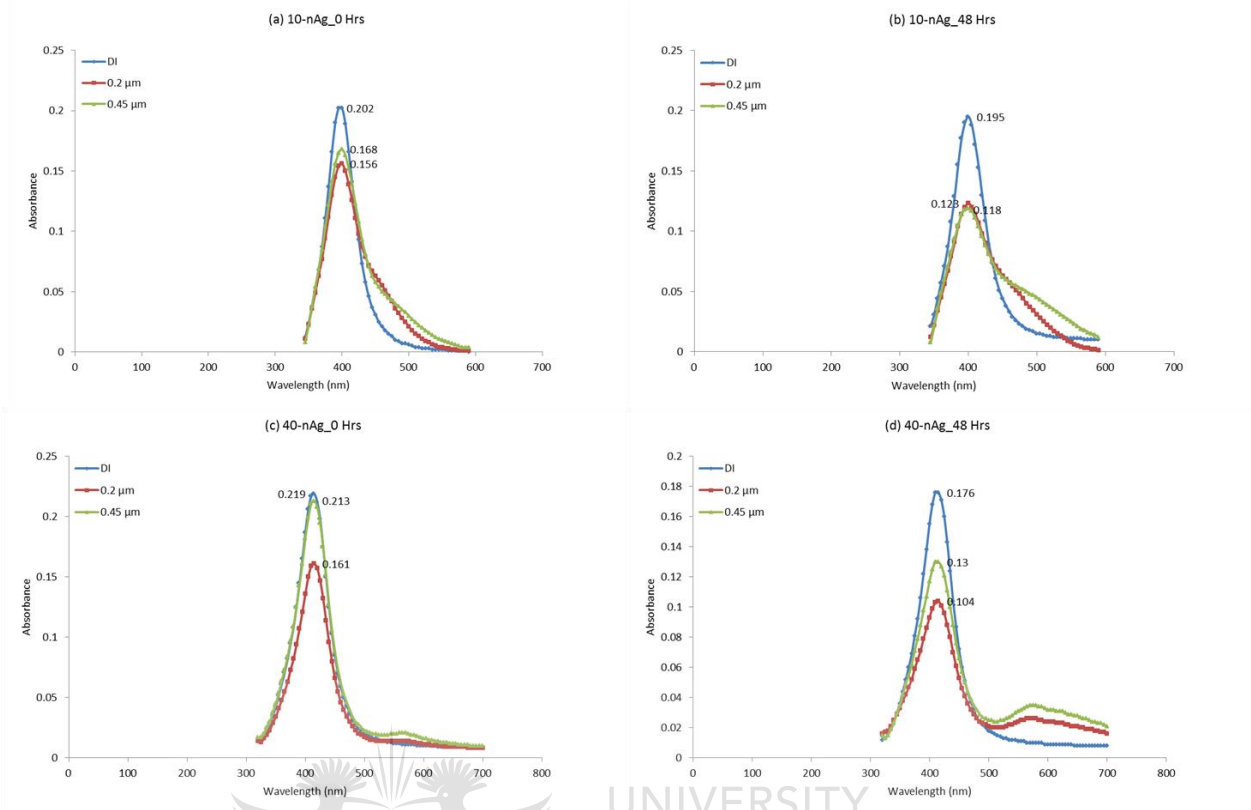

Figure 4.7: The UV-Vis spectra of 10-nAg at (a) 0 hours, (b) 48 hours and 40-nAg at (c) 0 hours and (d) 48 hours in DI water, as well as 0.2 and 0.45 µm filtered river water. Peak absorbance represented by value for each spectrum.

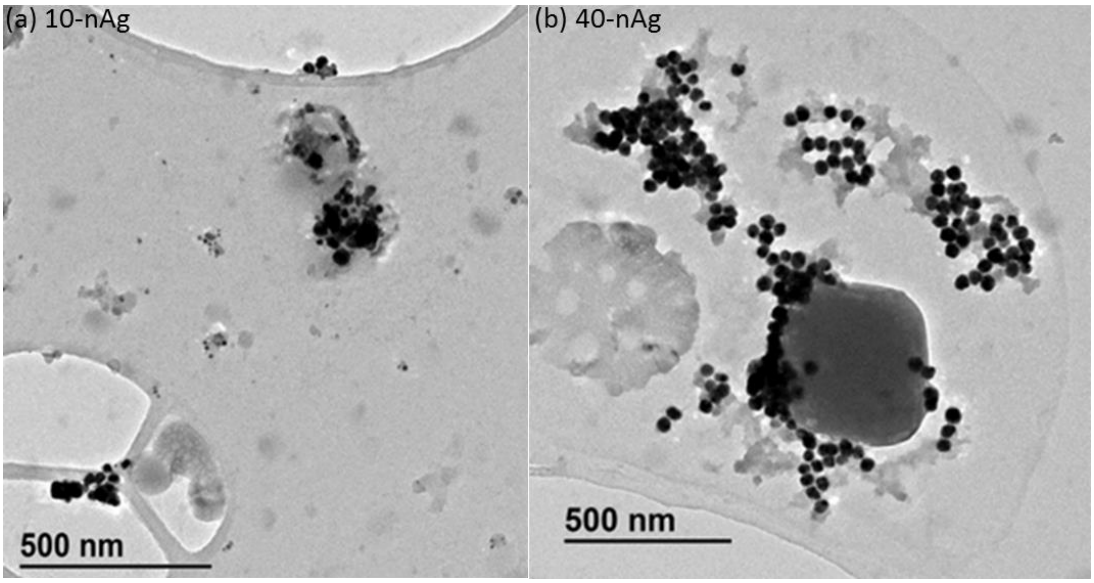

Figure 4.8: Images obtained with TEM illustrating high association of (a) 10-nAg and (b) 40-nAg with freshwater constituents (highly likely NOM) through adsorption during test.

4.3.2 Nanoparticles concentration

Particle concentration varied considerably between nAg sizes and water regimes (Figure 4.9). The concentration of 10-nAg across water treatments was remarkably lower than 40-nAg, the extent was unexpected considering the dosing concentration was the same for both nAg sizes. It is suggested that such differing observations on nAg concentration are mainly founded on NTA limitations rather than actual size induced effects. The NTA performs poorly when detecting and quantifying low-end nanoscale size particles, for both size and particle counts (Domingos *et al.* 2009; Farkas *et al.* 2010; Kittler *et al.* 2010a; Gallego-Urrea *et al.* 2011); hence it performed more favourably for 40-nAg detection in this instance. Therefore; there is little confidence in observed concentration differences between 10-nAg and 40-nAg in this instance, and therefore accurate comparison cannot be undertaken (Figure 4.9c). We suggest that 40-nAg were favourably detected because of their larger size, hence high concentrations relative to 10-nAg.

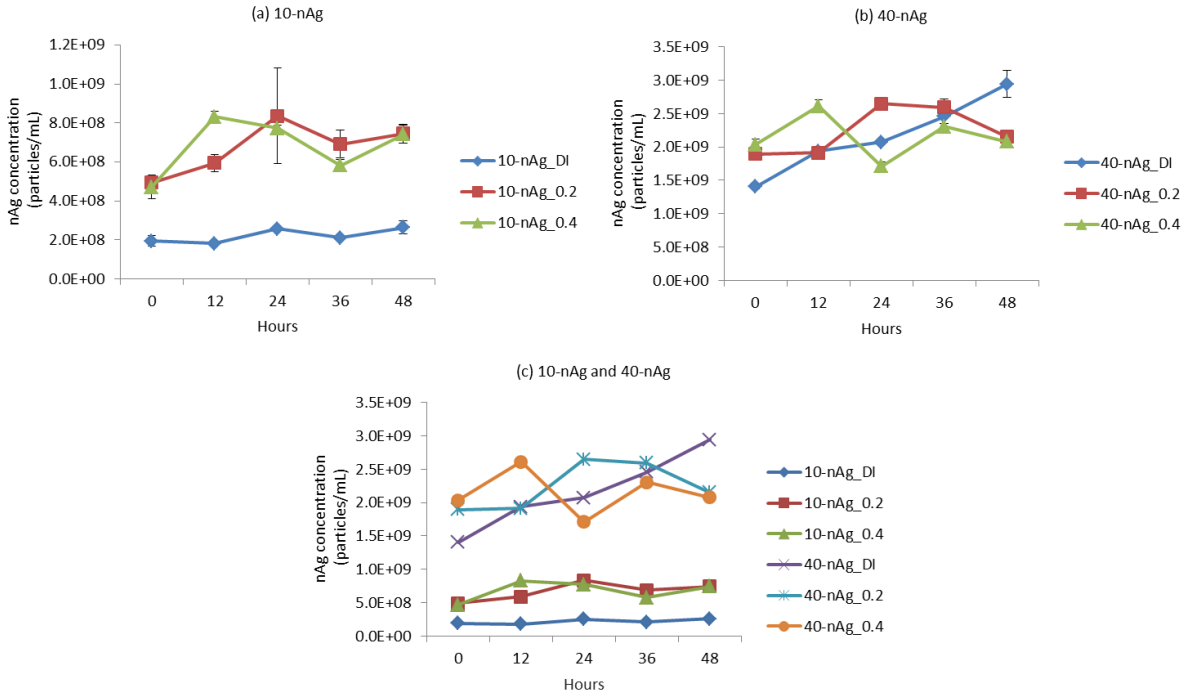

Figure 4.9: Concentration (particles/mL) of nAg in DI water, as well as 0.2 and 0.45 µm filtered river water obtained with NTA analysis for (a) 10-nAg, (b) 40-nAg and (c) comparison of 10-nAg and 40-nAg concentrations over 48 hours. Bars denote standard error (*n* = 3).

However there remains high confidence in sizing data for 10-nAg because particle counts per screen remained within NTA software acceptable levels as few counts are reported as error during video analysis. Even observable differences in 10-nAg particle concentration as a factor of water regime variation, where there were fewer particles in DI water compared to river water (Figure 4.9a), probably exist due to NTA limitations. Thus because 10-nAg agglomeration was enhanced in river water in comparison to DI water, therefore there is high likelihood that the low concentrations in DI water were only as a result of analytical limitation.

On the other hand, there was high confidence in obtained 40-nAg concentration results (Figure 4.9b). In DI water there was an overall concentration increase in 40-nAg whilst the trend was not similar and apparent in river water. Basis for such variation in river water is not understood since size remained highly uniform (Figure 4.3b), whereas size variation would have possibly influenced detection of particle numbers. Had there been size influence on concentration quantification for 40-nAg, then higher concentration values would have been obtained in natural

river water in where larger sizes were measured relative to DI water. Experience showed that NTA analysis to determine concentration of ENPs in environmental water is limited. Furthermore, the findings confirm NTA's poor detection capability of smaller ENPs (≤ 10 nm), as reported elsewhere (Domingos *et al.* 2009; Farkas *et al.* 2010; Kittler *et al.* 2010a; Gallego-Urrea *et al.* 2011). Likely the situation can be improved by coupling NTA with other techniques which are more capable in this analytical aspect, for instance, single particle ICP-MS as well as centrifugal liquid sedimentation.

4.3.3 Dissolution

Dissolution results after 48 hours are summarised in Figure 4.10. Average dissolution of 10-nAg after 48 hours was found to be 2.9, 17.63 and 1.9 µg/L in DI, 0.2 and 0.45 µm filtered river water respectively. For 40-nAg it was 3.2 and 1.1 µg/L in DI and 0.45 µm, whilst it was below 0.5 µg/L detection limit in 0.2 µm filtered river water. Overall, dissolution of 10-nAg was very low when considering the 600 µg/L nominal dosing concentration. Notably, there were even replicates below detection in DI and 0.45 µm filtered water. For the 40-nAg only in DI water were all replicates above detection limit, a single replicate in 0.45 µm filtered water, whereas all replicates were below detection in 0.2 µm filtered water. Such high occurrence of below detects challenges comparison between nAg sizes and between water treatments. However, based on dissolution averages it appears that dissolution of both sizes in DI and 0.45 µm filtered water were similar, whilst the strikingly high dissolution of 10-nAg in 0.2 µm filtered river water cannot be fully accounted for. For example, the hydrodynamic sizes of 10-nAg in 0.2 and 0.45 µm filtered river water were similar, hence differing dissolution could not be linked to size. Therefore, the typical size dependent dissolution of nAg (Liu *et al.* 2010; Park *et al.* 2011; Zhang *et al.* 2011) between 10-nAg and 40-nAg was not observed in this instance.

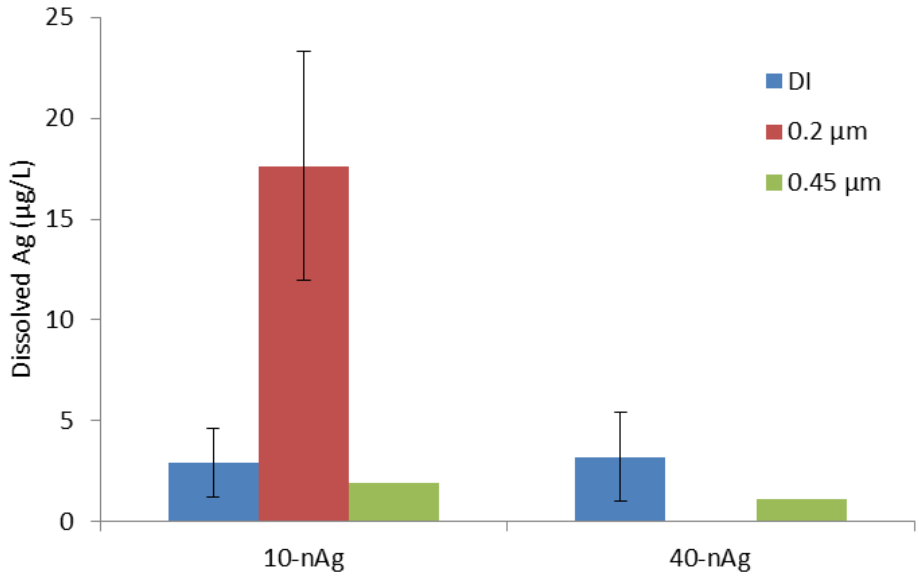

Figure 4.10: Dissolution of 10-nAg and 40-nAg as total dissolved Ag (µg/L) in DI water, 0.2 and 0.45 µm filtered river water. Bars denote standard error (*n* = 3).

Surface characteristics of 10-nAg measured as zeta potential (Figure 4.2) and absorbance spectra (Figure 4.7), do not indicate remarkable differences between the two filtering levels. Dissolution differences in river water appeared not to be founded on nAg surface characteristics. Overall, water quality characteristics effects on dissolution of both nAg sizes were not observed. However, the considerable low dissolution observed here, is typical for nAg forms (Navarro *et al.* 2008; Fabrega *et al.* 2009; Oukarroum *et al.* 2013; Yu *et al.* 2013).

4.4 Concluding remarks

- The study revealed the influential role of water characteristics in determining fate and transport of ENPs in aqueous solutions. Hence behaviour of nAg in inert DI water differed remarkable to river water, as a factor of water properties. The findings indicate the need for improved environmental realism in studies investigating fate, behaviour and effects of ENPs in aquatic systems by taking into consideration the crucial role of environmental factors and further incorporate such factors to levels manageable analytically. Efforts in that direction will assist rapid knowledge gain, to enable credible environmental risk assessment to expedite real world regulation of nano-enabled products.

- The behaviour of nAg was size dependent, further illustrating the need for detailed characterisation in fate and behaviour studies because even within nanoscale ENPs transformation is partly determined by particle size. The study revealed findings that challenge common logic: bigger hydrodynamic sizes resulted from smaller 10-nAg whilst the larger 40-nAg remained highly stable and retaining original size throughout testing period. Although the findings appear somewhat “unexpected”, they demonstrated the inverse relation between particle size and reactivity which resulted in 10-nAg forming larger agglomerates. The results are indicative of dynamic nanoscale behaviour requiring a differing set of thinking and analytical approach from regulation of bulk scale environmental contaminants. It should however be cautioned that the formation of large agglomerates by 10-nAg does not necessarily translates to reduced reactivity as small size characteristics (i.e. large surface area) within agglomerates may still be retained (Liu *et al.* 2010), and still result in higher bioaccumulation (Glenn and Klaine 2013), dissolution and toxicity (Sotiriou *et al.* 2010) by originally smaller ENPs.

- Detection and quantification of ENPs in environmental matrices remains a challenge, as demonstrated by limited ability to quantify concentration of smaller 10-nAg in this investigation. The NTA technique has brought along advances in the detection and quantification of ENPs, especially with respect to hydrodynamic size and distribution, as well as particle concentration in aqueous medium thereby enabling reporting of ENPs concentration in exposure relevant particles/mL units rather than mass/volume units. Highly advanced as it is, the NTA however experiences shortcomings under actual environmental scenarios, further demonstrating the need for complementary highly specialised and diverse analytical techniques when investigating behaviour, fate and effects of ENPs in the environment. International and national collaborations between institutions are recommended to overcome this challenge and enable access to diverse analytical techniques required in this field, because due to their costly nature cannot be expected to be housed in one laboratory or institution.

CHAPTER 5

Interaction of different sized nAg with an aquatic higher plant, *Salvinia minima* under different exposure water chemistries

5.1 Introduction

Water resources are predicted to receive increasing volumes of nano-scale pollutants arising from different life cycle phases of nano-enabled products (Kaegi *et al.* 2010; Musee 2011; Gaiser *et al.* 2012; Coleman *et al.* 2013; Musee *et al.* 2014); which has necessitated for health and safety information to protect ecological and human health. To date there has been remarkable efforts to elucidate fate, behaviour and effects of ENPs in aqueous environments (Jassby *et al.* 2012; Jiang *et al.* 2012; Wang *et al.* 2012; Yin *et al.* 2012; Oukarroum *et al.* 2013) and many reviews suggest increasing research activity in this field (Nowack 2009; Johnston *et al.* 2010a; Reed *et al.* 2012; Chang *et al.* 2012; Yu *et al.* 2013), yet, the state of knowledge remains poor owing to numerous controversial and inconsistent data. Such an information status largely arises from the dynamic behaviour of ENPs in environmental matrices and varying experimental protocols which complicates the ability to predict their chemical and physical state as well as their interaction with aquatic biota.

To protect ecological integrity from nano-pollutants more accurately and concurrently ensure nanotechnology sustainability; environmental risk assessment of ENPs is essential. This is more urgent especially for high volume produced and used ENPs such as silver nanoparticles (nAg) which have elevated potential for environmental release. Silver nanoparticles are widely incorporated in products for their favourable antibacterial properties in disinfectant sprays, for sterilisation of fabrics and air purification in vacuum cleaners and air conditioners (Benn and Westerhoff 2008; Nowack *et al.* 2012; Yang and Westerhoff 2014).

In aquatic ecosystems, plants form a critical life base in energy metabolism as producers and food source (Lahive *et al.* 2014). The vital function of aquatic plants in maintaining viable ecosystems warrants protection from potential toxic xenobiotic substances. However, increasing use of nano-enabled products raises probability for aquatic ecosystems and plants exposure to nano-pollutants; which in turn pose threat to ecological health and ecosystem services. Once in aquatic environments, ENPs undergo transformations that determine their fate, behaviour and effects. To date research on the interactions of ENPs with higher aquatic plants is still at infancy, (Kahru and Dubourgier 2010; Peralta-Videa *et al.* 2011; Miralles *et al.* 2012; Glenn and Klaine 2013; Ma *et al.* 2013; Yadav *et al.* 2014) thus poor knowledge on aspect of ENPs uptake,

accumulation and toxicity on aquatic higher plants. For instance, to date the influence of water chemistry on bioavailability of ENPs to aquatic higher plants have only been investigated for gold nanoparticles (nAu) with natural organic matter as experimental matrix variant (Glenn and Klaine 2013).

Therefore, better understanding of uptake and accumulation of ENPs by aquatic higher plants merits to be investigated as small ENPs size does not effectively guarantee internalisation (Glenn and Klaine 2013; Judy *et al.* 2012), as other factors like plant morphology, species and water chemistry exert influence. For nAg, only a single report on Ag accumulation was obtained accentuating the limited information in this aspect (Jiang *et al.* 2012). *Spirodela polyrhiza* was shown to accumulate elevated quantities of Ag when exposed to nAg compared to $AgNO_3$, suggesting possible size influence on interaction of aquatic higher plants with nAg.

Toxicity of nAg has been suggested to be size dependant towards bacteria, cellular, genetic and developmental endpoints (Sotiriou *et al.* 2010; Park *et al.* 2011). The bulk silver form is a well-known microbiocide (Schluesener and Schluesener 2013) and highly toxic to aquatic biota (Ratte 1999). In spite of increasing evidence of negative impacts associated with nAg toxicity to humans and the environment (Luoma 2008; Marambio-Jones and Hoek 2010; Fabrega *et al.* 2011), however data on nAg toxicity and ENPs in general to aquatic higher plants is very limited (Gubbins *et al.* 2011; Jiang *et al.* 2012; Kim *et al.* 2011; Oukarroum *et al.* 2013; Jiang *et al.* 2014), and hence factors that regulate bioavailability and accumulation remain largely unstudied.

In an attempt to narrow the data gap, accumulation and effects of citrate coated nAg of average size 10 (10-nAg) and 40 nm (40-nAg) were investigated on the higher aquatic plant, *Salvinia minima*. The aim was to investigate the interactive influence of nAg size and water quality properties on translocation and nAg bioaccumulation by free floating aquatic higher plants.

The investigation sought to understand potential toxicological effects induction mechanisms and nano-pollutant trophic transfer within aquatic ecosystems. Bioaccumulation of toxicants is generally a precursor and an indicator for potential effects to follow (Luoma and Rainbow 2008). Furthermore, because nAg in aqueous environments are susceptible to chemical and physical transformations, the role of exposure medium and nAg properties towards such transformations were investigated. *Salvinia minima* is a small free floating aquatic fern often establishing large populations in stagnant water resources in subtropical and tropical regions (Prado *et al.* 2010). The species was an attractive model because it can be easily maintained under laboratory, has

high growth rate, and provides sufficient plant biomass necessary for ecotoxicological assessments (Prado *et al.* 2010; Dhir *et al.* 2011). In addition, *S. minima* was suitable study specimen as it offered root biomass suitable for metal accumulation investigations unlike *Lemna* and *Spirodela* spp candidates that possess little root biomass.

5.2 Materials and methods

5.2.1 Nanoparticles and characterisation

Two sizes of citrate coated nAg suspensions, i.e. averaged 10 nm (10-nAg) and 40 nm (40-nAg) were purchased from Sigma-Aldrich, USA (catalog 730785-25 mL and 730807-25 mL) and stored on arrival at 4 ^{0}C according to manufacture specifications. Transmission electron microscopy (TEM; JEM 2100, JEOL), dynamic light techniques (DLS; Zetasizer Nano ZS, Malvern) and Nanoparticle Tracking Analysis (NTA; NS500, NanoSight) techniques were used to characterise nAg size. The DLS sizes are related to the Smoluchowski equation, in addition the zetasizer was utilised to determine zeta potential, whilst the NTA was further used to quantify nanoparticle concentration. Dissolved Ag was determined with inductively coupled plasma mass spectroscopy (ICP-MS; Agilent 7500 Series) after sample ultracentrifugation with 3 kDa Amicon® filter units and 5% acidification with HNO_3.

5.2.2 Test suspension

Moderately hard water (MHW) instead of the hydrophonic Hoagland's Medium (HM) was used as test water, so as to minimise test media influence on nAg stability (Chapter 3)- a similar strategy has been adopted by others (Prado *et al.* 2010; Miralles *et al.* 2012). The United States Environmental Protection Agency (USEPA) formulation was used to prepare MHW (Smith *et al.* 1997). To investigate the influence of test suspension chemistry on nAg interactions with *S. minima*; natural organic matter (NOM) and ionic strength (Ca^{2+}) in MHW were varied. Suwanee River NOM (IHSS, 1R101N) was used to prepare 5 mg/L NOM suspensions, whilst calcium sulphate was used to increase Ca^{2+} to 90 mg/L in MHW for the Ca^{2+} exposures. Following preparation the test suspensions were bath-sonicated (Fischer Scientific, FS30) for 30 minutes prior test initiation. The test media pH was kept at 8±0.2 in order to avoid discrepancies as a result of differing exposure pH.

5.2.3 Laboratory culture maintenance

A laboratory culture of *S. minima* was initiated with individuals obtained from the Biological Sciences Department Green House, University of Clemson, USA. The plants were transferred to Clemson University Institute of Environmental Toxicology laboratories (CU-ENTOX). On arrival plants were rinsed with tap water to remove attached debris, following culture initiation in 10% HM obtained from Sigma Aldrich (catalog number-H2395). The cultures were maintained in 10 L glass tanks in a REVCO incubation chamber at 24^0C; 16 h light to 8 h dark light dark photo period under white light at least 7 days prior to initiation of exposures to nAg.

5.2.4 Accumulation

To investigate Ag accumulation by *S. minima*, healthy individuals (non-chlorotic) were harvested from the plant cultures, blotted dry on paper towel until no water was absorbed and then 500 mg fresh weight biomass was selected for a test population per replicate. The plants were exposed to 50 mL 600 µg/L nAg suspension in 125 mL volumetric flasks for 48 hours under incubation conditions mentioned in previous section (Section 5.2.3). All exposures were triplicated. To reduce evaporation but still facilitate gaseous exchange; test vessels were covered with pierced parafilm (5 holes). After 48 hours the plants were harvested washed with distilled water and dried on paper towel for < 1 minute before weighing to determine fresh weight biomass. The roots and fronds were separated, dried at 80^0C for 4 hours in acid washed and pre-weighed 20 mL crucibles, and finally dry weight was obtained after cooling. Obtained dry biomass was ash dried at 530 ^{0}C for 14 hours in a furnace (Fischer Scientific) then digested with 250 µL HNO_3 until ash was well dissolved and finally diluted with Milli Q de-ionised (DI) water to achieve a 5% acid concentration. The resultant aqueous suspension was centrifuged at 3880 rpm for 10 minutes. Total silver in the supernatant was measured with ICP-MS and results reported as µg/mg.

5.2.5 Growth assay

The phytotoxicity of nAg on *S. minima* growth was investigated by quantifying plant biomass, before and after exposure to nAg. This was a 7 days investigation in MHW, NOM and Ca^{2+} as described Section 5.2.4. Fresh plant biomass of 350 mg was used per replicate, and all exposures were triplicated. Plants from each replicate were harvested after 7 days and fresh biomass measured after paper drying blot drying. Relative growth rate (RGR) was then determined following Hu *et al.* (2014). Growth reduction (%) was calculated from obtained RGR.

$$RGR = \frac{lnW_2 - lnW_1}{t} \quad (1)$$

where W_1 and W_2 are initial and final fresh weight (mg), and t is the incubation time (d).

5.2.6 Chlorophyll pigments assay

Furthermore, nAg influence on the photosynthetic system was investigated so as to gain insights on the energy metabolism under nAg exposure conditions. Following whole plant biomass determination in Section 5.2.5; the roots were separated from fronds, and fronds biomass obtained primarily to undertake chlorophyll pigments measurements. Immediately chlorophyll pigments were extracted using 5 mL 96% ethanol after fine homogenisation with a pestle and mortar. After centrifugation at 3880 rpm for 10 minutes, absorbance of supernatant was measured at 470, 649 and 664 nm wavelengths with an ultra violet visible spectrophotometer (Shimadzu, UV-2501PC), and pigments calculated following Lichtenthaler (1987).

Formulas as were as follows:

$$Chl_a = \frac{(13.36\ A664 - 5.19\ A649)8.1}{FW} \quad (2)$$

$$Chl_b = \frac{(27.43\ A649 - 8.12\ A664.2)8.1}{FW} \quad (3)$$

where Chl *a* and Chl *b* stand for chlorophylls *a* and *b* respectively.

5.2.7 Data analysis

All tests were conducted in triplicate and data are presented as means with their corresponding standard errors. Differences between treatments were undertaken using JMP Pro version 10, α = 0.05, following normality testing with Shapiro-Wilk W Test. The Student's t-test was used between two treatments whilst for more than two pairs the Tukey-Kramer HSD was applied. Furthermore, JMP Pro was used for principal component analysis (PCA).

5.3 Results and discussion

5.3.1 nAg characterisation: before testing

The sizes of nAg before adding to exposure medium were obtained in DI water using TEM, NTA and DLS analytical techniques. Size from TEM images averaged 8.8 nm (6.5-12.6) and 41.45 nm (35.72-47.9) for 10-nAg and 40-nAg, respectively (Figure 5.1a, c). The NTA modal particle size were 34.6 nm (31-38), and 47.67 nm (46-49) for 10-nAg and 40-nAg respectively (Figure 5.1b, d), whilst DLS measurements revealed averages of 40 nm (33.6-44.4) and 56.71 nm (52.5-60.21) for 10-nAg and 40-nAg respectively. The measurements obtained from the three techniques were reasonably comparable but slight discrepancies were expected owing to differences size derivation variation between the techniques.

For instance, TEM measures dry physical size whilst DLS and NTA are light scattering techniques that measure hydrodynamic size. The DLS tends to exhibit bias towards large size fractions, but the NTA overcomes such limitation by tracking individual particles at different sample positions (Cumberland and Lead 2009; Hole *et al.* 2013; Nickel *et al.* 2014). Analysis with DLS and NTA revealed immediate agglomeration in both nAg samples after introduction into test media, with smaller 10-nAg reflecting higher agglomeration rates than 40-nAg. It is assumed such phenomenon is illustrative of relative higher reactivity of smaller sized 10-nAg because they possess larger surface area and higher surface atom composition (Jolivet *et al.* 2004; Auffan *et al.* 2008; 2009; Park *et al.* 2011). Furthermore, average drift velocity for 10-nAg and 40-nAg were 1687 and 1338 nm/s respectively; which further points to higher reactivity for 10-nAg compared to 40-nAg.

Both nAg sizes were negatively charged in DI water with zeta potentials determined as -47.93 mV and -41.33 mV for 10-nAg and 40-nAg respectively (Figure 5.2). The results reflected the influence of citrate anions and are in agreement with earlier findings for citrate stabilised nAg (Liu *et al.* 2010; Baalousha *et al.* 2013), and because of such high charge (high repulsion) were considered highly stable (Pamies *et al.* 2014).

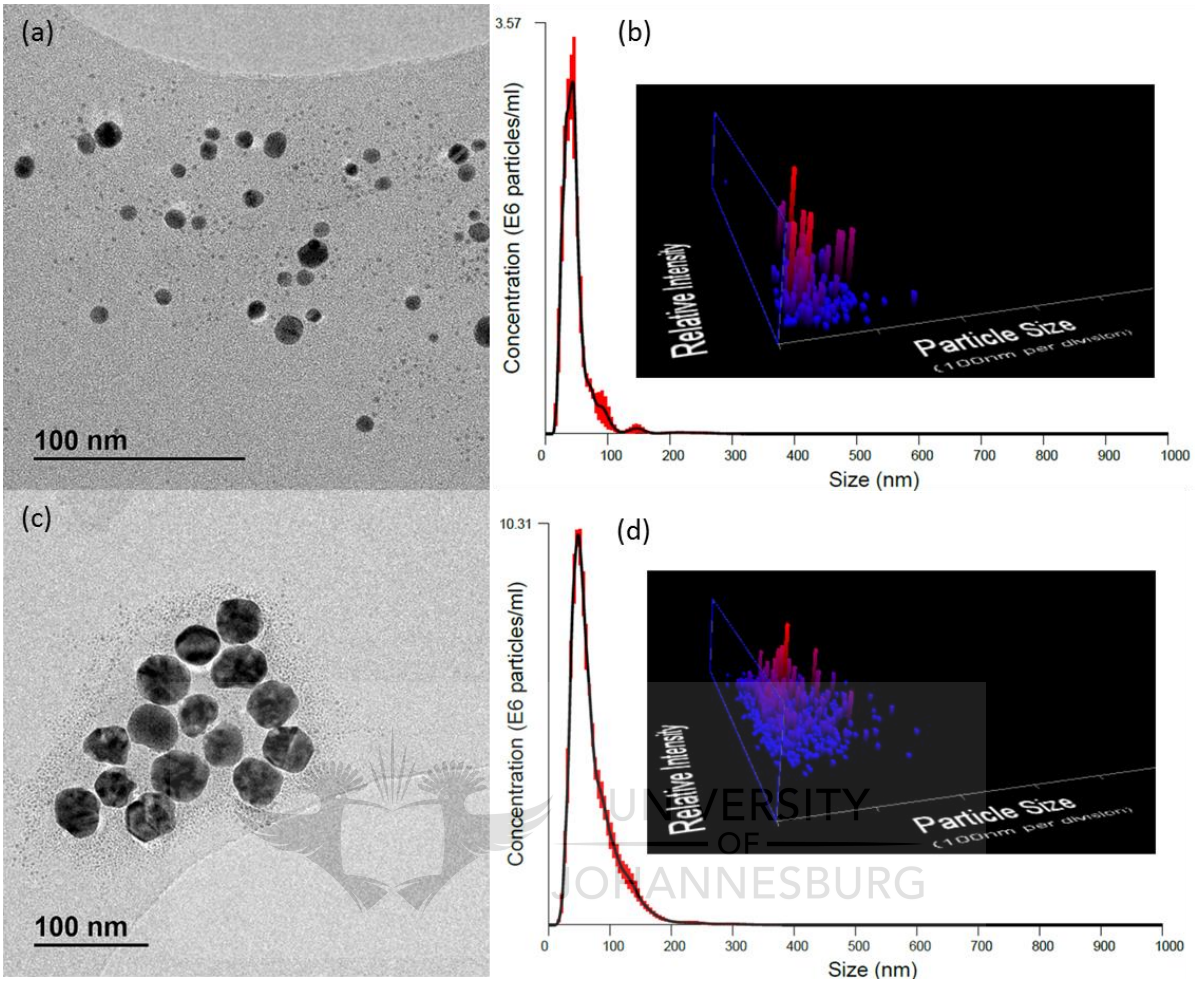

Figure 5.1: Sizes of nAg in DI water obtained before experimental exposures: (a) TEM image for 10-nAg and (b) NTA measurements for 10-nAg (red bars indicate standard error) (c) TEM image for 40-nAg and (d) NTA measurements for 40-nAg (red bars indicate standard error). Inserts in (b) and (d) illustrate relative nAg size intensities obtained with NTA.

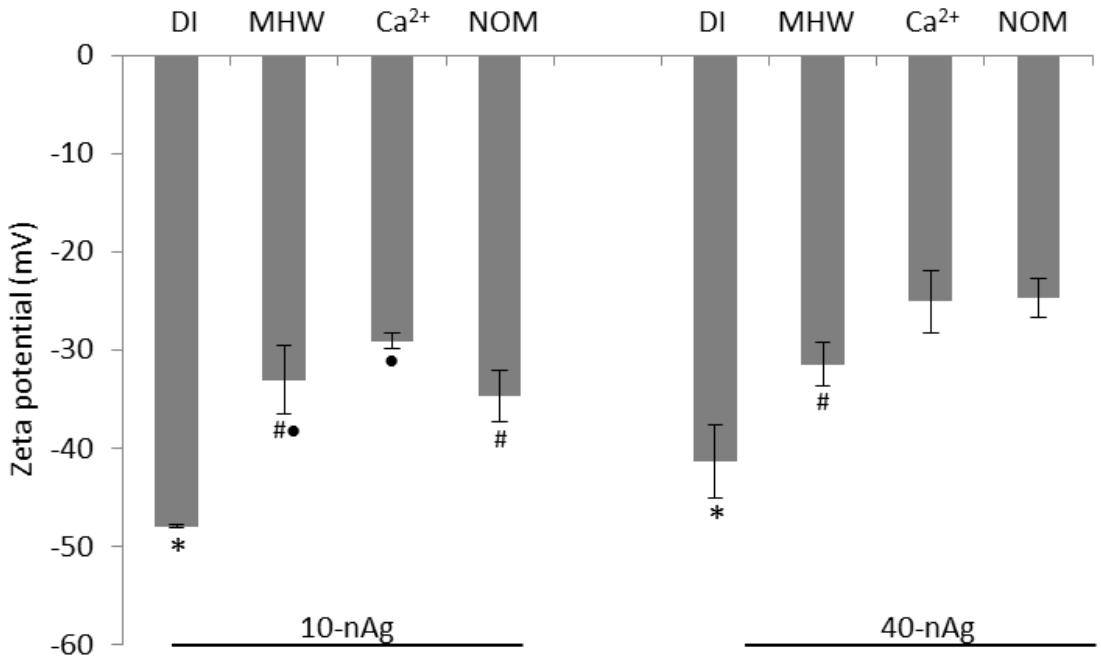

Figure 5.2: Zeta potentials of nAg measured in DI water at 0 hours and in MHW, NOM and Ca^{2+} water variations after 48 hours. Bars denote standard error (*n*=3). Differing symbols on top of error bars indicate statistical difference between water treatments within a single nAg size. Turkey Kramer HSD, $p < 0.05$.

5.3.2 nAg characterisation: during exposure period

To gain better understanding on nAg stability under different test conditions; zeta potential, size and concentration were monitored every 24 hrs over the 48 hrs exposure period. This was to estimate plausible nAg exposure dynamics towards the plants, and also how it relates to Ag bioaccumulation and effects observed following introduction of nAg into various water treatments (MHW, NOM, Ca^{2+}). The measurements were undertaken in experimental vials that did not contain the plants. All water treatments effectively reduced nAg zeta potentials (Figure 5.2), but the neutralising effect in Ca^{2+} was most prominent on 10-nAg but similar to 40-nAg in NOM. The effect is reflective of increased electrolyte composition in comparison to inert DI water conditions.

For instance, the coating effect of cations such as Ca^{2+} and Mg^{2+} neutralises the surface charge of citrate coated nAg and compresses the electric double layer (repulsive forces), and as a result enhances agglomeration (Delay *et al.* 2011; Baalousha *et al.* 2013). The coating effect of NOM and other organics shields the negative charge of nAg, an effect suggested to improve ENPs

stability through steric and charge stabilisation (Cumberland and Lead 2009; Liu and Hurt 2010; Delay *et al.* 2011). Furthermore, the reduction of surface charge across water treatments can also be accounted by partial release of Ag^{+}, which then adsorbs to nAg surfaces additionally neutralising the negative charge (Henglein 1998). Results on dissolution reported in later sections further added credence to this suggestion.

The effect of inter-particle repulsion compression was evident in observed nAg size transformation, in form of agglomeration (Figure 5.3). The sizes of 10-nAg in MHW and Ca^{2+} after 48 hours were larger than in NOM (Figure 5.3a). In fact, 10-nAg size remained relatively invariant over 48 hours, suggesting effective size stabilisation by NOM. The stabilising effect of NOM was more apparent on 40-nAg, whereby the size remained similar up to 48 hours and differed to MWH and Ca^{2+} treatments where in the latter treatments 40-nAg effectively agglomerated (Figure 5.3b). Additional evidence of NOM stabilising effect was observed based on concentration results in a given treatment.

The concentration of 10-nAg in NOM differed from other treatments (Figure 5.3e) because of the NTA's (NS500) limited analytical capability in detecting lower end sizes, hence nAg concentration in NOM was lowest, whilst due to agglomeration in MHW and Ca^{2+} nAg detection improved, and therefore higher concentrations were observed for the latter treatments. The poor detection of 10-nAg was even observable on overall concentration results whereby 10-nAg concentration were often lower than for 40-nAg although the dosing concentration was similar for both sizes. Conversely; 40-nAg highest concentrations were obtained in NOM, and appears highly related to size results (Figure 5.3f) thereby suggesting that in MHW and Ca^{2+} where 40-nAg underwent agglomeration, there could have been particle exposure loss due to sedimentation, however, in NOM the particles were highly stable as evidenced by higher detection. More evidence of NOM stabilising effect was observed for 40-nAg in form of narrow size distribution over 48 hours (Figure 5.5e, f), whilst in other water treatments the distribution widened.

Increasing Ca^{2+} concentration appeared to improve the stability of 10-nAg, as evidenced by narrow size range compared to other water treatments (Figure 5.4). However, it was most destabilising for 40-nAg (Figure 5.5). Such stabilisation was contrary to expectations based on Ca^{2+} effect of inter-particle repulsion reduction (Delay *et al.* 2011; Baalousha *et al.* 2013). In fact the stabilising effects of NOM and Ca^{2+} clearly varied between nAg sizes; notably Ca^{2+} had better stabilisation 10-nAg but poor with 40-nAg, and conversely, NOM was superior in stabilising 40-nAg but poor with 10-nAg. Such opposing stabilising trend between Ca^{2+} and NOM remains

unclear, but likely exists as result of size driven behaviour differences (chemical/physical). Interestingly, larger agglomerates were generally observed from 10-nAg compared to 40-nAg as depicted by both DLS (Figure 5.3c-d) and NTA results (Figure 5.3a-b). Although the results appear to oppose “common expectation”, they however can be accounted for and further illustrate unique size driven behaviour changes at nanoscale under different water chemistries.

First, as suggested in earlier (Section 5.3.2); higher reactivity of 10-nAg can be associated with larger surface area compared to 40-nAg (Jolivet *et al.* 2004; Auffan *et al.* 2008; 2009; Park *et al.* 2011) likely enhanced the agglomeration rate for 10-nAg. Secondly, superior reactivity of 10-nAg was evidenced by particle drift velocity where it averaged 1687 nm/s for 10-nAg compared to 1338 m/s for 40-nAg. Such data accounts for the higher agglomeration of 10-nAg an effect observed on NTA videos (videos not shown) where 10-nAg frequently collide with one another and agglomerated at a faster rate.

The NTA size distributions of 10-nAg in NOM remarkably differed from other water treatments which raised the possibility that suspended organic matter rather than 10-nAg agglomerates may have influenced the observed wide and polydispersed distributions. Here it is argued that this may not be the case because such an effect was absent for 40-nAg in NOM treatment, and therefore, the stabilising effect of NOM on nAg was probably size dependent. However, this needs to be regarded with caution since even though agglomeration destabilises ENPs; possibility of superior reactivity of smaller forms may remain unaltered (Liu *et al.* 2010). For example, reactivity retention was apparent with 10-nAg as to be shown under dissolution, bioaccumulation, and toxicity effects studies.

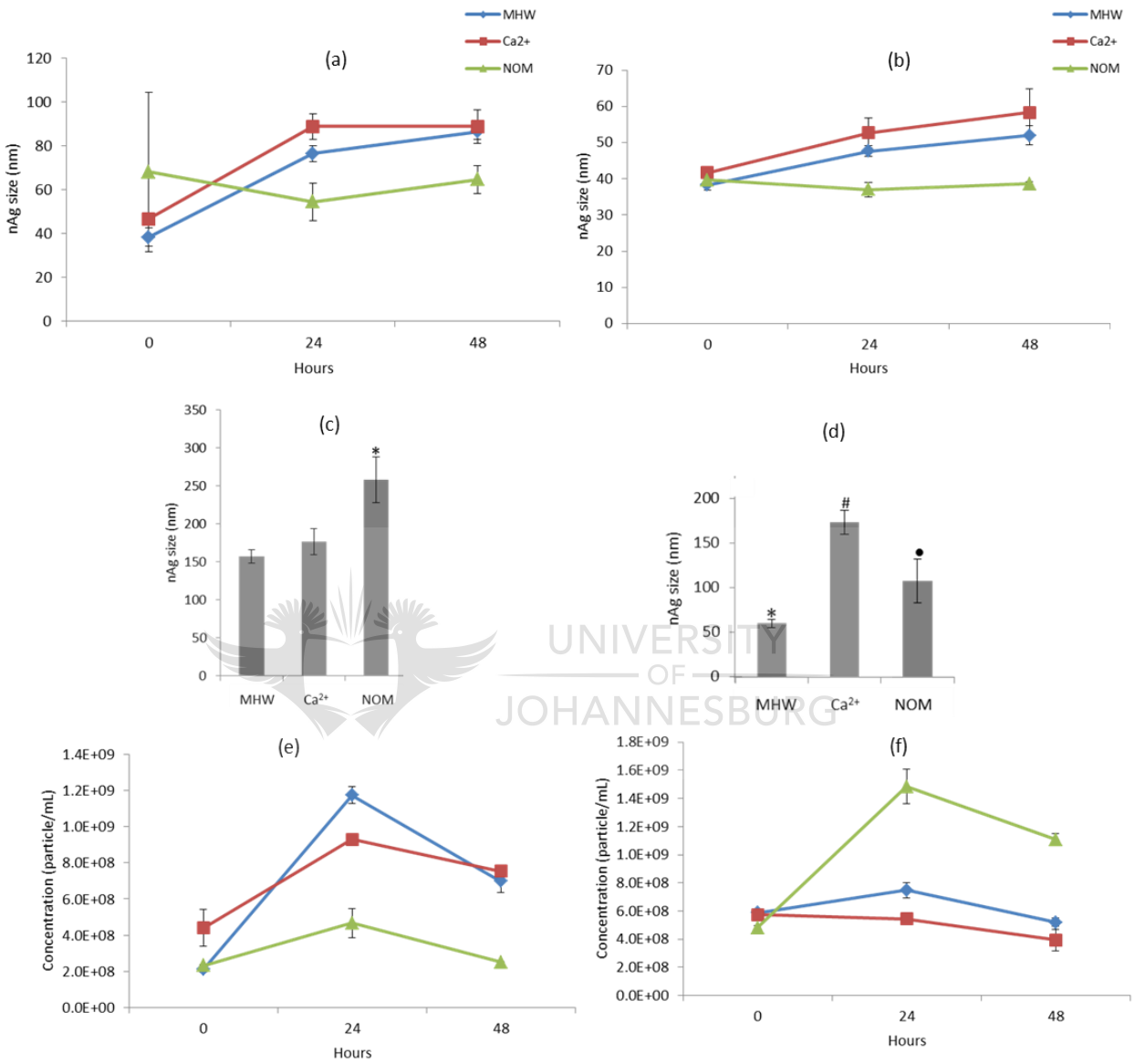

Figure 5.3: Illustrations of nAg modal particle size as well as concentration under test conditions. Modal particle size obtained with NTA for: (a) 10-nAg and (b) 40-nAg; average particle size obtained with DLS after 48 hrs for: (c) 10-nAg and (d) 40-nAg; as well as concentration over 48 hours for: (e) 10-nAg and (f) 40-nAg. All measurements undertaken in MHW, Ca^{2+} and NOM water variations. Bars denote standard error (n=3). Differing symbols on top of error bars indicate statistical difference within n-Ag size. Turkey Kramer HSD, $p < 0.05$.

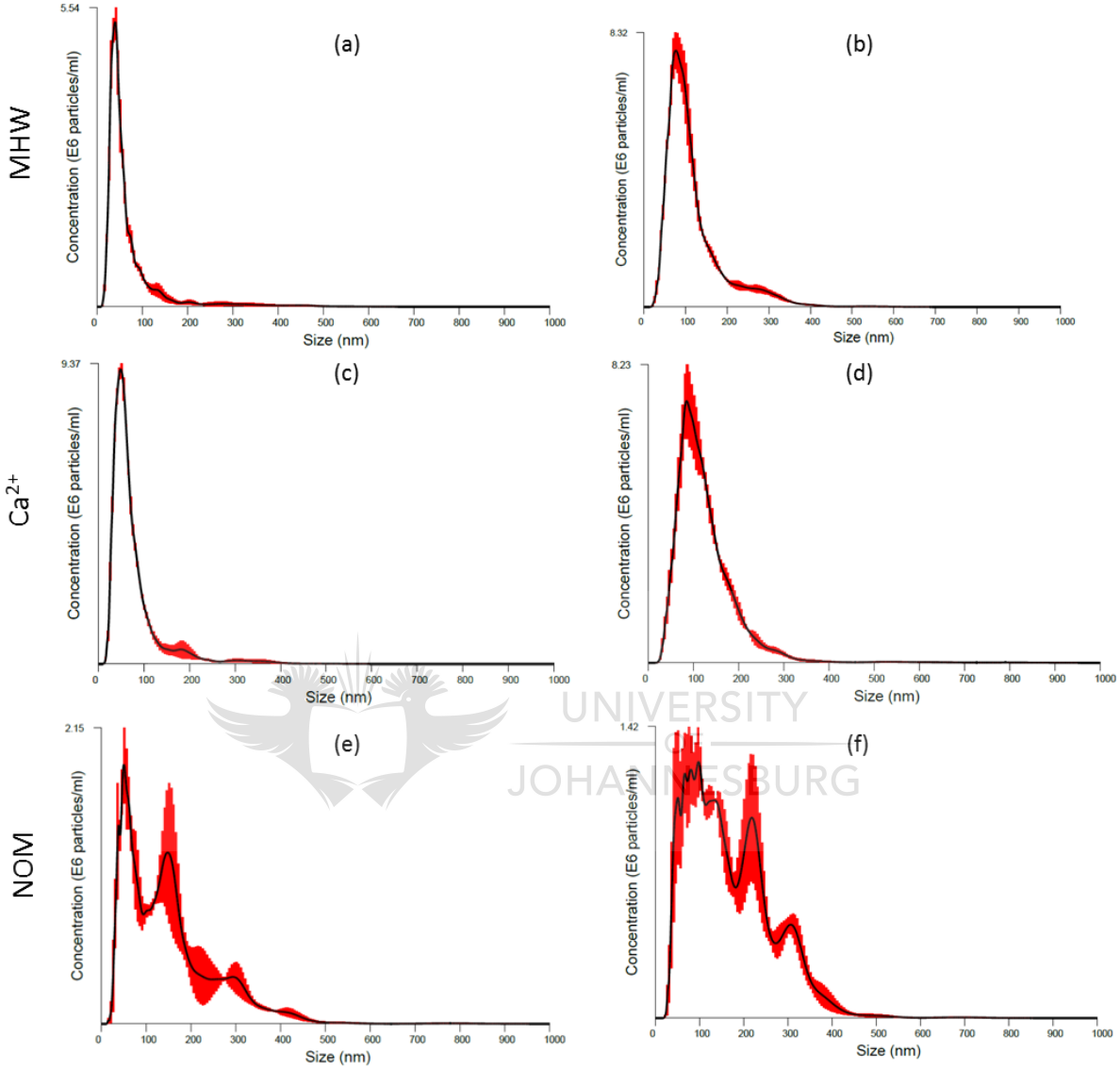

Figure 5.4: Size distributions obtained with NTA for 10-nAg in MHW: (a) 0 hrs, (b) 48 hrs; in Ca^{2+}: (c) 0 hrs, (d) 48 hrs; in NOM: (e) 0 hrs, (f) 48 hours. Red bars indicate standard error, *n*=3.

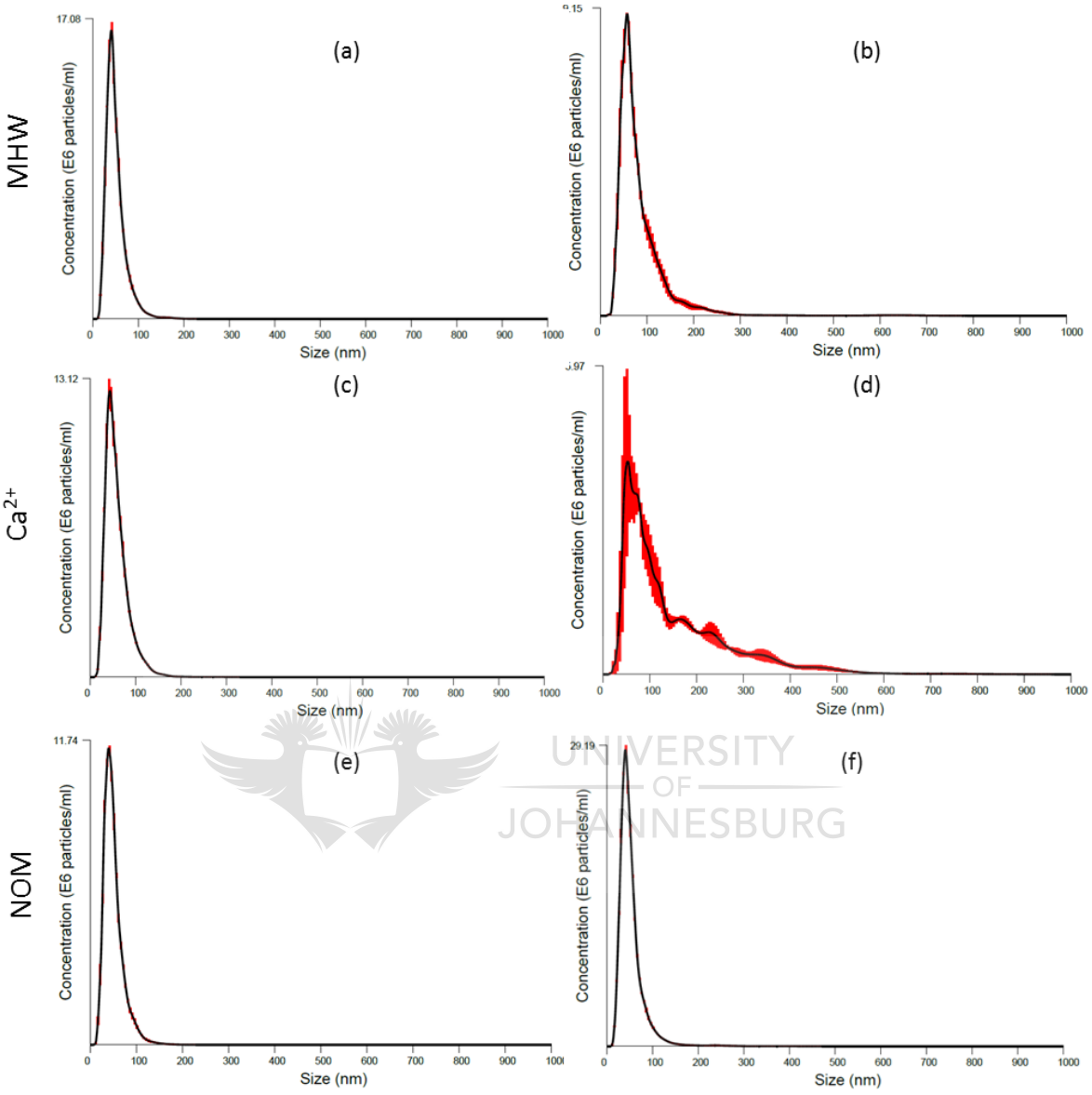

Figure 5.5: Size distributions obtained with NTA for 40-nAg in MHW: (a) 0 hrs, (b) 48 hrs; in Ca^{2+}: (c) 0 hrs, (d) 48 hrs; in NOM: (e) 0 hrs, (f) 48 hours. Red bars indicate standard error, *n*=3.

5.3.3 Dissolution

Dissolution of nAg is critical driver of dissolved Ag uptake (e.g. Ag^{+}, AgX, Ag^{+}adsorbed), bioaccumulation, and effects in aquatic environments (Fabrega *et al.* 2011). Even though nAg solubility is typically slow (Navarro *et al.* 2008; Fabrega *et al.* 2009) studies have shown the slow but constant release of dissolved Ag can translate to higher Ag bioaccumulation and toxicity effects over time (Hwang *et al.* 2008; Miao *et al.* 2009). For instance, aquatic plants can have

higher uptake rates for Ag^{+} compared to nAg (Jiang *et al.* 2012). It should be noted that in this chapter dissolution refers to total dissolved Ag without distinguishing between various species of dissolved Ag species (e.g. Ag+, $AgCl^{2-}$ and $AgCl_3^{2-}$).

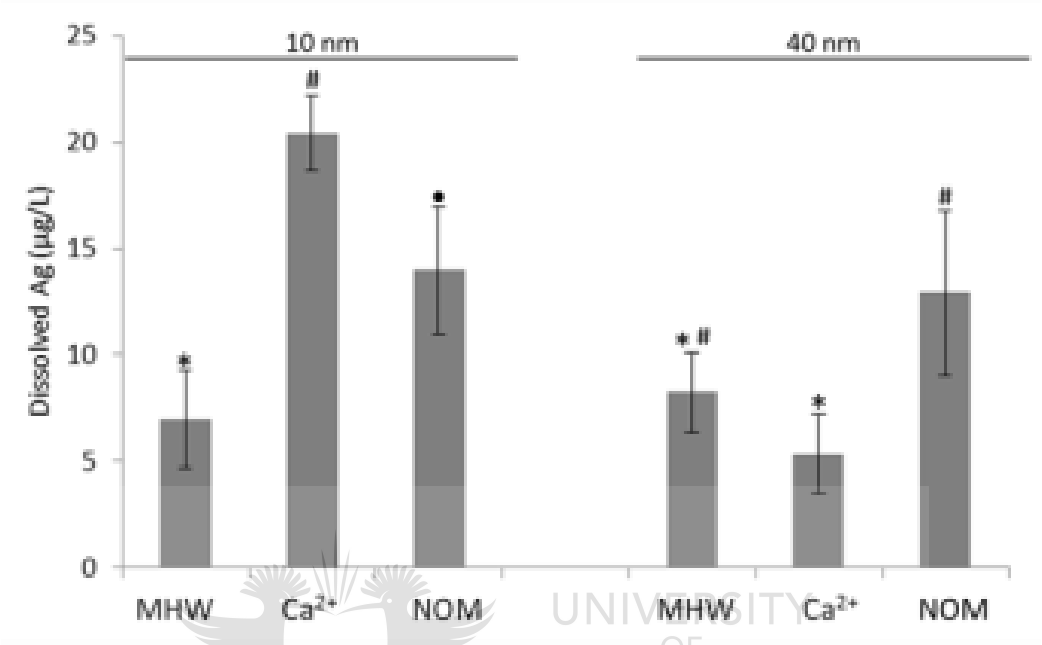

Figure 5.6: Dissolution of nAg as a factor of size and across water quality treatments after 48 hours. Bars denote standard error (*n*=3). Differing symbols on top of error bars indicate statistical difference within n-Ag size. Turkey Kramer HSD, $p < 0.05$.

Dissolution of nAg was size dependent in Ca2+, whereas in other exposures dissolution did not differ significantly (Figure 5.6), which is typical of nAg (Ho *et al.* 2010; Liu *et al.* 2010). In MHW, average dissolution of 40-nAg (8.23 µg/L) was higher than that of 10-nAg (6.96 µg/L). In Ca^{2+} treatment, dissolution was 20.4 and 6.96 µg/L for 10-nAg and 40-nAg respectively. Finally in NOM the dissolution was 13.96 and 12.9 µg/L for 10 nm and 40-nAg respectively. Furthermore, 10-nAg dissolution statistically differed across water chemistries being lowest in MHW, and highest in Ca^{2+} (Figure 5.6). A different trend was observed for 40-nAg dissolution being lowest in Ca^{2+}, and highest in NOM treatment (Figure 5.6). These findings point to plausible synergistic influence of nAg size and water variation on dissolution due to non-uniformity per nAg size across water treatments.

The relatively higher dissolution of smaller 10-nAg compared to larger 40-nAg, observed in Ca^{2+}, was not surprising. The 10-nAg are expected to possess higher surface area than the bigger 40-nAg, hence 10-nAg being soluble as a result of higher exposed surface fraction for oxidation (Sotiriou and Pratsinis 2010). Size reduction enhances particle curvature and reactivity which facilitate higher dissolution rates (Hannemann *et al.* 2006; Lok *et al.* 2007). Such accounts can explain the observation of relatively higher dissolution of 10-nAg in Ca^{2+}. Of interest is that 10-nAg had higher agglomeration rates (based on higher reactivity) relative to 40-nAg (Figure 5.3a, b). Despite 10-nAg forming larger agglomerates compared to 40-nAg, this did not effectively reduce dissolution by blocking/coating sites available for oxidation, as illustrated by higher 10-nAg dissolution findings in Ca^{2+} treatments. Such behaviour is not atypical for large ENPs agglomerates (Reinsch *et al.* 2012). Moreover; it is likely that 10-nAg agglomerate pockets possibly created a microlayer of adsorbed Ag^{+}, Ag0 and Ag, an environment characterised by high dissolution rates (Liu and Hurt 2010). Therefore our findings confirm earlier suggestions that within ENPs agglomerates most of the surface area is retained, and available for oxidation (Liu *et al.* 2010).

The influence of Ca^{2+} and NOM on nAg dispersion has been reported previously, and it has been suggested that resultant NOM-nAg complexes reduce surface area available for oxidation and reverse dissolved Ag to Ag^{0} thereby inhibiting dissolution (Dubas and Pimpan 2008; Sal'nikov *et al.* 2009; Liu *et al.* 2010), however the coating effect does not completely inhibit dissolution (Li *et al.* 2010). It was observed that NOM did not inhibit but rather enhanced dissolution when comparing NOM to MHW treatment for both nAg sizes. This was attributed to highly stable nAg within NOM-nAg complexes; which retained a certain degree of monodispersed properties (Cumberland and Lead 2009). The stabilising effect of NOM has also been observed to arise from the formation of NOM-nAu complexes (Glenn and Klaine 2013) and NOM-nAg complexes (Baalousha *et al.* 2013), and hence likely to significantly influence dissolution of ENPs in aquatic environments.

Increasing ionic strength generally destabilises ENPs (Cumberland and Lead 2009; Burns *et al.* 2013; Pamies *et al.* 2014). However, such destabilisation is linked to size characteristic, an effect observed in this study and elsewhere with citrate coated nAg due to Ca^{2+} (Baalousha *et al.* 2013). As illustrated in previously (Section 5.3.2), the destabilising effect of Ca^{2+} is attributed to its surface charge shielding activity. However, when viewed as dissolution potential, it appears Ca^{2+} enhances nAg dissolution in a size dependent manner because increased Ca^{2+} enhanced dissolution of 10-nAg whilst it was inhibitive of 40-nAg (Figure 5.6). Similar to NOM, the effect of

Ca^{2+} appear to be related to retention of the original size behaviour characteristics as evidenced by higher dissolution of 10-nAg relative to 40-nAg. Overall, our findings suggest that agglomeration promoting Ca^{2+} and NOM may have partly stabilised 10-nAg as small size behaviour was not completely lost, thereby accounting for high dissolution of 10-nAg which existed as larger agglomerates in Ca^{2+} and NOM treatments.

In the case of simple solutions such as DI water, the dissolution mechanisms and kinetics of Ag are relatively simpler and somehow predictable (Liu *et al.* 2010). However, in complex solutions such as those used in this study comprised of numerous oxidants and reductants; the dissolution of Ag becomes highly complex and dynamic –due to numerous chemical reactions that take place. That said, size induced differences were still observable although highly influenced by water quality variables. In summary, these findings confirm the limitation of simple models for actual environment prediction of nano-sized materials behaviour, as previously reported (Keller *et al.* 2010; Lowry *et al.* 2012; Collin *et al.* 2014).

5.3.4 Silver accumulation

Studies on accumulation had three-fold aims, namely to evaluate: (i) Ag accumulation differences between roots and fronds, (ii) nAg size influence on Ag accumulation, and (iii) the influence of water quality changes on Ag accumulation. However, it should be noted that Ag accumulation results presented herein may not have completely resulted from internalised nAg or dissolved Ag since traces of both forms may remain adsorbed to plants surfaces even after rinsing of the plants, as reported elsewhere (Glenn *et al.* 2012; Judy *et al.* 2012; Li *et al.* 2013).

Overall, more Ag was found accumulated in roots as compared to fronds (Figure 5.7). Only in 40-nAg NOM treatment did Ag accumulation not differ statistically between roots and fronds, but on average the roots accumulated higher Ag, thus rendering them plausible major sites of nAg/dissolved Ag uptake. Although *Salvinia* spp roots are modified frond elongation (Oliver 1993; Smith *et al.* 2006), they function as normal roots and the presence of numerous root hairs increases the surface area for uptake suggesting that to roots are more efficient compared to fronds with respect to nutrient uptake. It has been suggested that the presence of root hairs in aquatic higher plants can increase uptake rates of ENPs (Glenn *et al.* 2012).

Furthermore, *Salvinia* species are capable of nutrient uptake using both roots and fronds (Smith *et al.* 2006), therefore, low Ag accumulation by fronds observed herein supports the hypothesis that roots are major uptake sites but not necessarily an indication of low translocation from roots

to fronds. Higher deposition of metals in roots compared to fronds after exposure of aquatic vascular plants to metal-based ENPs has been reported (Glenn *et al.* 2012; Burns *et al.* 2013; Glenn and Klaine 2013). However, it appears such an accumulation trend is not always applicable as *S. minima* fronds have been reported to accumulate Zn at higher rates than roots after exposure to nZnO (Hu *et al.* 2014). Such controversies may be related to differences between ENP types and the likely influence of exposure duration

Furthermore, accumulation of Ag in whole plant as a function of nAg size was also evaluated. Higher Ag accumulation was found in plants exposed to 10-nAg, however, the difference between the sizes was found statistically insignificant. Even without statistical significance, the trend was well illustrated as the 10-nAg average values (Ag accumulation) were generally higher compared to 40-nAg. It was not surprising to observe the influence of nAg size on Ag accumulation because ENPs applications are generally founded on size induced differences based on physical and chemical properties. The novelty of this study is that no previous study has demonstrated this effect in aquatic plants exposed to nAg although similar accumulation trends have been documented for nAu (Glenn *et al.* 2012; Glenn and Klaine 2013). Even with terrestrial plant forms exposed to varying nAg size; higher Ag accumulation was established from smaller nAg sizes (Wang *et al.* 2013).

Moreover, theoretically it was expected that higher Ag accumulation will result from smaller sized nAg as a result of preferential internalisation since plant cell wall pores are approximately 20-50 nm in diameter (Adani *et al.* 2011; Judy *et al.* 2012); hence 10-nAg would likely to internalised at higher rates compared to larger 40-nAg. Contrary, 10-nAg *in-situ* formed larger agglomerates compared to 40-nAg expect in Ca^{2+} treatment (Figures 5.3-5), plausibly reducing internalisation of particulate 10-nAg. Therefore; suggest that internalisation of nAg was not the major driver for higher accumulation of Ag from 10-nAg exposures, as observed in this study. Multiple pathways therefore were possible involved in the uptake process. It is suggested that further investigations for internalisation, for instance with electron microscopy techniques will likely shed more light on this aspect.

.

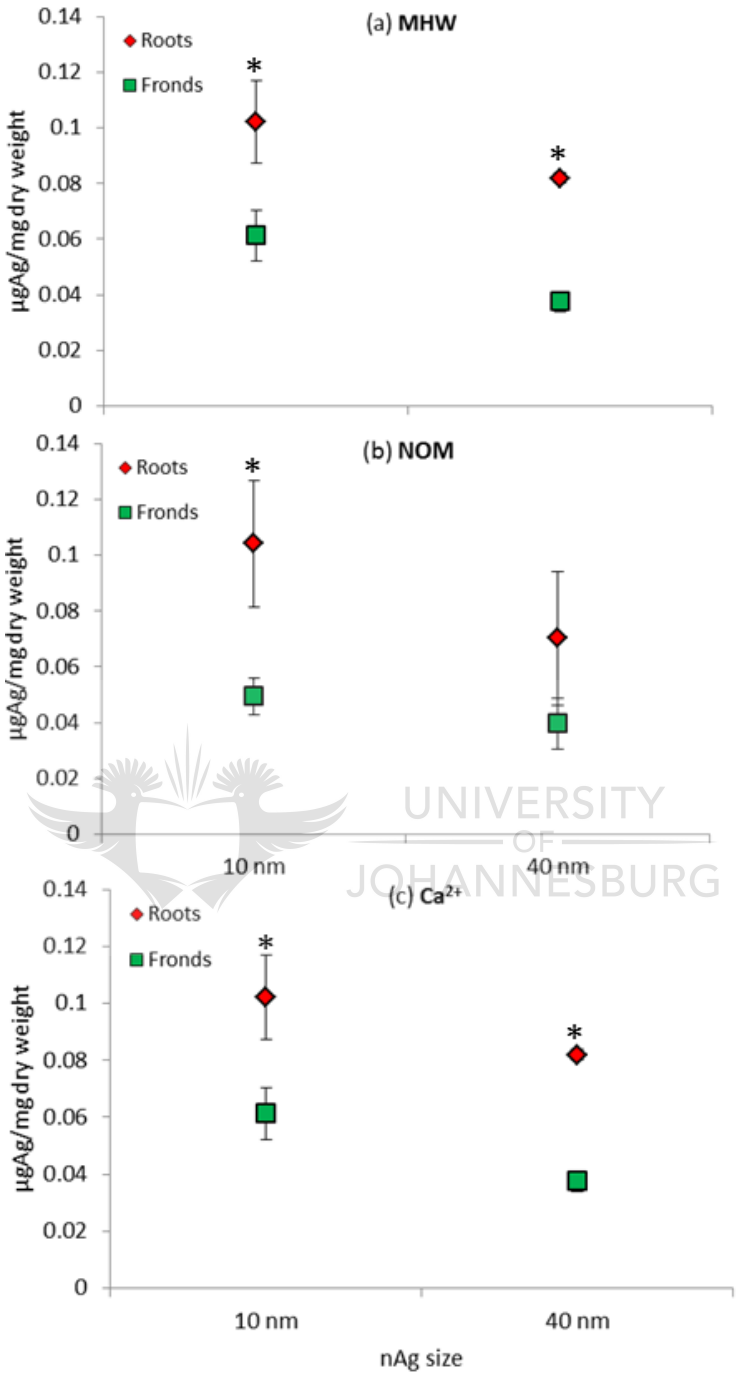

Figure 5.7: Accumulation of Ag by *S. minima* roots and fronds after 48 hours exposure to 10-nAg and 40-nAg in different holding water quality conditions: (a) moderately hard water, (b) natural organic matter (NOM) and (c) Ca^{2+}. Bars denote standard error (n=3). *indicates statistical difference between roots and fronds Ag accumulation within a specific nAg size exposure. Student's t-test, $p < 0.05$.

Two mechanisms then remained plausible to account for higher Ag accumulation from 10-nAg in Ca^{2+}: dissolution and adsorption. Dissolution of 10-nAg was higher than for 40-nAg (Figure 5.6), and therefore suggest this pathway partly accounted for higher Ag accumulation in 10-nAg exposures. Dissolved Ag^{+} can be easily internalised by higher plants relative to nAg forms and this has been illustrated in studies comparing Ag accumulation between nAg and Ag salts (Jiang *et al.* 2012; Wang *et al.* 2013; Jiang *et al.* 2014). Such evidence supports our suggestion that higher dissolution of 10-nAg partly accounted for higher bioaccumulation of Ag in plants exposed to 10-nAg compared to 40-nAg.

Secondly, higher reactivity of 10-nAg as evidenced by higher agglomeration rates could also account for size dependent Ag accumulation observed as 10-nAg likely had higher adsorption rate to plant surfaces. Although no adsorption evidence is presented here but there are substantial clues for plausible adsorption related to high Ag accumulation in 10-nAg regimes. As already mentioned, it is possible that washing of plants at test end did not remove all nAg from plants surfaces, and, 10-nAg probably exhibited higher adsorption potential than 40-nAg due to higher reactivity of the former. The association of nAg with biota surfaces has been reported to promote the release of free metal ions within the surface layers (Fabrega *et al.* 2011). Furthermore, *S. minima* is capable of accumulating metal derivatives through passive adsorption and also internalisation into tissues and cells (Sune *et al.* 2007); thus supporting adsorption as possible mechanism for Ag accumulation.

Further investigation of underlying pathways driving Ag accumulation observed; revealed that dissolution, particle size and concentration were all partly involved, but extent varied between nAg size and water quality regimes (Figure 5.8). It could not be determined which parameter between nAg and dissolution was the principal driving factor. These findings supported the suggestion for involvement of different pathways, as regulated by the interplay between nAg size and exposure medium chemistry. Therefore based on the PCA analysis, there is high likelihood that Ag accumulation was associated internalisation of both in nano-particulate and dissolved forms. This would not be unexpected since Ag accumulation has been observed in plants exposed to dissolved Ag (Jiang *et al.* 2012; Wang *et al.* 2013; Jiang *et al.* 2014) whilst cell wall pores are capable of mediating internalisation of ENPs (Glenn *et al.* 2012). Improved discrimination of the role of nAg parameters on Ag bioaccumulation could be achieved by monitoring of dissolution and accumulation at higher frequency than adopted here. Furthermore, detection and characterisation of internalised Ag (in plant tissue) can also shed light on the uptake dynamics of nAg by aquatic vascular plants.

Furthermore, the influence of water quality variation on whole plant Ag accumulation was probed. The trend was uniform between the two nAg sizes, whereby accumulation was least in NOM treatment, followed by MHW, and highest in Ca^{2+} treatment (Figure 5.9). However, only Ca^{2+} treatment of 40 nm statistically differed from other treatments within the same nAg size. The variation of Ag accumulation between water treatments were associated with nAg stability and hence bioavailability because stability ENPs is highly dependent on exposure chemistry (da Silva *et al.* 2011; Delay *et al.* 2011; Bian *et al.* 2013). Specifically, the presence of divalent Ca^{2+} has been reported to improve stability (concentration dependent manner) of citrate coated nAg (Cumberland and Lead 2009; Baalousha *et al.* 2013) above certain thresholds; thus plausibly accounts for the highest accumulation observed in Ca^{2+} treatments. In contrast, dissolution results in this instance only partly support this suggestion because dissolution in Ca^{2+} was only highest for 10-nAg and not at 40-nAg regimes.

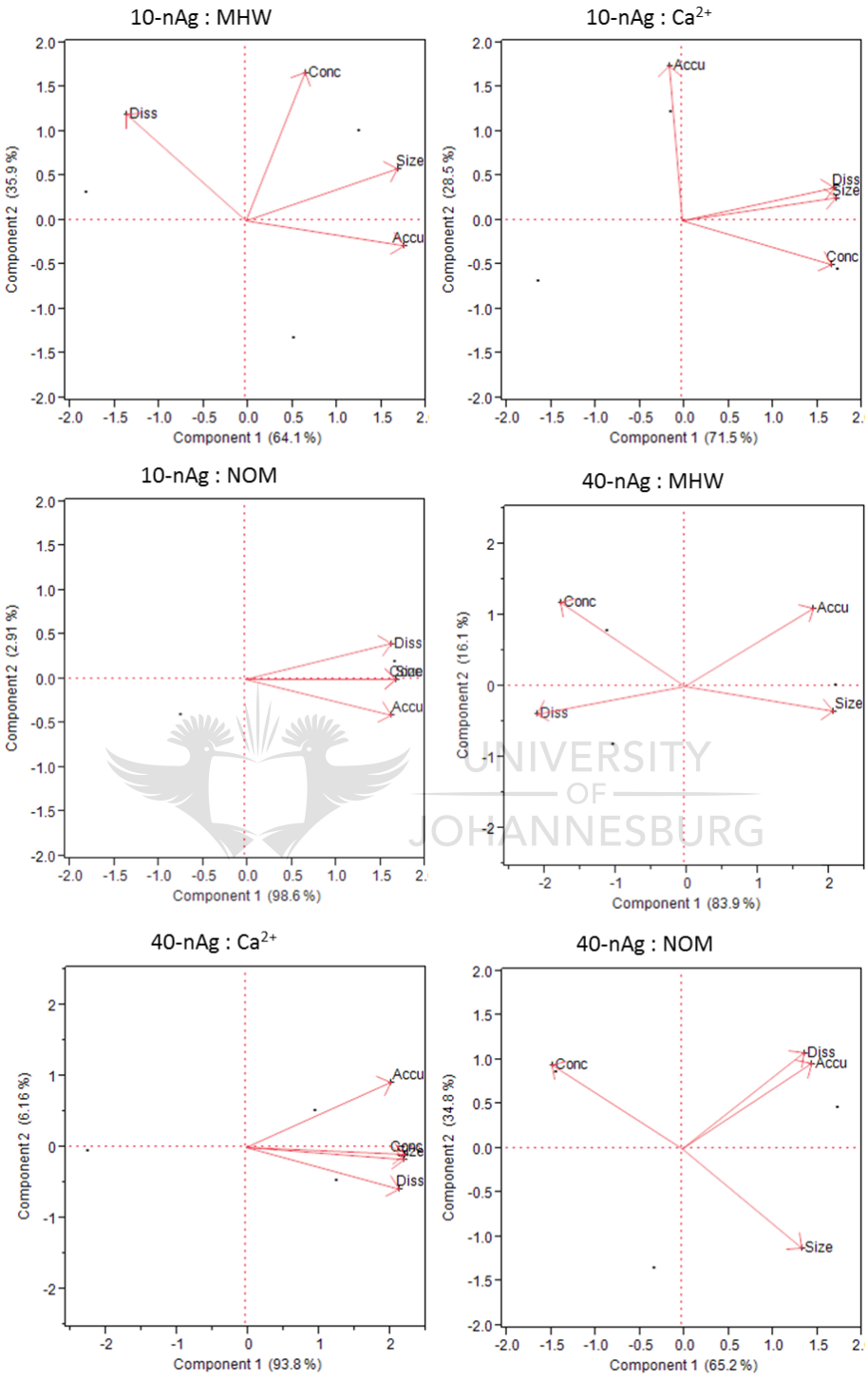

Figure 5.8: Principal component analysis plot illustrating association of Ag accumulation (Accu) with nAg size (Size), dissolution (Diss), and nAg concentration (Conc) parameters for 10-nAg and 40-nAg under differing water quality regimes (MHW, NOM and Ca^{2+}).

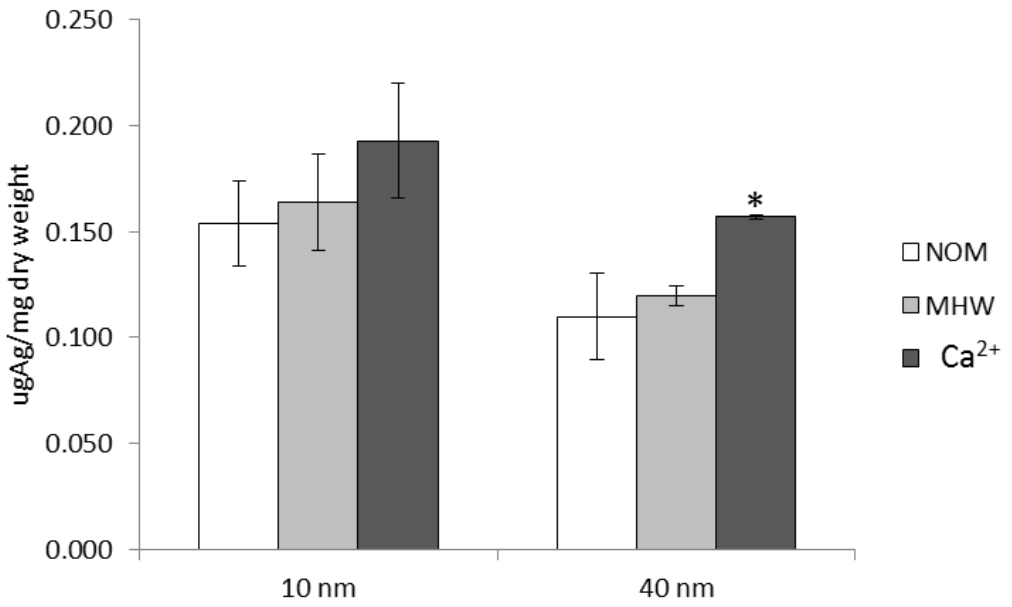

Figure 5.9: Pairwise comparison of whole plant Ag accumulation across water quality treatments within a single nAg size exposure (MHW, NOM and Ca^{2+}). Bars denote standard error (n = 3). Differing symbols on top of error bars indicate statistical difference between compared treatments within single nAg size. Turkey Kramer HSD, $p < 0.05$.

Even though NOM treatment generally improves the stability of ENPs (Cumberland and Lead 2009; Baalousha *et al.* 2013), the resultant large size NOM-ENPs complexes can hinder accumulation by aquatic plants (Glenn and Klaine 2013). Therefore, it is postulated that formation of such complexes in this case led to least Ag accumulation in NOM treatments, as large agglomerates were formed especially for 10-nAg. Therefore, these findings are not in conflict with current knowledge and appear to support arguments for the influential role of exposure water quality in influencing fate, bioavailability and effects of ENPs in aqueous environments. Although environmental behaviour of nano pollutants is highly dynamic, the current findings suggest that even within big data sets it is possible to identify certain patterns, and hence support calls for complementary approaches to nanotechnologies risk assessment (Praetorius *et al.* 2013).

5.3.5 Chlorophyll pigments and growth

Exposure of *S. minima* to nAg altered chlorophyll *a* and *b* content and the effect was size dependent but not uniform across water treatments (Figure 5.10). In MHW, both nAg sizes significantly reduced chlorophylls relative to controls, with 10-nAg being most inhibiting. In NOM

treatment, only 10-nAg reduced chlorophylls although not statistical significant whilst 40-nAg and control exposures were similar. However, in Ca^{2+} treatment whilst 40-nAg was highly inhibitive, 10-nAg stimulated chlorophylls production to levels even higher than control treatments. Effects on photochemical efficiency of plants (energy housing), suggests possible secondary effects on numerous active (energy requiring) physiological pathways, such as growth for instance, which was inhibited in this study.

Salvinia minima exposure to both nAg sizes across water treatments inhibited plant growth compared to respective control exposures (Figure 5.11). In MHW, 10-nAg were more growth inhibitive than larger 40-nAg counterparts. In NOM treatment 40-nAg exhibited higher growth inhibition than 10-nAg, but overall; both sizes significantly reduced growth. However in Ca^{2+}, the inhibiting effect of both nAg sizes was relatively similar with 10-nAg being slightly more toxic (not significantly different); nevertheless both sizes significantly inhibited plant growth. Overall growth inhibition effect (% reduction) was more severe in Ca^{2+} water treatment and 10-nAg being highly growth inhibiting except in NOM water treatment (Table 5.1); this probably as a result of additional harmful effects of Ca^{2+} at excessive concentrations (Sims *et al.* 1995; Lopez-Lefebre *et al.* 2001).

Table 5.1: Percentage growth reduction relative to respective controls. Analysis based on relative growth rate measurements.

	10-nAg	**40-nAg**
MHW	63.1	57
NOM	36.3	79
Ca^{2+}	1415	1276

Even though across water treatments 10-nAg resulted in bigger hydrodynamic sizes (Figure 5.3), they were still relatively highly inhibitive of chlorophylls and growth compared to 40-nAg (Figure 5.10; 5.11). With respect to growth; a slightly lower 7 days growth EC_{50} value was reported on *L. minor* exposed to larger citrate coated nAg (84.1 nm; DLS) compared to smaller forms (15.92 nm; DLS), although the trend was opposite after 14 days (Gubbins *et al.* 2011). Our findings are similar to those of Gubbins *et al.* (2011) after 7 days. No reports on photosynthetic effects as a factor of nAg size or water quality were found, and these results are first of this nature.

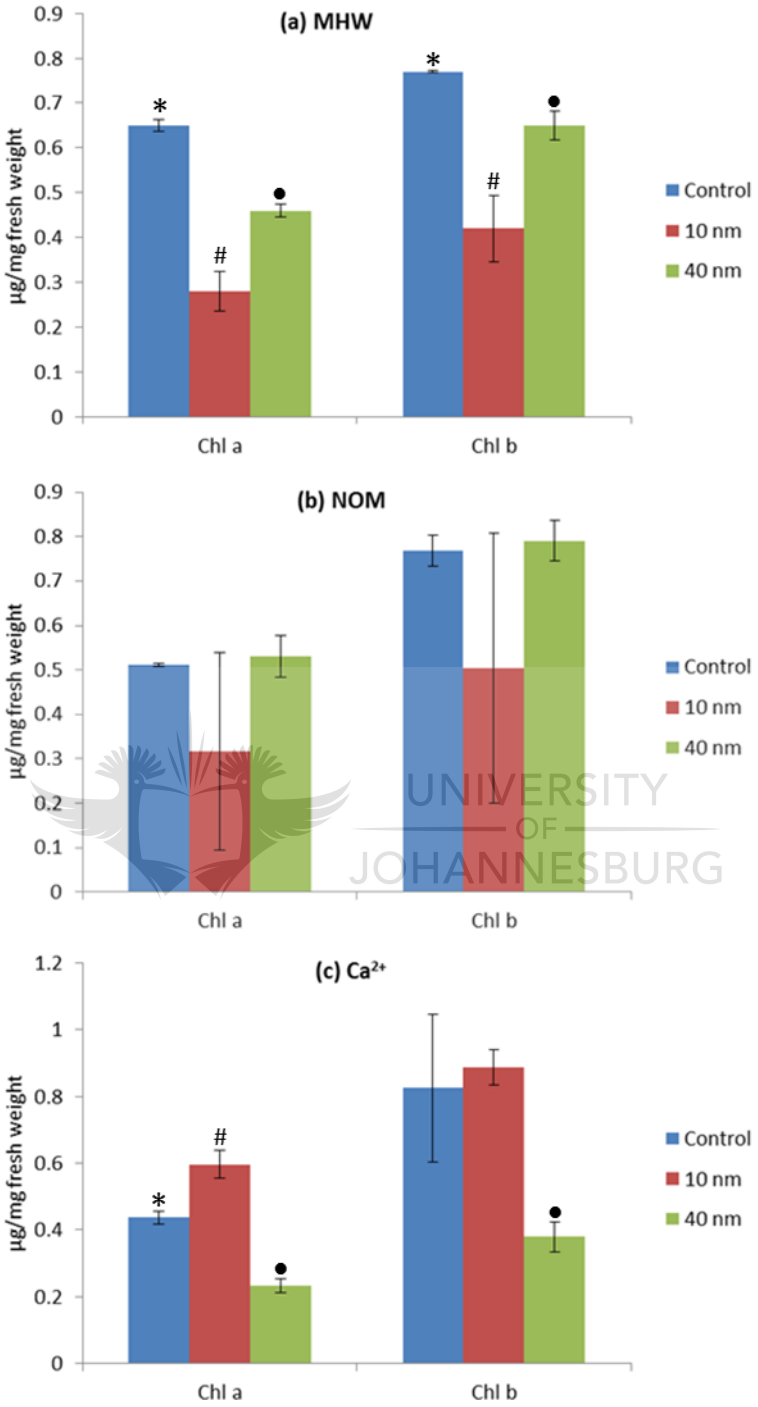

Figure 5.10: Quantification of chlorophyll pigments Chl *a*, Chl *b* in *S. minima* after exposure to 10-nAg and 40-nAg for 48 hours. Bars denote standard error (*n*=3). Differing symbols on top of error bars indicate statistical difference within photosynthetic parameter. Turkey Kramer HSD, $p < 0.05$.

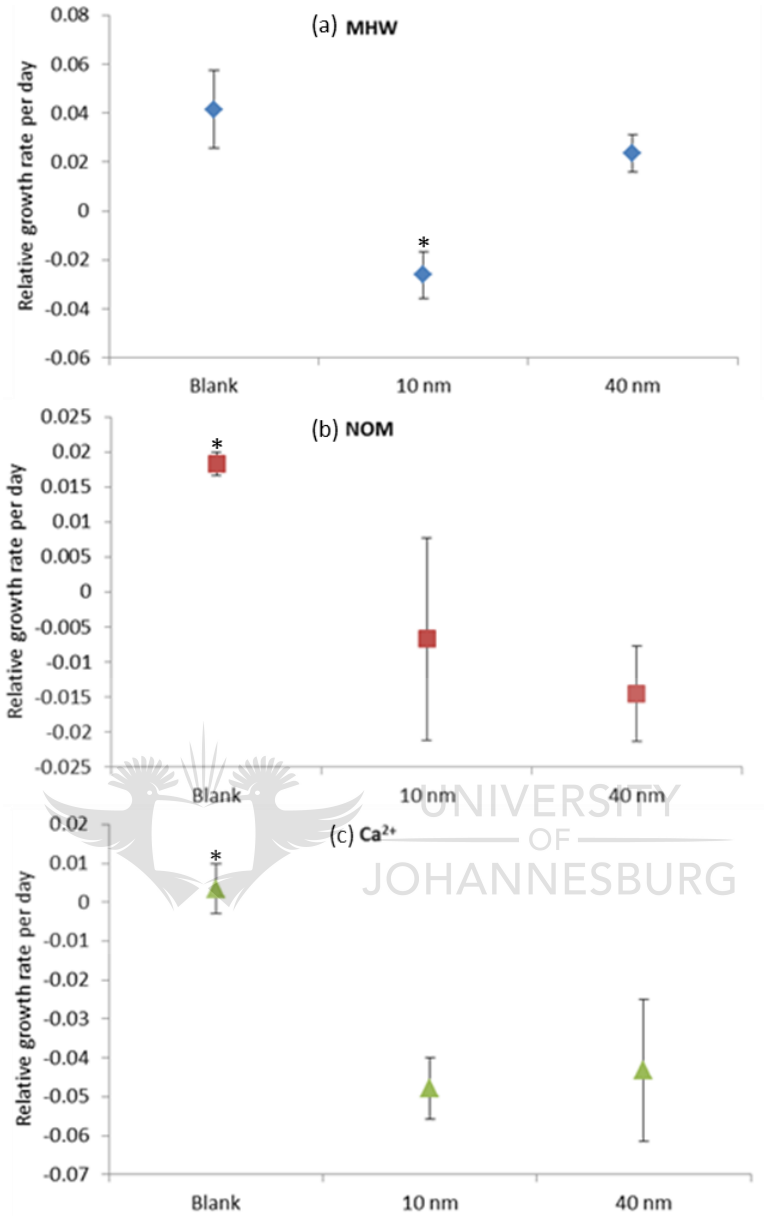

Figure 5.11: Relative growth rate of *S. minima* at different nAg exposures across varying water treatments: (a) moderately hard water, (b) natural organic matter and (c) Ca^{2+}. Bars denote standard error (n=3). * on top of error bars indicate differing growth rate between nAg exposures within a water treatment. Turkey Kramer HSD, $p < 0.05$.

Interestingly in Gubbins *et al.* (2011); bulk Ag was highly toxic and nAg dissolution was < 1%; therefore suggesting dissolution played an insignificant role in toxicity of nAg effects observed. Similar trend on photosynthetic effects were observed on *S. polyrhiza* exposed to nAg and $AgNO_3$ (0.5-10 mg/L), but the authors concluded that $AgNO_3$ was not always the most toxic Ag form. Furthermore; the toxicity of the two forms was generally similar but sensitivity varied between toxicity parameters (Jiang *et al.* 2012). Growth effects of metal-based ENPs towards aquatic higher plants have been attributed to both ionic species (Hu *et al.* 2013) and particulate/colloidal form (Shi *et al.* 2011) but also appeared to be growth end-point dependant (Jiang *et al.* 2012), whilst in certain instances the major driving factor was unclear (Hu *et al.* 2014). Therefore, our results and suggestions do not conflict the current body of knowledge.

The growth endpoint appeared as more sensitive compared to chlorophyll or can be suggested to better illustrate the effects of nAg for both sizes across treatments. However, it has been suggested that sensitivity of the photosynthetic pathway is endpoint dependent (Jiang *et al.* 2012); hence it is not suggested that the chlorophyll endpoints used here as completely insensitive/unresponsive. Rather, it is argued that chlorophyll and growth endpoints may be highly useful applied in a complementary bioassay package. Overall, the growth and photosynthetic effects observed in this study suggest possibility for adverse ecological effects in aquatic resources due to elevated pollutant concentrations of nAg. The exposure concentration in this study is environmentally not relevant, but utilised mainly to enable accurate nAg characterisation in test. Thus, it would be ideal for future research to investigate similar endpoints at lower and environmentally relevant concentrations. That said, the current findings indicate potential for nAg/Ag bioaccumulation by aquatic higher plants, and also trophic transfer potential.

5.4 Concluding remarks

- Silver ENPs are susceptible to chemical and physical transformations which are driven by nAg size and prevalent environmental conditions; as well demonstrated in this study by distinctive changes between DI water and different testing water treatments. The findings further stress the limited applicability of information obtained with simple water medium in actual environmental scenarios.

- Different forms of nAg characterisation undertaken in this investigation were complementary and helpful in understanding the observed and potential interactions of nAg with *S. minima*. This demonstrated the importance of continuous (start-end) ENP characterisation in-test as it partly determines what is “seen” by biota was illustrated, and

allows better understanding of uptake, bioaccumulation, and toxicity dynamics. For instance, the presence of 10-nAg having larger agglomerates to 40-nAg was not indicative of reduced bioavailability of the former, as illustrated by overall higher dissolution, bioaccumulation, and toxicity of 10-nAg.

- Furthermore, the elevated stability of 40-nAg under test conditions did not elevate interaction with *S. minima*, rather the enhanced reactivity of smaller 10-nAg dominated, and inreased its interaction with the plants in both dissolved and particulate form. The study therefore concluded that interaction of aquatic plants with nano-pollutants is not fully limited by ENPs bioaccessible size (i.e. encountering cell wall pores), where larger particles would be rejected and not interact with plants. However, the size, surface reactivity and dissolution of metal-based ENPs are all interactively influential determinants for bioaccumulation and toxicity effects. Examination of tissue cross sections, mainly the roots, would have provided more insights on uptake/internalisation kinetics; such an aspect requires consideration in future to better understand the role of cell wall pores in size mediated regulation of nAg-size driven uptake. Current findings; therefore challenge the common idea that ENPs agglomeration translates to their reduced reactivity and hazardness, but contrary suggest that in actual aquatic environments; ENPs' chemical and physical transformations may enhance their persistence as nano-pollutants with poorly known implications over wider temporal and spatial scales, as well as different trophic levels.

- The findings of this study supports suggestions that bioaccumulation of xenobiotics is generally a precursor for toxicity (Luoma and Rainbow 2008); as demonstrated by higher Ag accumulation from 10-nAg exposures; and consequent growth and photosynthetic effects. Although in this study no internalisation information was generated, it was observed that nAg interaction with aquatic plants was enhanced at lower-end nanoscales and not only elevated potential effects towards aquatic plants but also exerted overall aquatic health implications as bioaccumulation and potential trophic transfer were enhanced by exposure to smaller nAg. Therefore aquatic plants may serve as reservoirs of nano-pollutants irrespective of their physical and chemical forms in aquatic ecosystems.

CHAPTER 6

The oxidative toxicity of silver and zinc oxide nanoparticles towards the aquatic plant *Spirodela punctuta* and the role of testing media parameters

6.1 Introduction

Nanotechnology is a rapidly developing field characterized by increasing numbers of commercially available products including cosmetics, paints, food additives, clothing, medical and electronics to mention a few (BCC Research 2012). These positive commercial advances, have stimulated a rapidly increasing production of ENPs, thus greatly increasing the likelihood of their release into the environment (Klaine *et al.* 2008; Musee 2011; Tejamaya *et al.* 2012) in proportion to their uses and applications, and the trend is expected to increase dramatically in future (Hansen *et al.* 2008; Musee 2011). Many ENMs are known to be potentially toxic and earlier articles have highlighted several potential toxicity effects at nanoscale (Oberdörster 2004; Nel *et al.* 2006; Oberdörster *et al.* 2006). In addition, many reviews have suggested that the toxicity of ENMs is mainly a result of their size, as well as their large surface area to volume ratios, which renders them detrimental at very low concentrations (Handy *et al.* 2008a;b Klaine *et al.* 2008; Fabrega *et al.* 2011; Musee *et al.* 2011).

Among the ENMs that have been ranked as the most widely used are metallic silver (nAg) and zinc oxide nanoparticles (nZnO) (BCC Research 2012). Silver nanoparticles have attracted widespread interest as broad-spectrum antimicrobial agents in textiles, food preservation, cosmetics and biomedical applications (Tolaymat *et al.* 2010; Liu *et al.* 2012). Moreover, ENMs can be released unintentionally into the environment during their application phase, thereby necessitating an understanding of their potential impacts to biological life forms in aquatic ecosystems because they have the potential to compromise environmental health. For example, Benn and Westerhoff (2008) highlighted the release of nAg from washing machines. In addition, the environmental implications of nAg have been summarized in numerous reviews (Handy *et al.* 2008b; Navarro *et al.* 2008; Fabrega *et al.* 2011; Levard *et al.* 2012) although the mechanisms that are responsible for causing the observed toxicity are yet to be fully elucidated.

For example, there have been suggestions that the toxicity of nAg particles is caused primarily by dissolved Ag ions, which induce oxidative stress (Lee *et al.* 2007; Pal *et al.* 2007; Shahverdi *et al.* 2007; Navarro *et al.* 2008), while other studies suggest that the toxicity is not primarily induced by dissolved metallic species (Fabrega *et al.* 2009; Yin *et al.* 2011). Some evidence points to the influence of environmental conditions on the stability of nAg in the aquatic environment (El Badawy *et al.* 2010; Huynh and Chen 2011; Li *et al.* 2013; Tejamaya *et al.* 2012) which, in turn,

controls the eventual observed toxicity. The variability of the available information therefore indicates that detailed investigations aimed at establishing the mechanisms of nAg toxicity are needed in order to derive reliable data that can support a sound assessment of the potential risks associated with nAg in the aquatic environment.

To date, there are limited data on the toxicological effects of nZnO to aquatic biota (Kahru and Dubourguier 2010; Ma *et al.* 2013). For instance, a recent review listed forty eight (48) studies that documented the aquatic toxicity of nZnO (Ma *et al.* 2013), but none of these studies provided definitive information on the mode of toxicity. Instead, the toxic action of nZnO was attributed broadly to: (i) the release of Zn ions (Brunner *et al.* 2006; Heinllan *et al.* 2008; Auroja *et al.* 2009; Bian *et al.* 2011; Mudunkotuwa *et al.* 2012; Reed *et al.* 2012), (ii) the production of free radicals (Xia *et al.* 2008; Applerot *et al.* 2009; Ma *et al.* 2009; Feris *et al.* 2010; Ma *et al.* 2011), and (iii) the oxidative damage of biological compartments and membranes (Xia *et al.* 2008; Wahab *et al.* 2010; Xie *et al.* 2011). Most of these studies attribute nZnO toxicity to dissolved Zn forms (Ma *et al.* 2013).

Although there is currently insufficient statistically significant evidence to link nZnO toxicity with its physico-chemical parameters (Ma *et al.* 2013), however, the literature suggests that particle properties (e.g. size, morphology, chemical composition) and environmental parameters (e.g., pH, natural organic matter, etc.) control the dissolution process, and thereby influence the toxic mode of action. Despite these efforts aimed at evaluating the toxicity of nZnO in aquatic systems, no studies have been reported on the potential risks of nZnO to higher aquatic plants (Kahru and Dubourguier 2010; Ma *et al.* 2013), while only a handful of studies have reported the toxicity of nAg towards higher aquatic plants (Gubbins *et al.* 2011; Kim *et al.* 2011; Oukarroum *et al.* 2013). This situation highlights the clear gap in current knowledge of the risks posed by nAg and nZnO to higher aquatic plants.

For this study, a free-floating species *Spirodela punctuta* (commonly known as duckweed) was selected as representative of other primary producers at the same trophic level in the aquatic ecosystem. Higher aquatic plants play a significant role related to energy metabolism in aquatic ecosystems. Additionally, duckweeds have been widely used in toxicological tests because of their rapid growth rates, sensitivity to the toxic effects of pollutants, and ease of maintenance under laboratory conditions (Upadhyay and Panda 2010; Parlak and Yilmaz 2012; Oukarroum *et al.* 2013).

Therefore, the study aims were two-fold. First; to investigate the influence of nAg and nZnO on the health status of *Spirodela punctuta* by assaying impacts on the functioning of the oxidative defense system. The anti-oxidative system serves as an important protection mechanism against environmental pollutants in plants (Parlak and Yilmaz 2013). Secondly, examine the influence of environmental factors (e.g., pH, ionic strength, etc.) on the ENPs properties so as to derive an understanding of their implications in the observed toxicity. For instance, to estimate or predict the risks associated with the exposure of ENPs to biological life forms, it is critical to determine their stability in relevant testing conditions because this can influence on physicochemical properties such as the hydrodynamic size and surface charge of ENPs (Suttiponparnit *et al.* 2011).

6.2 M**aterials and methods**

6.2.1 Nanoparticles characterization

Batches of nZnO and nAg (dry powder) were purchased from Aldrich®, South Africa. According to the manufacturer's specifications, their particle sizes were <100 nm. Prior to toxicity testing, the ENPs were characterised in terms of their particle size and morphology using the TEM (JEOLJEM-2100®, Japan); particle surface area analysis was done by following the BET theory. Additional surface analysis was undertaken using XRD, using a PAN Analytical X'Pert PRO PW 3040/60 (Netherlands). In the testing media, the hydrodynamic size and zeta potential were analysed using a zetasizer (Nano-ZS, Malvern, USA). Both parameters were tested at the beginning and the end of each experimental exposure.

6.2.2 Chemical analysis

Forty mL of exposure water was pipetted from each exposure concentration and preserved using HNO_3. Each of the preserved samples contained a 5% HNO_3 concentration. Pipetting was done carefully to ensure that the particulates that had settled out of suspension were not re-suspended. Before the water samples were analysed, they were filtered through a 0.45 µm mesh size filter. The extent of dissolution of the ENPs was measured at the end of each experimental exposure period using ICP-OES (Optima 2100 DV PerkinElmer, Massachusetts, USA) at a detection limit of 0.025 mg/L.

6.2.3 Plant sample collection and laboratory maintenance

Samples of *Spirodela punctuta* were collected from the inlet of Rietvlei Dam at Rietvlei Nature Reserve situated South-East of Pretoria, South Africa (25°52′53.20″ S 28°17′43.40″ E). In the laboratory, the samples were rinsed in tap water (< 1 minute) to remove attached debris and no

sterilisation treatment was undertaken. The plants were then acclimatised in 10 L capacity glass tanks filled with 4-5 L high strength Hoagland's E+ medium prepared using deionised water (Environment Canada 2007) for 72 hours (hrs) under a 16 hrs white light: 8 dark photoperiod at 21±2 °C before the plants were exposed to the ENPs.

6.2.4 Testing water

A stock solution of 1 mg/L ENPs was prepared in Hoagland's E+ water medium, shaken vigorously for a minute, and stored under dark conditions to stabilise for 24 hrs before preparing dilutions for different exposure concentrations. After 24 hrs dilutions were made with the Hoagland's E+ water medium to achieve nAg and nZnO nominal exposure concentrations of 0.01, 0.1, 1 and 1000 mg/L whilst control exposures were not dosed with ENPs. The ENPs concentrations exceeding 1 mg/L are presently deemed environmentally irrelevant; however, they were used in the experiments for two specific reasons.

First, to investigate the effect of concentration on the agglomeration of ENPs and, secondly, to determine detectable dissolved ionic species that might be released from the ENPs. High concentrations of ENPs have been used elsewhere to systematically investigate the dissolution kinetics of metallic ENPs (Hu *et al.* 2009; Blinova *et al.* 2010). In addition, based on the ionic strength of the testing media, its influence on the agglomeration of ENPs was investigated to determine the potential removal of ENPs from suspension through sedimentation.

6.2.5 Toxicity testing

Five replicates were used for each exposure concentration and the control; each test contained 35 plants with 3-4 fronds, and 100 mL of test medium in a 250 mL glass beaker. Each experiment ran for 4 days (static) and 14 days (static) with the water medium renewed on day seven. The pH of the exposure water in the beakers was monitored continuously.

6.2.6 Tissue homogenate preparation and biochemical extraction

At the end of each test period all live plants from every exposure beaker were carefully transferred (with the minimum amount of water possible) into a glass mortar, and then immediately frozen in liquid nitrogen. Next, the samples were then crushed into a fine powder and suspended in 500 µL of 1X phosphate buffer saline (PBS; 137 mM NaCl, 2.7 mM KCl, 10 mM Na_2HPO_4, 2 mM KH_2PO_4) buffer in 2 mL capacity Eppendorf tubes. The tubes were then centrifuged at 10 000 g for 15 minutes at 4°C (HermLe Labortechnic GmbH, Z236K, Germany). Finally, the supernatant was stored at -80°C until biochemical analysis were undertaken. The

preparation of samples for biochemical analysis was done on ice unless required otherwise under a specific protocol.

6.2.7 Protein quantification

The Bio-Rad Bradford Protein Microplate Assay was used for the quantification of protein concentrations using the Bio-Rad Bovine Gamma-Globulin protein standard, according to Bradford (1976). This was undertaken so as to express activity of antioxidative enzymes as a factor protein quantity.

6.2.8 Free radicals quantification

Total ROS and RNS were measured using the dichlorodihydrofluorescin (DCFH-DiOxyQ) probe against the 2', 7'-Dichlorodihydrofluorescein (DCF) standard curve following the OxiSelect™ *In Vitro* ROS/RNS assay kit protocol. The hydrogen peroxide content was measured fluorometrically using the OxiSelect™ Hydrogen Peroxide/Peroxidase (H_2O_2) assay kit.

6.2.9 Antioxidant activity

Total antioxidant capacity (TAC) of samples was measured following the OxiSelect™ TAC assay kit protocol which measures the TAC of a sample by comparing with uric acid standards. The direct activity of antioxidant enzyme activity was measured for SOD following the OxiSelect™ Superoxide Dismutase Activity Assay. The assay is based on the ability of SOD to reduce the superoxide ion.

6.2.10 Data analysis

Statistical differences between samples were evaluated using a one-way ANOVA followed by a Student-Newman-Keuls Method test where the data had homogenous variances. In instances where the data failed the normality test, treatments were compared using the Kruskal-Wallis ANOVA followed by the Dunn's multiple comparison when necessary. Statistical significance was tested at $\alpha = 0.05$. The statistical software used was SigmaStat®.

6.3 Results and discussion

6.3.1 Nanoparticles characterisation: dry state

The textural characteristics of nAg and nZnO were investigated using BET analysis and the results are summarized in Table 6.1. The results suggest that nZnO had a larger surface area and pore volume relative to nAg. Notably, the nZnO had a size range from 10-130 nm suggesting

a wide size distribution. While the nZnO had smaller and larger crystals, its surface area characteristics were three times larger than those recorded for nAg. This was probably because nZnO has both inter- and intra-particle porosity as well as small particles (< 30 nm), consistent with the particle porosity values for nZnO (see Table 6.1).

Table 6.1: BET surface areas and pore volumes of nZnO and nAg

Sample	SA_{BET} (m^2/g)	Pore volume (cm^3/g)	Particle size (nm)
nZnO	11.44	0.03020	10-130
nAg	3.399	0.01509	40-60

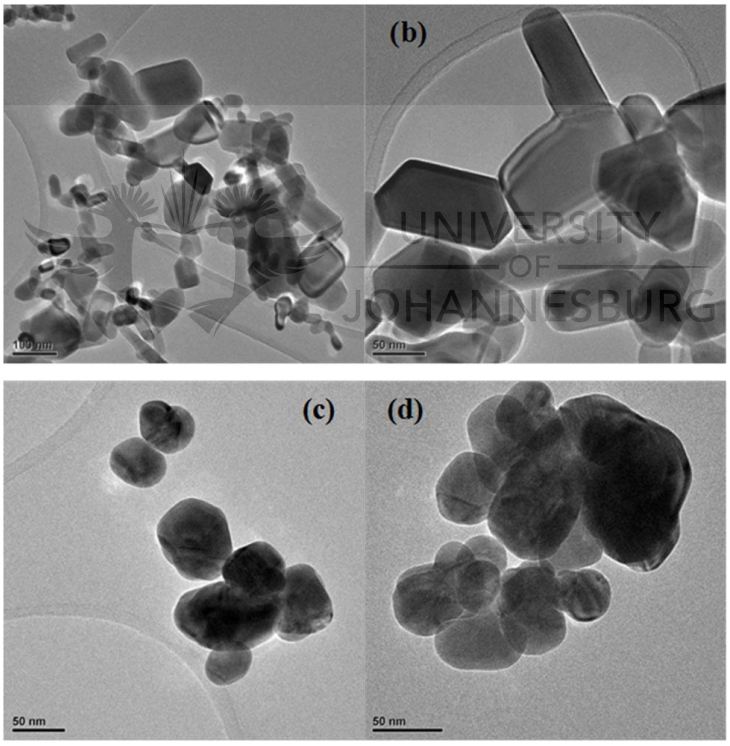

Figure 6.1: TEM images of (a-b) nZnO and (c-d) nAg (both samples are commercial materials).

The morphologies of nZnO and nAg are shown in Figs. 6.1 (a) and (b), respectively. The nZnO had poly-dispersed particles with different morphologies such as regular and irregular spheres, rods, hexagonal platelets, cubes, etc., and differed in size. The particle size trend appears to be related to the morphology of the particles. For instance, individual rods showed a diameter range

of 15-45 nm, cubes had diameter range of 10-130 nm, and the platelets gave a diameter range of 60-80 nm. Regular spheres gave a diameter ranging from 20 to 50 nm whilst irregular spheres had a size range of 80-120 nm. The formation of larger particles (e.g., cubes, spheres, etc.) with particle sizes up to 130 nm may have occurred through the random self-assembly of smaller particles. Therefore, particle growth must have occurred via the Ostwald ripening process. The differences in morphologies and a wide particle size distribution (10-130 nm) yielded a mixed range of properties. The TEM images in Figure 6.1 (c-d) show the morphology of nAg, and reveal presence of spheres with a uniform size distribution of about 40-60 nm, with an average size of 50 nm. However, larger particles of about 70 nm were also observed occasionally and thought to be due to coalescence.

The XRD pattern of nZnO had a poly-crystalline structure – characterised by a Wurtzite hexagonal structure (JCPDS Card No. 79-2205, *a* = 0.3249 nm, *c* = 0.5205 nm) with a high degree of crystallinity (Figure 6.2a). The crystal structure belongs to a hexagonal crystal system with the space group P63mc. All peaks were clearly identified, evidence that the material was phase pure. Thus, no characteristic peaks were observed for impurities [e.g., Zn or $Zn(OH)_2$]. The XRD pattern of nAg is shown in Figure 6.2b. The peaks confirm the presence of crystalline nAg. The XRD analysis also confirmed the spherical morphology that is characteristic of nAg.

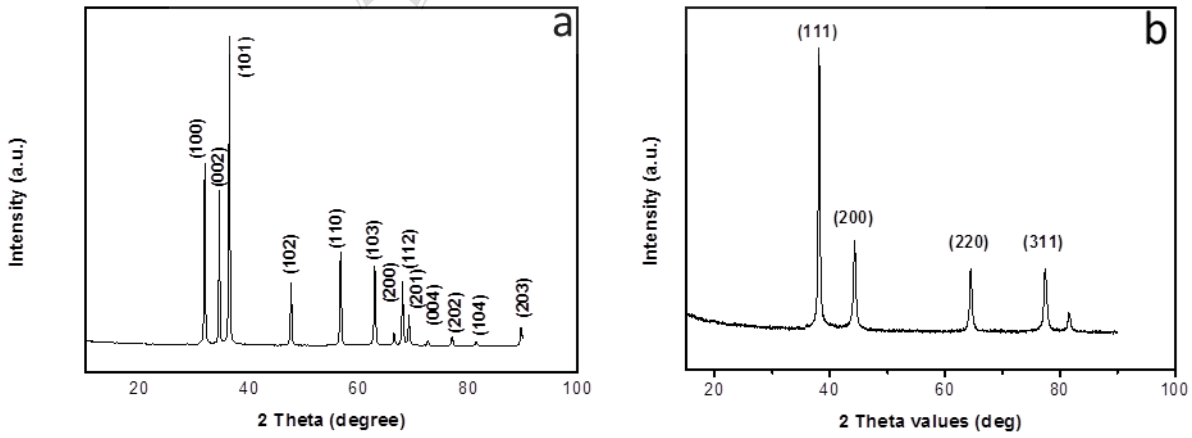

Figure 6.2: The XRD patterns of (a) nZnO and (b) nAg.

6.3.2 Nanoparticles characterisation: testing conditions

After the ENPs were introduced into the testing water, they underwent significant agglomeration at all the four exposure concentrations (Table 6.2); agglomeration of similar sized nAg has been reported elsewhere (Oukarroum *et al.* 2013). In this study, agglomeration was observed to be

influenced by the exposure concentration, although a definitive change to the size of the ENPs was not always observed between different concentrations. The largest particle sizes were observed for nZnO but this was not in the case of nAg. The agglomeration at these concentrations was so strong that the ENPs settled out of suspension and sedimented at the bottom of test beakers (Figure 6.3). There was no conclusive influence of any effect of exposure duration on agglomerate sizes. The particle surface charges were negative for both nAg and nZnO particles and their negative charge remained throughout the testing periods (Table 6.2). Notably; the particles at the highest exposure concentration (largest particles) recorded the lowest zeta potentials. These results are not in agreement with other studies (Zhang *et al.* 2011), where they observed that smaller particles carried lower zeta potentials than bigger particles. The zeta potentials appeared not to be influenced by the exposure period.

The overall agglomeration of ENPs and their change in particle size after introduction into testing media have previously been reported (Jiang *et al.* 2009; Zhang *et al.* 2009; Bian *et al.* 2011; Huynh and Chen 2011; Unrine *et al.* 2012). For instance, Zhang *et al.* (2011) reported significant agglomeration of nAg in Hoagland's medium similar to that used in this study. Similarly, Johnston *et al.* (2010b) highlighted that the size of agglomerated particles increased with increasing ENPs concentration – an observation in agreement with findings of this study. Notably, agglomeration can be so significant that ENPs can be in the µm size range far larger than the dry/starting state particles in the lower nm scale (Unrine *et al.* 2012). The high electrolyte composition of the very hard water used here provided favorable conditions for agglomeration especially because no surface modification or coating was applied to the nanoparticles.

Table 6.2: The hydrodynamic size (nm) and zeta potentials of the nanoparticles measured under experimental conditions.

		Hydrodynamic size (nm)				Zeta potential (mV)			
Concentration (mg/L)		0.01	0.1	1	1000	0.01	0.1	1	1000
Test start	*n*ZnO	326.5	822	1020	1299	-9.9	-7.7	-8.8	-5.1
	*n*Ag	667	716	639	1313	-9.2	-6.8	-8.4	-3.6
4 days-test end	*n*ZnO	422	726	1158	1350	-9.6	-11	-10.7	-6.4
	*n*Ag	402	900	1300	727	-7.5	-10.1	-11.6	-5.6
14 days-test end	*n*ZnO	574.6	531	426	1129	-9.3	-10.3	-8.9	-4.9
	*n*Ag	760.95	352	629	365	-9.6	-9.3	-8.8	-5.1

The hardness of water has been widely reported to exacerbate the agglomeration of ENPs (Jiang *et al.* 2009; Zhang *et al.* 2009; El Badawy *et al.* 2010; Liu and Hurt 2010; Bian *et al.* 2011; Delay *et al.* 2011; Unrine *et al.* 2012; Chernousova and Epple 2013; Yu and Liu 2013). The high ionic strength of water reduces the inter-particle electrostatic repulsion by "masking" the electric double layer, thereby promoting agglomeration of particles (Zhang *et al.* 2008; Jiang *et al.* 2009; Li *et al.* 2011; Zhang *et al.* 2011). The size of particles in testing media is very important because it has toxicity implications. This is because the testing media represents what the biota "get exposed to", and also influences the uptake dynamics (Singh *et al.* 2009; Hirn *et al.* 2011). Additionally, the change in size/agglomeration of ENPs in testing media alters their dissolution characteristics, and this aspect is addressed in section 6. 3.3.

6.3.3 Chemical analysis

After 4 days, silver ions were above the analytical detection level only at the highest exposure concentration (0.145 mg/L) as indicated in Table 6.3. This suggests that the dissolution of nAg was negligible as only about 0.015% of the total nominal silver was dissolved. Dissolved zinc ions were recorded at 0.25 mg/L and 12 mg/L in the 1 mg/L and 1000 mg/L exposure concentrations, respectively. The data indicate a higher dissolution rate (25% of the total nominal ZnO) at 1 mg/L exposure concentration compared to 1.2% at 1000 mg/L exposure concentration, although this translates to a significant 12 mg/L of Zn ions in solution.

Table 6.3: Measured dissolved ionic species (mg/L) for the nAg and nZnO particles.

ENPs	Duration (days)	0.01 (mg/L)	0.1 (mg/L)	1 (mg/L)	1000 (mg/L)
Ag	4	<0.025	<0.025	<0.025	0.145
	14	<0.025	<0.025	<0.025	ND
ZnO	4	<0.025	<0.025	0.250	12
	14	<0.025	<0.025	0.025	13

ND: not determined, since no plants survived at this exposure

Exposure time did not appear to influence the dissolution of the ENPs and in longer exposure tests, the dissolution of ENPs remained similar to the 4-day dissolved ions fraction. This suggests that saturation was reached by a 4-day exposure period; however, it should be noted that such equilibrium is not stable as the dissolved ions move in and out of solution depending on physico-

chemical parameters (Lee *et al.* 2012). No analysis was done at 1000 mg/L nAg because none of the plants survived exposure to 14 days and the experiment was therefore terminated.

The toxicity of metallic- and metal oxide-ENPs in aquatic systems has been associated with their ability to dissolve and produce ionic forms which then exert toxic effects (Franklin *et al.* 2007; Griffitt *et al.* 2008; van Hoecke *et al.* 2009). It is therefore necessary to distinguish between the toxicity of the particulates and the dissolved ion fraction of the ENPs in a given test medium. Dissolution results indicated negligible solubility (*ca* 0.1 mg/L at the highest exposure concentrations) for nAg and the toxic effects of the nAg observed in this study are therefore caused mainly by the particulates. These findings are in agreement with previous findings of low nAg dissolution and its observed toxicity was correlated to the particulates (Griffitt *et al.* 2008; Navarro *et al.* 2008; Choi *et al.* 2010; Oukarroum *et al.* 2013).

Although limited dissolution may have taken place, the resultant positively charged Ag ions could have played a role in reducing the negative surface charge of the ENPs at 1000 mg/L, an effect that has been quantified previously by Degen and Kosec (2006). One would have expected the lower pH (5.4-5.5) used in this study to be more favorable towards dissolution. However, the high electrolyte concentration and nutrient composition of the testing medium resulted in the agglomeration and sedimentation of nZnO in the test vessels (Figure 6.3). Silver nanoparticles are known to form complexes with anions (Unrine *et al.* 2012; Yu *et al.* 2013) – which are nutrient components of the water used in this study. Generally, ENPs agglomerates are prone to sedimentation and hence become less mobile (Yu *et al.* 2013), especially in high ionic strength media (Delay *et al.* 2011; Liu *et al.* 2012; Unrine *et al.* 2012). Also, because the test system was static (renewal after 7 days for the 14 days test), the dissolved oxygen was depleted, thereby further limiting the dissolution of nAg (Zhang *et al.* 2011; Liu *et al.* 2012). Liu *et al.* (2012), for instance, showed that even under favorable pH conditions for dissolution, nAg requires dissolved oxygen because anoxic conditions inhibits the dissolution process.

Figure 6.3: Image illustrating settling out from suspension of large nZnO particles in media test conditions.

Although metallic silver and nAg can be expected to release Ag ions (slow dissolution) after introduction into pure/inert water, this phenomenon is not directly applicable in "complex" media systems. This is because both dissolved and colloidal silver undergo complexation with other elements resulting in precipitation and transformation (Chernousova and Epple 2013). In essence, Ag ions occur in very low concentrations in natural aquatic environments because they easily bind to negatively charged ligands resulting in highly complex speciation patterns that are a factor of specific mixtures of ions (Liu *et al.* 2012; Levard *et al.* 2012; Unrine *et al.* 2012). The negative zeta potentials of the nAg measured in this study is evidence of an increased influence by negatively charged species in the testing media (Zhao *et al.* 2005; Degan and Kosec 2006; Li *et al.* 2011). Similar to other findings (Kittler *et al.* 2010b; Zhang *et al.* 2011), an increase in dissolution linked to the exposure period as suggested by Liu and Hurt (2010) was not observed, where the exposure was prolonged up to 120 days. These results are in agreement with previous findings regarding the influence of abiotic parameters on the behavior and fate of nAg. These findings further stress the importance of evaluating the chemical characteristics of test media and the analysis of dissolved ionic component in any studies aimed at evaluating the toxicity of nAg particles, to avoid what seems to be a general assumption that nAg toxicity is mainly driven by Ag ions.

It is clear that the behavior and fate of nAg in the aquatic environment is complex and variable as a result of the influence by numerous ambient abiotic factors. Therefore, this requires a case-by-case evaluation in order to clarify the behavioral dynamics of nAg in a given system. From these findings, the stability of nAg suggests that the particulates are able to accumulate, persist and be transported in the aquatic environment. It is also likely that, depending on the abiotic

characteristics, the ENPs can later de-agglomerate to form smaller particles, which then dissolve thus producing bioavailable ionic species that have largely unknown implications for aquatic biota.

Relative to nAg, nZnO yielded markedly high concentrations of dissolved Zn ions which increased with an increase in exposure concentration, but independent on the exposure time. It has earlier been reported that Zn ions can also account for toxicity effects observed for nZnO (Xia *et al.* 2008; Zhu *et al.* 2009; Blinova *et al.* 2010; Miller *et al.* 2010; Shaw and Handy 2011) and even lower dissolved Zn concentrations than reported in this study have been reported to induce oxidative stress in duckweeds (Parlak and Yilmaz 2012). The stability and sedimentation of nZnO particles observed in this study compares well with other findings (Bian *et al.* 2011). This effect is caused by the reduction of electric repulsion through the masking of the electric double layer energy by the media electrolytes as well as the reduction of van der Waals forces (Jiang *et al.* 2009; Li *et al.* 2011). Therefore, the presence of electrolytes reduced the inter-particle electric tension resulting in agglomeration accompanied by a reduction in zeta potential (see Table 6.2) as evidenced by marked sedimentation recorded in this study. A study by Zhang *et al.* (2008) showed the dominance of the repulsive electric double layer between nZnO in inert pure water; however, such electric repulsion is reduced to negligible levels in exposure media that have a high ionic strength - such as the media used in this investigation.

The low solubility of nZnO in hard water recorded in here agrees with earlier findings by Reed *et al.* (2012), where particles settled out of suspension. Agglomeration of nZnO up to micrometre range in high IS has also been reported (Li *et al.* 2011). These results are in agreement with these findings where it was observed that large agglomerated particles, which confirm the settling out of the particles from suspension as shown in Figure 6.3. Other investigators have reported that increasing water IS results in an increase in agglomeration and the hydrodynamic size of ENPs (Jiang *et al.* 2009; Li *et al.* 2011). The presence of anions in the testing media can adsorb to surfaces of ENPs and influence the zeta potential (Zhao *et al.* 2005; Li *et al.* 2011; Wang *et al.* 2012), for example, a reduction in zeta potential leads to rapid formation of aggregates.

It has also been argued that in moderate to very hard water, Zn ions can either adsorb to large particulates that settle out of suspension, or remain on filters during filtration and are therefore effectively removed from the solution – thereby further reducing dissolution (Reed *et al.* 2012; Li *et al.* 2011). The adsorption of electrolytes was inevitable because of the high inorganic electrolyte composition of exposure media used. This process accounts for reduced zeta potential values on the largest nZnO particles because the surface charge of the particle in solution is

known to be influenced by adsorbed species (Degen and Kosec 2006). Generically larger particles possess relatively less reactive surfaces. Therefore, it is likely that fewer anions were adsorbed to larger particles at the highest exposure concentrations (thereby low zeta potentials) compared to smaller particles at lower exposure concentrations, which had relatively stronger surface charges. These findings confirm the work of Johnston *et al.* (2010b) but are not in agreement with Zhang *et al.* (2011), where the latter observed that smaller ENPs carried lower zeta-potential values than larger particles.

In addition, there is a strong likelihood that the higher quantity of positively charged dissolved Zn^{2+} species adsorbed to nZnO and contributed to the reduction of the negative nZnO zeta potentials by increasing the positive surface charge (Degen and Kosec 2006), hence lowered zeta potentials as observed. Such an effect is highly likely in the case of nAg zeta potentials at the highest exposure concentration tested. These results indicate that the media parameters, mainly electrolyte ions in this case, play a significant role in influencing the surface charge of ENPs (Li *et al.* 2011), and therefore the surface charge of nanoparticles is not simply a function of their size. Also, current findings suggest – contrary to previous general assumptions (Auroja *et al.* 2009; Kasemets *et al.* 2009; Shaw and Handy 2011) – that nZnO actually does not dissolve relatively easily and that the dissolved Zn becomes the dominant component. Although these previous assumptions are not necessarily flawed, current findings suggest that such dynamics are highly dependent on media characteristics, and should be interpreted carefully on that basis.

One other aspect that was observed was that a combination of media buffering capacity (caused by the high IS of the media) and sedimentation of ENPs masked pro-dissolution pH conditions, and hence did not favour nZnO dissolution. Low pH conditions are known to promote the dissolution of nZnO, an effect that was not observed in this study but one which has been reported by other authors (Zhang *et al.* 2008; Bian *et al.* 2011).

Theoretical classical thermodynamics (Noyes-Whitney equation) dictates that smaller particles dissolve at a higher rate than larger particles. However, this was not observed in this study, particularly at lower exposure concentrations (smaller particle sizes), where the dissolved Zn was found to be below analytical quantification concentrations. Current findings therefore support the earlier results reported by Bian *et al.* (2011), who argued that, quantitatively, such a theory is inadequate to offer a “perfect-fit” account. The morphology of the ENPs (nAg and nZnO) could have played a pivotal role in their dissolution but this aspect was not explored in detail the current study. For instance, the differences in particle morphology between nAg (spherical) and nZnO

(multi morphologies) (Figure 6.1) suggests such a possibility. This aspect will be investigated further in future research.

6.3.4 Free radicals

An analysis of total free radicals (OxiSelect™ *In Vitro* ROS/RNS) on samples exposed to nAg revealed an initial increase (though not statistically significant) in free radicals (0.01-0.1 mg/L), followed by a reduction in samples exposed to 1 and 1000 mg/L over 4 days (Figure 6.4a). However, after 14 days, the amount of free radicals for nAg increased significantly at 0.01 and 1 mg/L whilst samples exposed to 0.1 mg/L remained similar to the control (Figure 6.4b). No plants survived exposure to 1 000 mg/L over 14 days.

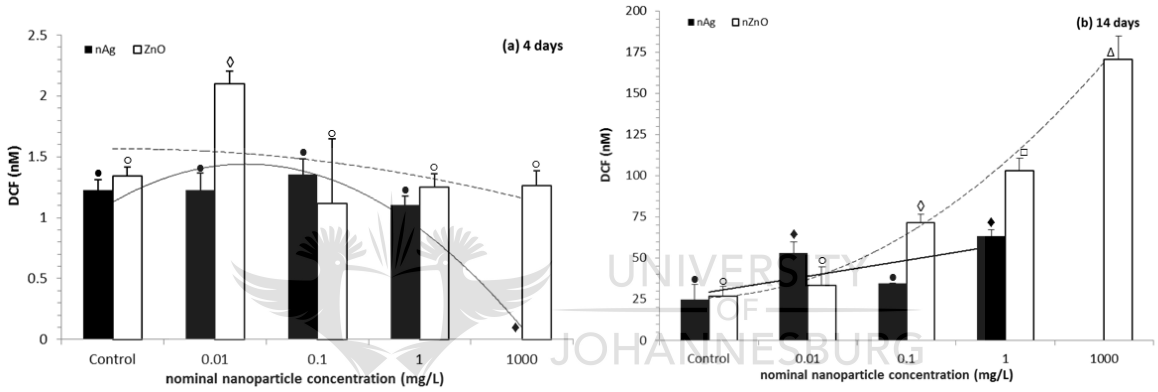

Figure 6.4: Quantitative levels of ROS and RNS measured in plant tissue after exposure to nAg and nZnO for; (a) 4 days and (b) 14 days. Different symbols indicate significance difference between treatments where $p < 0.05$, whilst similar symbols indicate no significant difference.

On the 4-day exposures to nZnO, the quantity of free radicals increased in samples in 0.01 mg/L whilst in the other concentrations, they were statistically similar to the controls (Figure 6.4a). After 14 days, a concentration-dependent influence was observed in nZnO exposed samples. An initial free radical increase at 0.01 mg/L (not statistically significant relative to control) was followed by statistically significant increases as the nZnO exposure concentration increased (Figure 6.4b).

The quantitative analysis of H_2O_2 on plants exposed to nAg for 4 days revealed significantly lower H_2O_2 amounts in samples exposed to the highest nAg concentration. Moreover, samples in 0.01-1 mg/L nAg had significantly higher H_2O_2 levels than the controls (Figure 6.5a). Samples exposed to nZnO for 4 days had statistically similar H_2O_2 levels compared to the control, although these samples had higher average H_2O_2 concentrations than the control (Figure 6.5a). After 14 days, H_2O_2 significantly increased in samples exposed to 0.1 mg/L nAg, relative the control samples.

On the other hand, samples exposed to 1000 mg/L nZnO particles had significantly increased H_2O_2 volumes in comparison to the control samples.

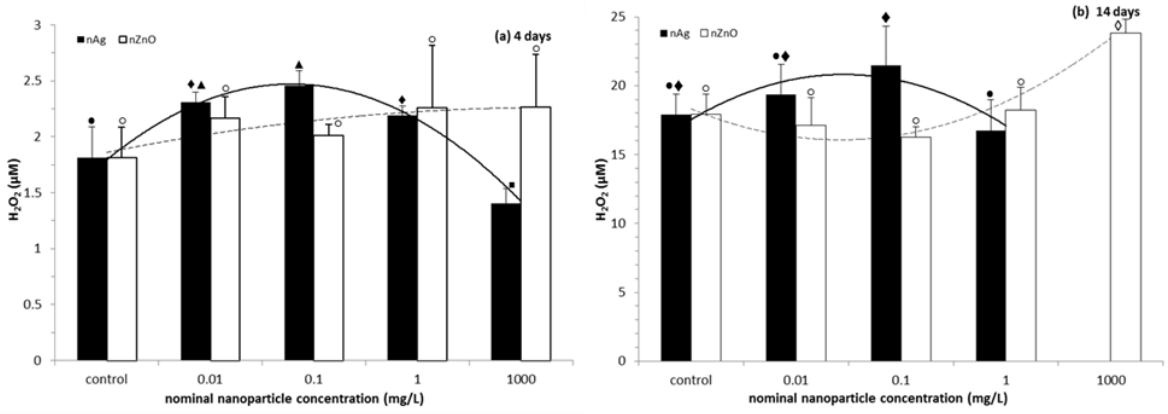

Figure 6.5: Quantitative levels of H_2O_2 measured in plant tissue after exposure to nAg and nZnO particles for; (a) 4 days and (b) 14 days. Different symbols indicate significance difference between treatments where $p<0.05$, whilst similar symbols indicate no significant difference.

Quantitative analysis of free radicals indicated varying degrees of oxidative attack by nAg and nZnO on plant samples. It was also observed that free radical activity on control samples increased with exposure time. The increased oxidative activity in the control samples can be accounted by the fact that free radical production is a natural process which takes place in healthy samples (not exposed to chemical toxicants) and is known to increase with age (Alscher *et al.* 2002; Mittler 2002; Blokhina *et al.* 2003; Asada 2006). The above-normal generation of free radicals as a result of exposure to ENPs has been previously suggested as one possible route through which they induce toxic effects to duckweeds (Hu *et al.* 2009; Jiang *et al.* 2012; Oukarroum *et al.* 2013) as well for other organisms (Choi and Zhu 2008). For instance, Oukarroum and colleagues (Oukarroum *et al.* 2013) reported a concentration-dependant increase of ROS production by nAg but this was only significantly higher than the blank at a 1 mg/L exposure concentration. Another study on *Spirodela polyrhiza,* only found a significant oxidative related effect at exposure to 5 mg/L of nAg (Jiang *et al.* 2012). Current results indicate that, even at a low exposure concentration of 0.01 mg/L, the ENPs generated markedly high free radical concentrations, in agreement with findings reported by Toduka *et al.* (2012). However, a distinct concentration-related effect was observed after 14 days exposure (ROS/RNS) particularly in the case of plant samples exposed to nZnO.

The quantification of H_2O_2 in plants exposed to nAg revealed an inverted bell-shaped response curve which was concentration related. It was hypothesized that the observed reduction in plant

growth/frond number at higher concentrations tracked this phenomenon. Although this was only noted in current study, the phenomenon has also been quantified elsewhere (Gubbins *et al.* 2011; Jiang *et al.* 2012; Oukarroum *et al.* 2013). Based on dissolution analysis findings, it is suggested that the observed free radical activity in plants exposed to nAg were caused by the particulate form, whilst at higher concentrations during an exposure of 14 days; dissolved Ag^{+} species may have caused additional effects. A similar hypothesis appears to hold for nZnO exposures < 1 mg/L. The highest ROS/RNS was recorded after 4 days exposure at the lowest nZnO concentration, which suggests a higher toxicity of particulates relative to dissolved Zn species. Similar findings have been reported for nAg (Choi and Hu 2008).

The study findings add further support for the opinion among scientists in the field of nanoecotoxicity that the mass per volume unit metric may not be the most suitable way to represent nanotoxicity results because highly toxic effects can be observed at low concentrations of ENPs (Warheit 2008; Dhawan *et al.* 2009; Fubini *et al.* 2010; Bouwmeester *et al.* 2011; Maynard *et al.* 2011). The oxidative influence of dissolved metallic ions from ENPs clearly remains significant for metallic- and metal oxides-ENPs; this is not surprising because metal toxicity is known to be linked to ROS production (Upadhyay and Panda 2010; Parlak and Yilmaz 2012; 2013). The significance of these results is that as the concentrations of ENPs in the aquatic environment increases, the effects of both particulates and ionic forms may synergistically cause adverse effects to higher aquatic plants, resulting in unpredictable adverse ecosystem effects.

6.3.5 Anti-oxidant activity

6.3.5.1 Total antioxidant capacity

Exposure to nAg over a 4-day period induced a significant loss in TAC only in samples exposed to 1000 mg/L; however, the TAC levels were similar to those of control samples in plants that had been exposed to lower nAg concentrations (Figure 6.6a). Samples exposed to nZnO for the same period had a significant increase in TAC at the lowest exposure concentration but samples at other (higher) concentrations remained similar to the control (Figure 6.6a). The 14-day nAg exposure results were inconclusive because the TAC values remained similar for all the exposure concentrations, whilst samples exposed to nZnO over the same period revealed a concentration-dependent reduction of TAC that was statistically significant in most cases (Figure 6.6b). An increase in the quantity or activity of biomolecules in the defense against free radicals has been reported to increase after exposure to chemical toxicants including ENPs (Oberdörster 2004; Arora *et al.* 2009; Wang *et al.* 2009; Choi *et al.* 2010; Jiang *et al.* 2012). Therefore, current results

reveal a significant influence in some cases by the ENPs on the biological anti-oxidative defense mechanism of aquatic plants.

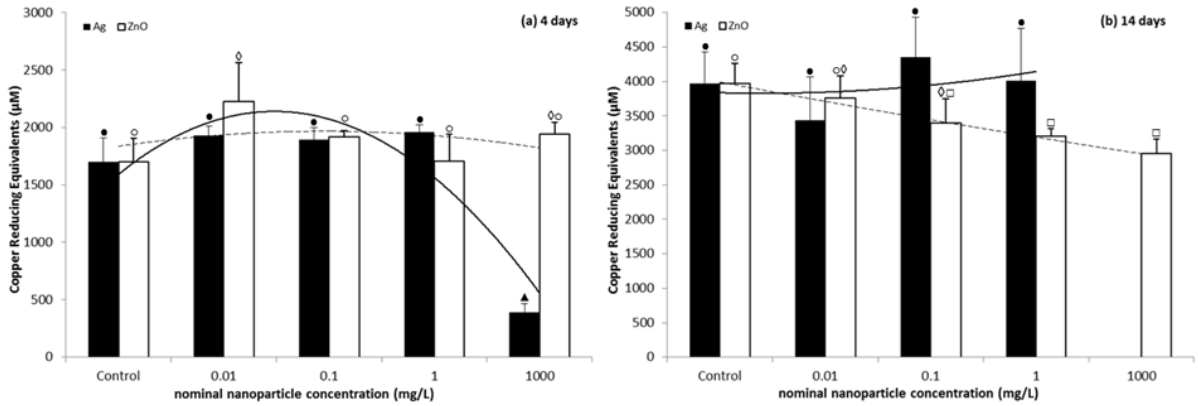

Figure 6.6: The total antioxidant capacity (TAC: µM copper reducing equivalents) measured in plant tissue after exposure to nAg and nZnO particles after (a) 4 days and (b) 14 days. Different symbols indicate significance difference between treatments where $p<0.05$, whilst similar symbols indicate no significant difference.

Based on the dissolution of nAg after 4 days, it was assumed that the loss of TAC observed at 1000 mg/L was driven by dissolved Ag ionic species. The role of particulate silver could have been better elucidated if the particles concentration per unit volume had been investigated, for example using the nano tracking analysis, however the equipment was not available and this will be pursued in future work. The TAC results obtained from nAg exposures appeared to relate partly to the free radical activity results. From the 4-day exposure to nAg, the TAC at 0.01-1 mg/L appeared to be less influenced by significantly higher amounts of H_2O_2 recorded at these levels, yet the TAC results related well to the ROS/RNS results for the same samples, thereby suggesting an "attack-response" relationship. However, no such direct relationship could be established for samples exposed to nAg for 14 days between free radical activity (both ROS/RNS and H_2O_2), and the TAC. The significant increase of TAC in samples exposed to 0.01 mg/L nZnO over a 4-day period relates well to the high ROS/RNS observed at the same concentration (see Figure 6.6a). Such results (0.01 mg/L nZnO; 4 days) illustrate an increased oxidative offence (ROS/RNS) as result of exposure to ENPs accompanied by a responsive antioxidant defense mechanism (TAC) in plants.

As mentioned earlier, such oxidative attack is assumed to arise from the particulate form of nZnO, based on the dissolution results presented in section 6.3.3. Additionally, the TAC results from nZnO exposure over a 14-day period reveal that the plants continuously lost their anti-oxidative

strength as they defended against increasing oxidative attack caused by exposure concentration increases. These TAC results relate well to ROS/RNS findings over the same exposure period. It is not uncommon for the oxidative effects to be most severe at the lowest exposure concentrations (Choi *et al.* 2010; Balen *et al.* 2011). The loss of TAC seems to be related to cellular damage (Choi *et al.* 2010), or protein degradation (Cheng 2012) as a result of the effects of ENPs compromising the plants physical and metabolic integrity. This is because biological samples are known to lose their antioxidative capacity as a result of the accumulation of free radicals, inactivation of proteins, and/or damage of cellular and sub-cellular membranes (Castex *et al.* 2010; Parlak and Yilmaz 2013).

6.3.5.2 Superoxide dismutase (SOD) activity

The 4-day exposure to both ENPs indicated an influence on the activity of SOD relative to the control samples (Figure 6.7). Samples exposed to 0.01 and 1000 mg/L nAg had higher SOD activity than the control samples; however, the samples exposed to 0.1 and 1 mg/L exhibited inhibited SOD activity relative to the controls. The observed inhibition of SOD activity relates well to H_2O_2 levels for the same exposure period and concentrations (Figure 6.5a). The increasing levels of H_2O_2 up to 0.1 mg/L likely inhibited the activity of SOD. Although the H_2O_2 appeared to decrease at the two highest concentrations, this was as a result of a reduction in plant tissue mass (observed but not quantified) and the view is held that per unit of plant tissue mass, the H_2O_2 levels may have increased even further at these concentrations.

The SOD activity was, however, assessed per unit protein concentration rather than on the available tissue biomass. The assumption that the reduction in plant tissue biomass masked the increase of H_2O_2 quantity was supported by significantly higher SOD activity at the highest nAg exposure concentration, driven by the concentration of dissolved Ag. Overall there was an inhibition of SOD activity in plants exposed to nZnO for 4 days (Figure 6.7a), except for a significant increase at 0.1 mg/L, which could not be accounted for by the observed free radical activity or the results on dissolution and agglomeration.

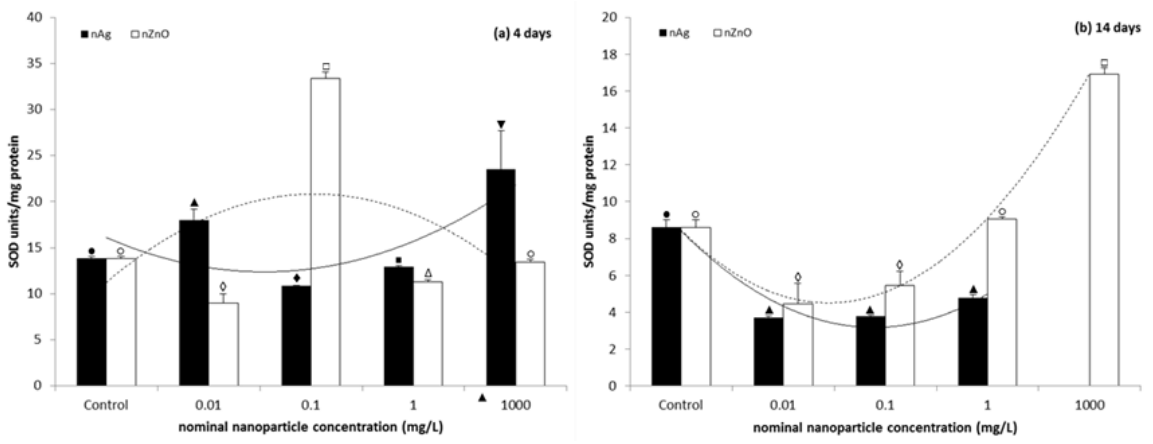

Figure 6.7: The activity of superoxide dismutase (SOD) measured in plant tissue after exposure to nAg and nZnO particles after: (a) 4 days and (b) 14 days. Different symbols indicate significance difference between treatments where $p<0.05$, whilst similar symbols indicate no significant difference.

After a 14-day exposure to nAg, an inhibition effect was observed for SOD activity at all exposure concentrations; this was significantly lower than the controls. However, plants exposed to nZnO had an inhibition of SOD activity at the two lowest concentrations followed by an increase at 1 mg/L (similar to control), and significantly higher activity in plants exposed to 1000 mg/L. It was observed that, after 4 days, the control samples had relatively higher SOD activity than the same control samples after a 14–day exposure.

The 14-day results for plants exposed to both ENPs indicated good relation to the H_2O_2 quantities observed for a similar exposure period. The plants that were exposed to nZnO had a higher inhibition of the antioxidant activity at the lowest exposure concentration, elevated toxicity at lowest exposure concentrations caused by reduced ENP size, and elevated available reactive surface area (Nair *et al.* 2009; Auffan *et al.* 2010; Wong *et al.* 2010; Maynard *et al.* 2011); this behavior of ENPs remains one of their distinguishing features in comparison to their counterpart bulk materials.

As mentioned earlier, the decrease of plant biomass at the highest exposure concentrations masked the concentration-driven increase of H_2O_2 because the former was assessed on total available sample rather than the unit mass of each sample. The SOD activity in samples exposed to nAg over 4 days could not be directly linked to levels of ROS/RNS and H_2O_2. Similar findings reported earlier that SOD activity could not be linked to oxidative stress (Choi *et al.* 2010; Wong *et al.* 2010). The SOD activity in plants exposed to metal contaminants is highly variable but, overall, presents a case of deviation from “healthy” control samples (Sharma and Dietz 2009).

One key lesson from this study is that the non-uniform relationship in certain instances between ROS and SOD supports the importance of using multiple lines of evidence on a tiered approach when assessing oxidative stress. This is because both inhibition and activation of SOD activity can be related to oxidative stress. On the other hand, samples exposed to nZnO over 14 days suggest that concentration-related increase of ROS/RNS over the same period induced a systematic inhibition of SOD activity (from 0.01 mg/L onwards). This is an effect that is related to the observed depletion of TAC in the same samples. Furthermore, levels of ROS/RNS and H_2O_2 on samples exposed to nAg over 14 days were often not statistically different to control samples, and anti-oxidative analysis (SOD activity and TAC) appeared to relate to such free radical activity.

The activation of SOD activity (relative to controls) is linked to its detoxification of accumulated superoxides (Cheng 2012; Cheng and Cheng 2012) but, additionally, accumulated superoxides can overcome the defense mechanisms by initiating lipid peroxidation as well as the formation of more destructive hydroxyl radicals that suppress the production of SOD, and hence inhibit its activity (McCord 2008; Foyer and Noctor 2009; Cheng and Cheng 2012; Parlak and Yilmaz 2013).

The direct inhibition of SOD activity has been linked to the deactivation of the enzyme bound heme group, which suppresses the activity of SOD (Willekens *et al.* 1997; Parlak and Yilamz 2013) and the oxidation of amino acid side chains which induce carbonyl groups on antioxidants (Balen *et al.* 2011). McCord (2008) reported a direct relationship between the inhibition of SOD activity and the peroxidation of cellular lipids. Therefore, it is hypothesized that to better account for the observed inhibition of SOD activity it is important to systematically study protein integrity as a higher tier assessment. For instance, the loss of cellular integrity caused by oxidative damage can account for the observed reduction in plant growth (though this was not investigated in detail here).

Nonetheless, other studies have shown that increasing free radical attack can be related with reduced photosynthesis and plant growth (Wong *et al.* 2010; Gubbins *et al.* 2011; Zhang *et al.* 2011; Jiang *et al.* 2012; Wang *et al.* 2012). Severe effects of oxidative stress include, but are not limited to, lipid peroxidation and the damage of cellular and sub-cellular membranes (Castex *et al.* 2010; Parlak and Yilmaz 2012), which can alter the physiological state of healthy plants, including interruption to photosynthesis which is an essential process for energy synthesis and for plant growth.

6.4 Concluding remarks

In this study, the findings strongly suggest that the potential risks of nAg and nZnO towards higher aquatic plants are dependent on environmental abiotic parameters. Thus conclude with the following remarks:

- Current results stressed the absolute necessity of determining the primary size of ENPs before they are introduced into test media as well as size in test, so as to avoid the derivation of misleading conclusions based on the influence of particle size on the observed toxicity.

- Based on current results and existing literature, it is clear that both particulates and dissolved species accounts for the toxicity of nAg and nZnO. However, it is argued that this is mainly determined by the exposure media chemistry and physical parameters.

- The high stability of ENPs observed in this study supports the contention that the evaluation of their impacts in aquatic environments should not only consider present fate and biological effects, but should also take account of future implications because changes in the physicochemical environment can result in ENPs that are more hazardous to aquatic life forms.

- Although earlier findings suggested that the toxicities of dissolved Zn and nZnO are similar [65, 103, 104], this should not be taken as an “umbrella” assumption. This is because current results and the results of other studies indicate that the toxicity of nZnO is controlled by ambient media chemistry, and therefore, the interpretation/comparison of the toxicity of ENPs (especially metallic forms) should take into account the properties of the testing media used. As an example, the IS and nutrient composition of the water used in this investigation provided buffering capacity relevant to toxicity to a certain extent. As a result, a direct comparison of current toxicity results to those of any other study would be misleading if the media characteristics and toxicity influence are not taken into consideration.

- In this study, evidence of free radical activity arising from nAg and nZnO on *Spirodela punctuta* was provided. Without the use of the Ag and Zn salts, no definite conclusions could be made regarding the free radical activity and anti-oxidative defence observed in those concentrations where dissolution occurred. However, based on the evidence of

oxidative stress arising from ENPs as well as the presence of dissolved ionic forms, it was concluded that the toxicity of nAg and nZnO was driven both by particulates as well as the dissolve ionic species, and was directly influenced by environmental conditions (e.g., IS, pH, organic matter, etc.).

- The results reported here indicate that nAg and nZnO can pose risks towards higher aquatic plants. However, additional data need to be generated for the uptake dynamics of these ENPs by aquatic higher plants, and on the specific mechanisms by which media chemistry parameters influences their uptake. The future work will aim to more clearly understand the dissolution dynamics of these ENPs through detailed speciation analysis based on results obtained here, and a determination of the mechanisms that influence their uptake by higher aquatic plants so that the risks that can potentially arise from ENPs can be more clearly understood.

CHAPTER 7
Summary, concluding remarks and future perspectives

7.1 Summary and concluding remarks

As an overall aim; this study sought to investigate fate and behaviour of metal-based ENPs in aqueous environments, as well as their interaction and toxicity effects towards free floating vascular plants. The foundation hypothesis was that the interaction of nAg and nZnO with higher aquatic plants is interactively influenced by the physical and chemical characteristics of the ENPs and experimental aqueous media. To achieve the task, research questions were formulated in order tackle specific objectives. These were broken down as follows:

Objective 1: Review the current state of knowledge on the interaction of ENPs with higher aquatic plants.

The literature survey undertaken revealed that interaction of aquatic higher plants with ENPs results from adsorption of ENPs onto plant surfaces, and also internalisation into plant tissue, with roots being the major sites of uptake. This may lead to bioconcentration and toxicological effects; the former indicating potential for trophic transfer of ENPs within aquatic ecosystems. Interaction was observed to be highly dynamic and driven mainly by physico-chemical properties of ENPs and experimental medium, as well as plant species phenotypic and physiological traits. For instance, water quality properties can induce higher agglomeration rates which further result in size exclusion of larger agglomerates by plants (Hu *et al.* 2013). Conversely; water quality properties can improve stability of ENPs by enhancing retention of primary size, hence improve internalisation; this has been demonstrated with NOM through steric stabilisation of nAu (Glenn and Klaine 2013). The role of ENPs size in regulating internalisation was well demonstrated with nAu by Glenn *et al.* (2012), indicating that small primary size alone does not effectively guarantee internalisation, as water chemistry can alter bioavailable size, and plant characteristics play a major role.

It has been previously illustrated that plants with more developed root systems accumulate ENPs at a higher rate compared to those with simple roots or that lack root systems (Glenn *et al.* 2012). In fact; the lack of root system can effectively reject internalisation of ENPs, irrespective of their size (Glenn *et al.* 2012). Further important plant features that regulate internalisation of ENPs are the plant cell wall pores; which based on bioavailable ENPs size control their entry. Knowledge surrounding ENPs uptake dynamics by aquatic plants remain poorly known, this aspect still requires further investigations focussing on ENPs bioavailable state (chemical and physical), as well as plant properties.

An understanding of ENPs uptake dynamics is important because uptake rate can directly be linked to toxicity effects. To date, toxicity of metal-based ENPs towards aquatic plants has been mainly associated with dissolved metallic forms, and rarely with nano particulates. This information emphasises solubility of metal-based ENPs as a dominating mechanism for toxicity effects induction. Hence, detailed dissolution analysis is highly recommended for investigations on interaction, internalisation and toxicity effects of metal-based ENPs towards aquatic plants. This will assist generate a quality data pool to gain better insights into hazard, exposure, and risk dynamics of metal-based ENPs in aquatic ecosystems.

Objective 2: Investigate the physical and chemical transformations of nAg and nZnO in aqueous media in order to gain insights into environmental fate and behaviour dynamics of the ENPs in water bodies.

Behaviour of nAg was observed to be size dependent under different exposure conditions. For instance; the behaviour of 10-nAg and 40-nAg in modified river water was different. Generally size transformation tended to favour agglomeration, but interestingly, larger size agglomerates resulted from primarily smaller 10-nAg compared to 40-nAg. As a result of their small size and larger surface are; 10-nAg were more reactive resulting to higher agglomeration rates compared to 40-nAg. This was evidenced by higher drift velocity of 10-nAg compared to 40-nAg. Such findings illustrated the dynamic behaviour of ENPs, which requires non-conventional approaches from regulation of bulk scale contaminants. On the other hand; less reactive 40-nAg were mostly stable under various water conditions which can translate to prolonged persistence, exposure and effects in water ecosystems compared to smaller counterparts. However; expected differences in solubility between 10-nAg and 40-nAg were not observed, this was mainly attributed to few sampling period and replicates which limited establishment of trends and enable statistically sound comparison.

The influence of exposure water chemistry on fate of ENPs was illustrated by differing physical and chemical behaviour of nAg and nZnO on variation of HM ionic strength, and filtering levels of modified river water. When comparing DI water and modified river water, nAg size (10-nAg and 40-nAg) in DI water was smaller and more uniform in DI water compared to river water where larger agglomerates resulted. The presence of numerous organic and inorganic factors in river water weakened inter-particle repulsion by adsorption, shielding of primary particle charge, hence conditions favoured higher agglomeration compared to DI water. However; there were insignificant differences between stability of nAg in 0.2 and 0.45 µm filtered water, as nAg size, concentration, and absorbance spectra between the two filtration levels remained relatively

similar. However; observed differences in dissolution between the two filtration levels for both 10-nAg and 40-nAg could not be supported as a result of low statistical confidence.

In the case of HM; ionic strength increase (50HM to 100HM) resulted in considerable size differences of nAg powder forms. Agglomerates were larger in higher ionic strength, and this was attributed to higher surface charge shielding effect of 100HM which possessed about 2 times more electrolytes than 50HM. Ionic strength also influenced solubility of powder nAg and nZnO. Dissolution of both ENPs was relatively inhibited in 100HM, this being always significant for nZnO and no always for nAg. This was attributed to high proportion of adosrbants in 100HM which reduced available reactive surface area for oxidation.

It was further expected that concentration of nAg and nZnO will differ considerably between 50HM and 100HM. However; poor dispersion of powder form ENPs resulted in poor quantification with NTA technique, which was not successful for nZnO. Even though there were wide data spread in nAg concentrations obtained with NTA; generally particle concentration was higher in 100HM compared to 50HM. These findings were in contradiction to expectations; as it was expected that resultant larger nAg agglomerates in 100HM would succumb to gravitational sedimentation at a higher rate to smaller counterparts in 50HM, an effect that would reduce particle numbers in suspension.

Overall, in aqueous environments ENPs undergo chemical and physical transformations which are interactively driven by primary ENPs characteristics, and exposure medium chemistry. These forms transformation were observed with nAg and nZnO introduced into artificial HM and modified river water. The results illustrated the highly dynamic behaviour of ENPs in aqueous environments, requiring complementary analytical tools to quantify. Furthermore, the risk posed by ENPs in aqueous environments can be expected to vary temporally and spatially, dependent on water quality regimes and physical properties of a water resource.

Objective 3: Investigate the role of ENPs size and aqueous media characteristics on uptake, accumulation and effects of nAg and nZnO on free floating higher aquatic plant specimen; *Salvinia minima* and *Spirodela punctuta*.

Investigations undertaken under this objective enabled generation of new knowledge with respect to interaction of metal-based ENPs with higher aquatic plants.

First, it was illustrated with cit-coated nAg that interaction of ENPs with aquatic plants is highly driven by particle size, where bioconcentration of Ag by *S. minima* was higher in specimen

exposed to smaller 10-nAg compared to 40-nAg. Partly this was ascribed to relatively higher reactivity of 10-nAg as a result of their larger surface areas which probably resulted in higher adsorption to plant surfaces. Furthermore, relatively higher dissolution of 10-nAg under some water quality regimes was suggested to have contributed to elevated Ag accumulation from these nAg forms. Even though 10-nAg had elevated agglomeration rates and were highly instable, however; it was hypothesized that this probably did not completely exclude internalisation of individual particles and smaller agglomerates by plant cell wall pores. Overall, the study findings were in agreement with current literature (see Chapter 2) regarding accumulation of metallic forms in particulate as well as dissolved species.

Even toxicity effects in *S. minima* exposed were generally more pronounced to samples exposed to 10-nAg; further corroborating earlier suggestions of elevated toxicity at nanoscale where lower end scale tends to be more hazardous (Colvin 2003; Oberdorster 2004; Nel *et al.* 2006). This was in good agreement with findings on Ag accumulation; further illustrating that bioaccumulation of xenobiotics is generally a precursor of toxicity (Luoma and Rainbow 2008).

However; caution is required when assessing ENPs risk, and not simply associate higher risk with smaller ENPs. For instance; high stability of 40-nAg under different water chemistries suggested that exposure from these nAg forms can be prolonged and results in chronic effects compared to 10-nAg which were highly toxic over short time period. Therefore risk assessment of ENPs should not only consider present fate and biological effects, but should also take into account future implications because changes in the physicochemical environment can result in ENPs that are more hazardous to aquatic life forms effects.

Exposure water chemistry was highly influential on the ENPs' behaviour and toxicity effects. For instance; particle size for both 10-nAg and 40-nAg obtained in NOM varied to Ca^{2+} and MHW regimes where significantly larger sizes resulted. This suggested that NOM was highly stabilising of nAg in aqueous environments. The stabilising effect of NOM was further illustrated in Ag accumulation, where highest Ag accumulation was recorded in NOM water regime. Such findings suggested that nAg was relatively more bioavailable in NOM water treatments.

Furthermore, dissolution of 10-nAg and 40-nAg was dependent on exposure water chemistry, which indicated varying chemical transformations between the water regimes. This revealed the interplay between water chemistry and nAg characteristics on interaction with *S. minima*. Most importantly, such results indicated that internalisation of nAg was probably in the form of both particulate nAg and dissolved Ag species dependent on water chemistry, because nAg size and dissolution dominated Ag accumulation at varying water chemistries. Similar findings were

obtained on the toxicity of nAg and nZnO (powder forms) towards *S. punctuta*, where both particulates and dissolved species of Ag and Zn accounted for toxicity of the ENPs, as a factor of exposure water chemistry. Further influence of water chemistry was observed with cit-coated nAg toxicity on *S. minina*, where toxicity severity was altered between MWH, Ca^{2+} and NOM water regimes.

Findings of this study provided further credence of oxidative stress induction as amongst precursors of ENPs toxicity. Firstly; samples of *S. punctuta* exposed to nAg and nZnO experienced increased free radical activity, where accumulation of ROS and RNS increased more prominently over 14 days, whilst accumulation of H_2O_2 was highly increased at lower ENPs concentration over a 4 days exposure period. Extent of increased free radical activity was further evidenced in concurrent increase of antioxidant mechanisms to counteract (detoxify) above normal free radical concentrations. The nAg were relatively more toxic than nZnO resulting in reduced biomass and no plant survival at highest exposure concentration. Toxicity of nAg was mainly attributed to particulate nAg forms compared to dissolved Ag species because of poor solubility of nAg under test conditions. Conversely, nZnO toxicity was mainly driven by dissolved Zn species because of notable dissolution of nZnO recorded.

In closing; few outcomes of this study are worth highlighting:

- Research on the interaction of ENPs with aquatic higher plants is still at infancy. There is still poor knowledge regarding ENPs uptake kinetics by the plants; where the role of ENPs characteristics, water physico-chemical properties, and plants traits (physiological, phenotypic) remains poorly understood.
- Fate and behaviour of metal-based ENPs in aquatic environments primarily depend on ENPs characteristics and water chemistry. Across the board behaviour differences between nAg sizes, were observed. Furthermore; water chemistry was also shown to be highly influential in determining: (i) ENPs stability and transformations, (ii) interaction with plants, and (iii) toxicity mechanisms to plant species.
- Toxicity of metal-based ENPs is dependent on ENPs size and water chemistry, resulting from both dissolved metallic species and nano-particulates, as driven by interplay of water chemistry and ENPs properties.
- Aquatic higher plants accumulate nano-pollutants, hence in aqueous environments can be reservoirs of such pollutants and facilitate their trophic transfer.

7.2 Future perspectives

- Long term studies investigating the stability and transformations of ENPs in aqueous environments are needed to establish persistence of ENPs and long term implications. This can be achieved through complementary coupling of analytical techniques that track behaviour and fate of ENPs, for instance over months, even years where possible. Continuous ENPs characterisation in such studies can never be over emphasized as behaviour of ENPs is highly dynamic, and the ENPs properties at start of an experiment can be significantly altered in a few minutes.
- To improve knowledge on interactions of ENPs and aquatic plants; detailed analytical efforts need to be given towards characterising physical and chemical properties of ENPs and exposure water, in order to understand bioaccessibility. Furthermore, the biology of test species needs to be well known and taken into consideration as that will give better insights about processes at play, which can be associated to nutrient uptake and regulation.
- Detailed ENPs characterisation in nanotoxicity studies is highly essential. Over long term, the data pool generated by the research community will enable discrimination and ranking of drivers of ENPs toxicity. Hopefully this will develop safer-by-design approaches, where manufacturing of nano-enabled products strives to inhibit nanotoxicity whilst still maintaining good product performance.
- Accumulation of ENPs by higher aquatic plants may hold potential for *green* and cheaper bioremediation for removal of nano-pollutants in aquatic ecosystems. Research investigations in this aspect are highly encouraged.

CHAPTER 8

References

Adani F, Papa G, Schievano A, Cardinale GD, Imporzano G and Tambone F. 2011. Nanoscale structure of the cell wall protecting cellulose from enzyme attack. *Environmental Science and Technology*, 45(3): 1107-1113.

Allen HJ, Impellitteri CA, Macke DA, Heckman JL, Poynton HC, Lazorchak JM, Govindaswamy S, Roose DL, Nadagouda MN. 2010. Effects from filtration, capping agents, and presence/absence of food on the toxicity of silver nanoparticles to *Daphnia magna. Environmental Toxicology and Chemistry*, 29(12): 2742-2750.

Alscher RG, Erturk N and Heath LS. 2002. Role of superoxide dismutases (SODs) in controlling oxidative stress in plants. *Journal Experimental Botany,* 53(372): 1331-1341.

American Society for Testing and Materials (ASTM). 2006. Standard terminology relating to nanotechnology. E 2456-06. West Conshohocken, PA.

Applerot G, Lipovsky A, Dror R, Perkas N, Nitzan Y, Lubart R and Gedanken A. 2009. Enhanced antibacterial activity of nanocrystalline ZnO due to increased ROS-mediated cell injury. *Advanced Functional Materials*, 19 (6): 842-852.

Arora S, Jain J, Rajwade JM and Paknikar KM. 2009. Interactions of silver nanoparticles with primary mouse fibroblasts and liver cells. *Toxicology and Applied Pharmacology,* 236(3): 310-318.

Asada K. 2006. Production and scavenging of reactive oxygen species in chloroplasts and their functions. *Plant Physiology* 141(2): 391-396.

Auffan M, Rose J, Proux O, Borschneck D, Masion A, Chaurand P, Hazemann JL, Chaneac C, Jolivet JP, Wiesner MR, Geen AV and Bottero JY. 2008. Enhanced adsorption of arsenic onto maghemites nanoparticles: As(III) as a probe of the surface structure and heterogeneity. *Langmuir*, 24(7): 3215-3222.

Auffan M, Rose J, Wiesner MR and Bottero J. 2009. Chemical stability of metallic nanoparticles: A parameter controlling their potential cellular toxicity in vitro. *Environmental Pollution*, 157: 1127-1133.

Auffan M, Bottero J, Chaneac C and Rose J. 2010. Inorganic manufactured nanoparticles: how their physicochemical properties influence their biological effects in aqueous environments. *Nanomedicine*, 5(6): 999-1007.

Auroja V, Dubourguier HC, Kasemets K and Kahru A. 2009. Toxicity of nanoparticles of CuO, ZnO and TiO_2 to microalgae *Pseudokirchneriella subcapitata*. *Science of the Total Environment*, 407(4): 1461-1468.

Balen B, Tkalec M, Sikic S, Tolic S, Cvjetko P, Pavlica M and Vidakovic-Cifrek Z. 2011. Biochemical responses of *Lemna minor* experimentally exposed to cadmium and zinc. *Ecotoxicology*, 20(2011): 815-826.

Baalousha M, Nam Y, Cole PA, Gaiser B, Fernandes TF, Hriljac JA, Jepson MA, Stone V, Tyler CR and Lead JR. 2012. Characterisation of cerium oxide nanoparticles- part 1: size measurements. *Environmental Toxicology and Chemistry*, 31(5): 983-993.

Baalousha M, Nur Y, Romer I, Tejamaya M and Lead JR. 2013. Effect of monovalent and divalent cations, anions and fulvic acid on aggregation of citrate coated silver nanoparticles. *Science of the Total Environment*, 454-455: 119-131.

Baalousha M, Arkill KP, Palmer RE and Lead JR. 2015.Transformations of citrate and Tween coated silver nanoparticles reacted with Na_2S. *Science of the Total Environment*, 502(2015): 344-353.

Baun A, Sorensen SN, Rasmussen RF, Hartmann NB and Koch CB. 2008. Toxicity and bioaccumulation of xenobiotic organic compounds in the presence of aqueous suspensions of aggregates of nano-C_{60}. *Aquatic Toxicology*, 86(2008): 379-387.

BCC Research, 2012. Nanotechnology: a realistic market research. NANO31E, Wellesley, USA.

Behra R and Krug H. 2008. Nanoecotoxicology-nanoparticles at large. *Nature Nanotechnology*, 3: 253-254.

Behra R, Sigg L, Clift MJD, Herzog F, Minghetti M, Johnston B, Petri-Fink A and Rothen-Rutishauser B. 2013. Bioavailability of silver nanoparticles and ions: from a chemical and biochemical perspective. *Journal of the Royal Society Interface*, 10(8): 1-15.

Benn TM and Westerhoff P. 2008. Nanoparticle silver released into water from commercially available sock fabrics. *Environmental Science and Technology,* 42(11): 4133-4139.

Bian SW, Mudunkotuwa IA, Rupasinghe T and Grassian VH. 2011. Aggregation and dissolution of 4 nm ZnO nanoparticles in aqueous environments: influence of pH, ionic strength, size, and adsorption of humic acid. *Langmuir,* 27(10): 6059-6068.

Bian J, Berninger JP, Fulton BA and Brooks BE. 2013. Nutrient stoichiometry and concentrations influence silver toxicity in the aquatic macrophyte *Lemna gibba*. *Science of the Total Environment*, 449: 229-236.

Blinova I, Ivask A, Heinlaan M, Mortimer M and Kahru A. 2010 Ecotoxicity of nanoparticles of CuO and ZnO in natural water. *Environmental Pollution*, 158(1): 41-47.

Blokhina O, Virolainen E and Fagerstedt KV. 2003. Antioxidants, oxidative damage and oxygen deprivation stress: a review. *Annals of Botany*, 91(2): 179-194.

Bondarenko O, Juganson K, Ivask A, Kasemets K, Mortimer M and Kahru A. 2013. Toxicity of Ag, CuO and ZnO nanoparticles to selected environmentally relevant test organisms and mammalian cells in vitro: a critical review. *Archives of Toxicology*, 87(7): 1181-1200.

Bone AJ, Colman BP, Gondikas AP, Newton KM, Harrold KH, Cory RM, Unrine JM, Klaine SJ, Matson CW and Di Giulio RT. 2012. Biotic and abiotic interactions in aquatic microcosms determine fate and toxicity of Ag nanoparticles: Part 2-toxicity and Ag speciation. *Environmental Science and Technology*, 46(13): 6925-6933.

Bouwmeester H, Lynch I, Marvin HJ, Dawson KA, Berges M, Braguer D, Byrne HJ, Casey A, Chambers G, Clift MJ, Elia G, Fernandes TF, Fjellsbø LB, Hatto P, Juilerat L, Klein C, Kreyling WG, Nickel C, Riediker M and Stone V. 2011. Minimal analytical characterization of engineered nanomaterials needed for hazard assessment in biological matrices. *Nanotoxicol*ogy, 5(1): 1–11.

Bradford MM. 1976. A rapid and sensitive method for the quantification of microgram quantities of protein utilizing the principle of protein-dye binding. *Analytical Biochemistry*, 72(1-2): 248-254.

Brain RA and Solomon KR. 2007. A protocol for conducting 7-day daily renewal tests with *Lemna gibba*. *Nature Protocols*, 2(4): 979-987.

British Standards Institution (BSI). 2007. Terminology for nanomaterials. PAS 136:2007. London, UK.

Brumfiel G. 2003. Nanotechnology: a little knowledge. *Nature*, 424: 246–248.

Brunauer S, Emmett PH, Teller E. 1938. Adsorption of gases in multimolecular layers. *Journal of American Chemical Society*, 60(2): 309-319.

Brunner TJ, Wick P, Manser P, Spohn P, Grass RN, Limbach LK, Bruinink A and Stark WJ. 2006. In vitro cytotoxicity of oxide nanoparticles: comparison to asbestos, silica, and the effect of particle solubility. *Environmental Science and Technology*, 40(14): 4374-4381.

Burns JM, Pennington PL, Sisco PN, Frey R, Kashiwada S, Fulton MH, Scott GI, Decho AW, Murphy CJ, Shaw TJ and Ferry JL. 2013. Surface charge controls the fate of Au nanorods in saline estuaries. *Environmental Science and Technology*, 47(22): 12844-12851.

Casals E, Pfaller T, Duschl A, Oostingh G J and Puntes V. 2010. Time evolution of the nanoparticle protein corona. *ACS Nano*, 4**:** 3623-3632.

Castex M, Lemarie P, Wabete N and Chin L. 2010. Effects of probiotic *Pediococcus acidilactici* on antioxidant defences and oxidative stress of *Litopenaeus stylirostris* under *Vibrio nigripilchritudo* challenge. *Fish and Shellfish Immunology,* 28(4): 622-631.

Chae YJ, Pham CH, Lee J, Bae E, Yi J and Gu MB. 2009. Evaluation of the toxic impact of silver nanoparticles on Japanese medaka (*Oryzias latipes). Aquatic toxicology*, 94(4): 320-327.

Chang Y, Zhang M, Xia L, Zhang J and Xing G. 2012. The toxic effects and mechanisms of CuO and ZnO nanoparticles. *Materials* 5(12): 2850-2871.

Chaúque EFC, Zvimba JN, Ngila C and Musee N. 2014. Stability studies of commercial ZnO engineered nanoparticles in domestic wastewater. *Journal of Physics and Chemistry of the Earth*, 67-69: 140-144.

Chen R, Ratnikova TA, Stone MB, Lin S, Lard M, Huang G, Hudson JS and Ke PC. 2010. Differential uptake of carbon nanoparticles by plant and mammalian cells. *Small*, 6 (5): 612-617.

Cheng TS. 2012. The toxic effects of diethyl phthalate on the activity of glutamine synthetase in greater duckweed (*Spirodela polyrhiza* L.). *Aquatic Toxicology*, 124– 125: 171– 178.

Cheng LJ and Cheng TS. 2012. Oxidative effects and metabolic changes following exposure of greater duckweed (*Spirodela polyrhiza*) to diethyl phthalate. *Aquatic Toxicology,* 109: 166-175.

Chernousova S and Epple M. 2013. Silver as antibacterial agent: ion, nanoparticle, and metal. *Angewandte Chemie International Edition*, 52(6): 1636-653.

Choi O and Hu Z. 2008. Size dependent and reactive oxygen species related to nanosilver toxicity to nitrifying bacteria. *Environmental Science and Technology,* 42(12): 4583-4588.

Choi JE, Kim S, Ahn JH, Youn P, Kang JS, Yi J and Ryu DY. 2010. Induction of oxidative stress and apoptosis by silver nanoparticles in the liver of adult zebrafish. *Aquatic Toxicology*, 100(2): 151-159.

Coleman JG, Kennedy AJ, Bednar AJ, Ranville JF, Laird JG, Harmon AR, Hayes CA, Gray PE, Higgins CP and Steevens JA. 2013. Comparing the effects of nano silver and coating variations on bioavailability, internalization and elimination, using *Lumbriculus variegatus. Environmental Toxicology and Chemistry,* 32(9): 2069–2077.

Collin B, Auffan M, Johnson AC, Kaur I, Keller AA, Lazareva A, Lead JR, Ma, X, Merrifield RC, Svendsen C, White JC and Unrine JM. 2014. Environmental release, fate and ecotoxicological effects of manufactured ceria nanomaterials. *Environmental Science: nano*, 1: 533-548.

Colvin VL. 2003. The potential environmental impact of nanomaterials. *Nature Biotechnology*, 21(10): 1166-1170.

Cumberland SA and Lead JR. 2009. Particle size distributions of silver nanoparticles at environmentally relevant conditions. Journal of Chromatography A, 1216:9099–105.

da Silva BF, Pe´rez S, Gardinalli P, Singhal RK, Mozeto AA, Barcelo D. 2011. Analytical chemistry of metallic nanoparticles in natural environments. *Trends in Analytical Chemistry*, 30(3):528-540.

Dasari TP and Hwang H. 2010. The effect of humic acids on the cytotoxicity of silver nanoparticles to a natural aquatic bacterial assemblage. *Science of the Total Environment*, 408(23): 5817-5823.

Degen A and Kosec M. 2006. Effect of pH and impurities on the surface charge of zinc oxide in aqueous solution. *Journal of European Ceramic Society*, 20 (2000): 667-673.

Delay M and Frimmel FH. 2012. Nanoparticles in aquatic systems. *Analytical and Bioanalytical Chemistry*, 402(2): 583–592.

Delay M, Dolt T, Woellhaf A, Sembritzki R and Frimmel FH. 2011. Interactions and stability of silver nanoparticles in the aqueous phase: influence of natural organic matter (NOM) and ionic strength. *Journal of Chromatography A*, 1218: 4206-4214.

Department of Science and Technology (DST). 2005. The National Nanotechnology Strategy. Department of Science and Technology, Pretoria. South Africa.

Department of Science and Technology (DST). 2010. Nanoscience and Nanotechnology: 10 Year research plan.

Department of Science and Technology (DST). 2012. South African National Survey of Research and Experimental Development. Statistical Report: 2011/12. Department of Science and Technology, Pretoria. South Africa.

Dhawan A, Sharma V, and Parmar D. 2009. Nanomaterials: a challenge for toxicologists. *Nanotoxicology,* 3(1): 1-9.

Dhir B, Sharmila P, Saradhi PP, Sharma S, Kumar R and Mehta D. 2011. Heavy metal induced physiological alterations in *Salvinia minima*. *Ecotoxicology and Environmental Safety,* 74(6): 1678-1684.

Dietz K and Herth S. 2011. Plant nanotoxicology. *Trends in Plant Science*, 16(11): 582-589.

Domingos RF, Baalousha MA, Ju-Nam Y, Reid MM, Tufenkji N, Lead JR, Leppard GG,Wilkinson KG. 2009. Characterizing manufactured nanoparticles in the environment: multimethod determination of particle sizes. *Environmental Science and Technology,* 43(19): 7277-84.

Dubas ST and Pimpan V. 2008. Humic acid assisted synthesis of silver nanoparticles and its application to herbicide detection. *Materials Letters*, *62* (17-18): 2661-2663.

El Badawy A, Luxton TP, Silva RG, Scheckel KG, Suidan MT and Tolaymat MT. 2010. Impact of environmental conditions (pH, ionic strength, and electrolyte type) on the surface charge and aggregation of silver nanoparticles suspensions. *Environmental Science and Technology,* 44(4): 1260-1266.

Environment Canada. 2007. Biological test method: test for measuring the inhibition of growth using the freshwater macrophyte, *Lemna minor.* Method Development and Applications Section, Environmental Technology Centre. EPS 1/RM/37 Second Edition.

European Union (EU). 2011. European Union Commission recommendation on the definition of nanomaterial. *Official Journal of the European Union*, 2011/696/EU.

Fabrega J, Fawcett SR, Renshaw JC and Lead JR. 2009. Silver nanoparticle impact on bacterial growth: effect of pH, concentration, and organic matter. *Environmental Science and Technology*, 43 (19): 7285−7290.

Fabrega J, Luoma SN, Tyler CR, Galloway TS and Lead JR. 2011. Silver nanoparticles: behaviour and effects in the aquatic environment. *Environment International,* 37(2): 517-531.

Farkas J, Christian P, Urrea JA, Roos N, Hassellov M, Tollefsen KE, and Thomas KV. 2010. Effects of silver and gold nanoparticles on rainbow trout (*Oncorhyncus mykiss*) hepatocytes. *Aquatic Toxicology*, 96(1): 44-52.

Feris K, Caitlin O, Tinker J, Wingett D, Punnoose A, Thurber A, Kongara M, Sabetian M, Quinn B, Hanna C and Pink D. 2010. Electrostatic interactions affect nanoparticle-mediated toxicity to the Gram-negative bacterium *Pseudomonas aeruginosa* PAO1. *Langmuir*, 26(6): 4429-4436.

Ferry JL, Craig P, Hexel C, Sisco P, Frey R, Pennington PL, Fulton MH, Scott IG, Decho AW, Kashiwada S, Murphy CJ and Shaw T. 2009. Transfer of gold nanoparticles from the water column to the estuarine food web. *Nature Nanotechnology*, 4: 441-444.

Foyer CH and Noctor G. 2009. Redox regulation in photosynthetic organisms: signaling, acclimation, and practical implications. *Antioxidants and Redox Signaling*, 11(4): 861–905.

Franklin NM, Rogers NJ, Apte SC, Batley GE, Gadd GE and Casey PS. 2007. Comparative toxicity of nanoparticulate ZnO, bulk ZnO, and ZnCl2 to a freshwater microalga (*Pseudokirchneriella subcapitata*): The importance of particle solubility. *Environmental Science and Technology*, 41(24): 8484–8490.

Fubini B, Ghiazza M and Fenoglo I. 2010. Physico-chemical features of engineered nanoparticles relevant to their toxicity. *Nanotoxicolology*, 4(4):347-363.

Gaiser BK, Fernandes TF, Jepson MA, Lead JR, Tyler CR, Baalousha M, Biswas A, Britton GJ, Cole PA, Johnston BD, Ju-Nam Y, Rosenkranz P, Scown TM and Stone V. 2012. Interspecies Comparisons on the Uptake and Toxicity of Silver and Cerium Dioxide Nanoparticles. *Environmental Toxicology Chemistry,* 31(1): 144–154.

Gallego-Urrea JA, Tuoriniemi J and Hassellöv M. 2011. Applications of particle-tracking analysis to the determination of size distributions and concentrations of nanoparticles in environmental, biological and food samples. *Trac-Trends in Analytical Chemistry*, 30 (3):473-483.

Gao F, Liu C, Qu C, Zheng L, Yang F, Su M and Hong F. 2008. Was improvement of spinach growth by nano-TiO_2 treatment related to the changes of rubisco activase? *Biometals*, 21(2): 211–217.

Gao J, Youn S, Hovsepyan A, Llaneza VL, Wang Y, Bitton G, Bonzongo JC. 2009. Dispersion and toxicity of selected manufactured nanomaterials in natural river water samples: effects of water chemical composition. *Environmental Science and Technology*, 43(9): 3322-3328.

Glenn JB and Klaine SJ. 2013. Abiotic and biotic factors that influence the bioavailability of gold nanoparticles to aquatic macrophytes. *Environmental Science and Technology*, 47 (18): 10223-10230.

Glenn JB, White SA and Klaine SJ. 2012. Interactions of gold nanoparticles with aquatic macrophytes are size and species dependent. *Environmental Toxicology and Chemistry*, 31(1): 194−201.

Gottschalk F, Sonderer T, Scholz RW and Nowack B. 2009. Modeled environmental concentrations of engineered nanomaterials (TiO2, ZnO, Ag, CNT, fullerenes) for different regions. *Environmental Science and Technology*, 43(24): 9216–9222.

Gottschalk F, Ort C, Scholz RW, Nowack B. 2011. Engineered nanomaterials in rivers—Exposure scenarios for Switzerland at high spatial and temporal resolution. *Environmental Pollution*, 159(12): 3439-3445.

Griffitt RJ, Luo J, Gao J, Bonzongo J and Barber DS. 2008. Effects of particle composition and species on toxicity of metallic nanomaterials in aquatic organisms. *Environmental Toxicology and Chemistry,* 27(9): 1972-1978.

Gubbins EJ, Batty LC and Lead JR. 2011. Phytotoxicity of silver nanoparticles to *Lemna minor* L. *Environmental Pollution*, 159(6): 1551-1559.

Hamilton RF, Buckingham S and Holian A. 2014. The effect of size of Ag nanosphere toxicity in macrophage cell models and lung epithelial cell lines in dependent on particle dissolution. *International Journal of Molecular Science*, 15(4): 6815-6830

Handy RD and Shaw BJ. 2007. Toxic effects of nanoparticles and nanomaterials: implications for public health, risk assessment and the public perception of nanotechnology. *Health Risk and Society*, 9(2): 125–144.

Handy RD, Owen R and Valsami-Jones E. 2008a. The ecotoxicology of nanoparticles and nanomaterials: current status, knowledge gaps, challenges, and future needs. *Ecotoxicology*, 17(5): 315–325.

Handy RD, von der Kammer F, Lead JR, Martin Hassellov M, Richard Owen R and Crane M. 2008b. The ecotoxicology and chemistry of manufactured nanoparticles. *Ecotoxicology*, 17(4): 287–314.

Handy RD, Cornelis G, Fernandes T, Tsyusko O, Decho A, Sabo-Attwood T, Metcalfe C, Steevens J, Klaine SJ, Koelmans AA and Horne N. 2012. Ecotoxicity test methods for

engineered nanomaterials: practical experiences and recommendations from the bench. *Environmental Toxicology and Chemistry*, 31(1): 1-17.

Hannemann S, Grunwaldt JD, Krumeich F, Kappen P and Baiker A. 2006. Electron Microscopy and EXAFS Studies on Oxide-Supported Gold-Silver Nanoparticles Prepared by Flame Spray Pyrolysis". *Applied Surface Sci*ence*,* 252(22): 7862.

Hansen SF, Michelson EV, Kamper A, Borling P, Stuer-Lauridsen F, and Baun A. 2008. Categorization framework to aid exposure assessment of nanomaterials in consumer products. *Ecotoxicology,* 17(5): 438-447.

Hendren CO, Mesnard X, Droge J and Wiesner MR. 2011. Estimating production data for five engineered nanomaterials as a basis for exposure assessment. *Environmental Science and Technology*, 45(7): 2562-2569.

Henglein A. 1998. Colloidal silver nanoparticles: photochemical preparation and interaction with O_2, CCl_4 and some ions. *Chemical Materials*, 10(1): 444-450.

Heinlaan M, Ivask A, Blinova I, Dubourguier H and Kahru A. 2008. Toxicity of nanosized and bulk ZnO, CuO and TiO2 to bacteria *Vibrio fischeri* and crustaceans *Daphnia magna* and *Thamnocephalus platyurus. Chemosphere,* 71(7): 1308-1316.

Hirn S, Semmler-Behnke M, Schleh C, Wenk A, Lipka J, Schaffler M, Takenaka S, Moller W, Schmid G, Simon U, and Kreyling WJ. 2011. Particle size-dependent and surface charge-dependent biodistribution of gold nanoparticles after intravenous administration. *European Journal of Pharmaceutics and Biopharmaceutics,* 77(3): 407-416.

Ho C, Yau S, Lok C, So M and Che CM. 2010. Oxidative dissolution of silver nanoparticles by biologically relevant oxidants: a kinetic and mechanistic study. *Chemistry- an Asian Journal*, 5(2): 285-293.

Holden PA, Nisbet RM, Lenihan HS, Miller RJ, Cherr GN, Schimel JP and Gardea-Torresdey JL. 2013. Ecological nanotoxicology: Integrating nanomaterial hazard considerations across the subcellular, population, community, and ecosystems levels. *Accounts of Chemical Research*, 46(3); 813–822.

Hole P, Sillence K, Hannell C, Maguire CM, Roesslein M, Suarez G, Capracotta S, Magdolenova Z, Horev-Azaria L, Dybowska A, Cooke L, Haase A, Contal S, Manø S, Vennemann A, Sauvain J, Staunton KC, Anguissola S, Luch A, Dusinska M, Korenstein R, Gutleb AC, Wiemann M, Prina-Mello A, Riediker M and Wick P. 2013. Interlaboratory comparison of size measurements on nanoparticles using nanoparticle tracking analysis (NTA). *Journal of Nanoparticle Research*, 15: 2101-2113.

Hu X, Cook S, Wang P and Hwang HM. 2009. In vitro evaluation of cytotoxicity of engineered metal oxide nanoparticles. *Science of the Total Environment,* 407(8): 3070–3072.

Hu C, Liu Y, Li X and Li M. 2013. Biochemical responses of duckweed (*Spirodela polyrhiza*) to zinc oxide nanoparticles. *Archives of Environmental Contamination and Toxicology*, 64: 643-651.

Hu C, Liu X, Li X and Zhao Y. 2014. Evaluation of growth and biochemical indicators of *Salvinia natans* exposed to zinc oxide nanoparticles and zinc accumulation in plants. *Environmental Science and Pollution Research*, 21(1): 732-739.

Huynh KA and Chen KL. 2011. Aggregation kinetics of citrate and polyvinylpyrrolidone coated silver nanoparticles in monovalent and divalent electrolyte solutions. *Environmental Science and Technology,* 45(13): 5564-5571.

Hwang E, Lee JH, Chae YJ, Kim YS, Kim BC, Sang B, and Gu MB. 2008. Analysis of the toxic mode of action of silver nanoparticles using stress-specific bioluminescent bacteria. *Small*, 4(6): 746-750.

International Organisation for Standardisation (ISO). 2005. Water Quality- Determination of the toxic effect of water constituents and waste to Duckweed (Lemna minor)- Duckweed Growth Inhibition Test. International Organization for Standardization, Geneva, Switzerland.

Jassby D, Budarz JF and Wiesner M. 2012. Impact of aggregate size and structure on the photocatalytic properties of TiO_2 and ZnO nanparticles. *Environmental Science and Technology*, 46(13): 6934-6941.

Jiang JK, Oberdoorster G and Biswas P. 2009. Characterization of size, surface charge, and agglomeration state of nanoparticle dispersions for toxicological studies. *Journal of Nanoparticle Research*, 11(1): 77–89.

Jiang H, Li M, Chang F, Li W and Yin L. 2012. Physiological analysis of silver nanoparticles and $AgNO_3$ toxicity to *Spirodela polyrhiza. Environmental Toxicology and Chemistry,* 31(8): 1880-1886.

Jiang H, Qui X, Li G, Li W and Yin L. 2014. Silver nanoparticles induced accumulation of reactive oxygen species and alteration of antioxidant systems in the aquatic plant *Spirodela polyrhiza. Environmental Toxicology and Chemistry*, 33(6): 1398-1405.

Jin X, Li M, Wang J, Marambio-Jones C, Peng F, Huang X, Damoiseaux R and Hoek EMV. 2010. High throughput screening of silver nanoparticle stability and bacterial inactivation in aquatic media: influence of specific ion. *Environmental Toxicology and Chemistry*, 44(19): 7321-7328.

Johnston HJ, Hutchison G, Christensen FM, Peters S, Hankin S and Stone V.2010a. A review of the in vivo and in vitro toxicity of silver and gold particulates: Particle attributes and biological mechanisms responsible for the observed toxicity. *Critical Reviews in Toxicology* 40(4): 328-346.

Johnston BD, Scown TM, Moger J, Cumberland SA, Baalousha M, Linge K, van Aerle R, Jarvis K, Lead JR and Tyler CR. 2010b. Bioavailability of nanoscale metal oxides TiO_2, CeO_2 and ZnO to fish. *Environmental Science and Technology*, 44(3): 1144-1151.

Jolivet J, Froidefond C, Pottier A, Chanéac C, Cassaignon S, Tronc E and Euzen P. 2004. Size tailoring of oxide nanoparticles by precipitation in aqueous medium: a semi-quantitative modelling. *Journal of Materials Chemistry*, 14: 3281-3288.

Judy JD, Unrine JM, Rao W, Sue W and Bertsch PM. 2012. Bioavailability of gold nanomaterials to plants: importance of particle size and surface coating. *Environment Science and Technology*, 46(15): 8467-8474.

Juhel G, Batisse E, Hugues Q, Daly D, van Pelt F, O'Halloran J and Jansen MAK. 2011. Alumina nanoparticles enhance growth of *Lemna minor*. *Aquatic Toxicology*, 105(3-4): 328-336.

Kaegi R, Sinnet B, Zuleeg S, Hagendorfer H, Mueller E, Vonbank R, Boller M and Burkhardt M. 2010. Release of silver nanoparticles from outdoor facades. *Environmental Pollution,* 158(9): 2900–2905.

Kahru A and Dubourguier HC. 2010. From ecotoxicology to nano-ecotoxicology. *Toxicology*, 269(2-3): 105–119.

Kahru A and Ivask A. 2013. Mapping the dawn of nanoecotoxicological research. *Accounts of Chemical Research,* 46(3): 823-833.

Kasemets K, Ivask A, Dubourguier HC and Kahru A. 2009. Toxicity of nanoparticles of ZnO, CuO and TiO_2 to yeast *Saccharomyces cerevisiae*. *Toxicology In Vitro*, 23(6): 1116–1122.

Keller AA, Wang H, Zhou D, Lenihan HS, Cherr G, Cardinale BJ, Miller R and Ji Z. 2010. Stability and aggregation of metal oxide nanoparticles in natural aqueous matrices. *Environmental Science and Technology*, 44(6):1962–1967.

Kim E, Kim S, Kim H, Lee SG, Lee SJ and Jeong SW. 2011. Growth inhibition of aquatic plant caused by silver and titanium oxide nanoparticles. *Toxicology and Environmental Health Sciences*, 3(1): 1-6.

Kittler S, Greulich C, Gebauer JS, Diendorf J, Treuel L, Ruiz L, Gonzalez-Calbet JM, Vallet-Regi M, Zellner R, Ko¨ ller M, Epple M. 2010a. The influence of proteins on the dispersability and cell-biological activity of silver nanoparticles. *Journal of Materials Chemistry*, 20:512-518. DOI: 10.1039/B914875B.

Kittler S, Greulich C, Diendorf J, Koller M and Epple M. 2010b. Toxicity of silver nanoparticles increases during storage because of slow dissolution under release of silver ions. *Chemistry of Materials,* 22(16): 4548-4554.

Klaine SJ, Alvarez PJJ, Batley GE, Fernandes TF, Handy RD, Lyon DY, Mahendra S, McLaughlin MJ and Lead JR. 2008. Nanomaterials in the environment: behavior, fate, bioavailability, and effects. *Environmental Toxicology and Chemistry*, 27(9): 1825-1851.

Klaine SJ, Koelmans AA, Horne N, Carley S, Handy RD, Kapustka L, Nowack B and von der Kammer F. 2012. Paradigms to assess the environmental impact of manufactured nanomaterials. *Environmental Toxicology and Chemistry*, 31(1): 3-15.

Kreyling W, Semmler-Behnke M and Möller W. 2006. Health implications of nanoparticles. *Journal of Nanoparticle Research*, 8 (5): 543−562.

Laban G, Nies LF, Turco RF, Bickham JW and Sepu´lveda MS. 2010. The effects of silver nanoparticles on fathead minnow (Pimephales promelas) embryos. *Ecotoxicology* 19(1):185–195.

Lahive E, O'Halloran J and Jansen M. 2014. A marriage of convenience; a simple food chain comprised of *Lemna minor* (L.) and *Gammarus pulex* (L.) to study the dietary transfer of zinc. *Plant Biology*, Early online version, DOI: 10.1111/plb.12179.

Lai SL, Guo JY, Petrova V, Ramanath G and Allen LH. 1996. Size-dependent melting properties of small tin particles: nanocalorimetric measurements. *Physical Review Letters,* 77**:** 99-102.

Lead JR and Wilkinson KJ. 2006. Environmental colloids: Current knowledge and future developments. In Wilkinson KL, Lead JR, eds, *Environmental Colloids: Behaviour, Structure and Characterization.* John Wiley, Chichester, UK, pp 1–15.

Lee HY, Park HK, Lee YM, Kim K and Park SB. 2007. A practical procedure for producing silver nanocoated fabric and its antibacterial evaluation for biomedical applications. *Chemical Communications*, 28(28): 2959−2961.

Lee Y, Kim J, Oh J, Bae S, Lee S, Hong IN and Kim S. 2012. Ion release kinetics and ecotoxicity effects of silver nanoparticles *Environmental Toxicology and Chemistry*, 31(1): 155–159.

Levard C, Hotze EM, Lowry GV and Brown GE. 2012. Environmental transformations of silver nanoparticles: impact on stability and toxicity. *Environmental Science and Technology*, 46(13): 6900-6914.

Li T, Albee B, Alemayehu M, Diaz R, Ingham L, Kamal S, Rodriguez M, Bishnoi SW. 2010. Comparative toxicity study of Ag, Au, and Ag–Au bimetallic nanoparticles on *Daphnia magna*. *Analytical and Bioanalytical Chemistry,* 398(2): 689-700.

Li X, Lenhart JJ, Walker HW. 2011. Aggregation kinetics and dissolution of coated silver nanoparticles. *Langmuir*, 28(2): 1095-1104

Li L, Sillanpaa M, Tuominen M, Lounatmaa K and Schultz E. 2013. Behavior of titanium dioxide nanoparticles in *Lemna minor* growth test conditions. *Ecotoxicology and Environmental Safety*, 88: 89-94.

Li X and Lenhart JJ. 2012. Aggregation and dissolution of silver nanoparticles in natural surface water. *Environmental Science and Technology,* 46(10): 5378-5386.

Lichtenthaler HK. 1987. Chlorophylls and carotenoids: pigments of photosynthetic membranes. *Methods in Enzymology*, 148(87): 350-382.

Lin D and Xing B. 2008. Root uptake and phytoxoxicity of ZnO nanoparticles. *Environmental Science and Technology*, 42(15): 5580-5585.

Lin S, Reppert J, Hu Q, Hunson JS, Reid ML and Ratnikova T. 2009. Uptake, translocation and transmission of carbon nanomaterials in rice plants. *Small*, 5(10): 1128-1132.

Liu JY and Hurt RH. 2010. Ion release kinetics and particle persistence in aqueous nano-silver colloids. *Environmental Science and Technology*, 44(6): 2169-2175.

Liu Q, Chen B, Wang Q, Shi X, Xiao Z, Lin J and Fang X. 2009a. Carbon nanotubes as molecular transporters for walled plant cells. *Nano Letters*, 9 (3): 1007-1010.

Liu J, Aruguete DM, Murayama M and Hochella MF. 2009b. Influence of size and aggregation on the reactivity of an environmentally and industrially relevant nanomaterial (PbS). *Environmental Science and Technology*, 43(21): 8178-8183.

Liu X, Lee PY, Ho CM, Lui VC Chen Y, Che CM, Tam PK, Wong KK. 2010. Silver nanoparticles mediate defferential responses in keratinocytes and fibroblasts during skin wound healing. *Chem, Med, Chem*, 5(3): 468-475.

Liu J, Wang Z, Liu FD, Kane AB and Hurt RB. 2012. Chemical transformations of nanosilver in biological environments. *ACS Nano,* 6(11): 9887-9899.

Lopez-Lefebre L, Rivero RM, Garcia PC, Sanchez E, Ruiz JM and Luis Romero. 2001. Effect of calcium on mineral nutrient uptake and growth of tobacco. *Journal of the Science of Food and Agriculture*, 81(14): 1334-1338.

Lowry GV, Gregory KB, Apte SC and Lead JR.2012. Transformations of nanomaterials in the environment. *Environment Science and Technology*, 46(13): 6893−6899.

Luoma SN. 2008. Silver Nanotechnologies and the Environment: old problems or new challenges? *Project on Emerging Technologies*, PEN 15, 72 pp.

Luoma SN and Rainbow PS. 2008. Metal contamination in aquatic environments: science and lateral engagements. 588, Cambridge University Press, London.

Lok C, Ho C, Chen R, He Q, Yu W, Sun H, Tam PK, Chiu J and Che C. 2007. Silver nanoparticles: partial oxidation and antibacterial activities. *Journal of Biological and Inorganic Chemistry*, 12(14): 527-534.

Luyts K, Napierska D, Nemery B and Hoet PHM. 2013. How physico-chemical characteristics of nanoparticles cause their toxicity: complex and unresolved interrelations. *Environmental Science: Processes and Impacts*, 15: 23-38.

Ma H, Bertsch PM, Glenn TC, Kabengi NJ and Williams PL. 2009. Toxicity of manufactured zinc oxide nanoparticles in the nematode *Caenorhabditis elegans*. *Environmental Toxicology and Chemistry*, 28 (6): 1324-1330.

Ma X, Geiser-Lee J, Deng Y and Kolmakov A. 2010. Interactions between engineered nanoparticles (ENPs) and plants: phytotoxicity, uptake and accumulation. *Science of the Total Environment*, 408 (16): 3053−3061.

Ma H, Kabengi NJ, Bertsch PM, Unrine JM, Glenn TC and Williams PL. 2011. Comparative phototoxicity of nanoparticulate and bulk ZnO to a free-living nematode *Caenorhabditis elegans*: the importance of illumination mode and primary particle size. *Environmental Pollution*, 159(6): 1473-1480.

Ma R, Levard C, Marinakos SM, Cheng Y, Liu J, Michel FM, Brown GE and Lowry GV. 2012. Size controlled dissolution of organic coated silver nanoparticles. *Environmental Science and Technology*, 46(2): 752-759

Ma H, Williams PL and Diamond SA. 2013. Ecotoxicity of manufactured ZnO nanoparticles: a review. *Environmental Pollution*, 172: 76-85.

Majedi SM, Kelly BC and Lee HK. 2014. Role of combinatorial environmental factors in the behavior and fate of ZnO nanoparticles in aqueous systems: A multiparametric analysis. *Journal of Hazardous Materials*, 264: 370–379.

Maksymiec W. 1997. Effect of copper on cellular processes in higher plants. *Photosynthetica* 34(3): 321-342

Marambio-Jones C and Hoek EMV. 2010. A review of the antibacterial effects of nanomaterials and the potential implications for human health and the environment. *Journal of Nanoparticle Research*, 12(5): 1531-1551.

Maynard MD, Warheit DB and Philbert MA. 2011. The new toxicological of sophisticated materials: nanotoxicology and beyond. *Toxicological Science*, 120(S1): 109-129.

McCord JM. 2008. Superoxide dismutase, lipid peroxidation, and bell-shaped dose response curves. *Dose Response*, 6(3): 223–238.

Merdzan V, Domingos RF, Monterio CE, Hadioui M and Wilkinson KJ. 2014. The effects of different coatings on zinc oxide nanoparticles and their influence on dissolution and bioaccumulation by the green alga, C. reinhardtii. *Science of the Total Environment*, 488–489: 316–324.

Metrevelli G, Philippe A and Schaumann GE. 2014. Disaggregation of silver nanoparticle homoaggregates in a river water matrix. *Science of the Total environment*, In Press, corrected proof.

Miao AJ, Schwehr KA, Xu C, Zhang SJ, Luo ZP, Quigg A and Santschi PH. 2009. The algal toxicity of silver engineered nanoparticles and detoxification by exopolymeric substances. *Environmental Pollution,* 157(11): 3034–3041.

Miller RJ, Lenihan HS, Muller EB, Tseng N, Hanna SK and Keller AA. 2010. Impacts of metal oxide nanoparticles on marine phytoplankton. *Environmental Science and Technology,* 44(19): 7329-7334.

Miralles P, Church TL and Harris AT. 2012. Toxicity, uptake, and translocation of engineered nanomaterials in vascular plants. *Environmental Science and Technology*, 46(17): 9224-9239.

Mittler R. 2002. Oxidative stress, antioxidants and stress tolerance. *Trends in Plant Science*, 7(9): 405-410.

Moore MN. 2006. Do nanoparticles present ecotoxicological risks for the health of the aquatic environment? *Environmental International*, 32(8): 967–976.

Moos PJ, Chung K, Woessner D, Honeggar M, Cutler NS and Veranth JM. 2010. ZnO particulate matter requires cell contact for toxicity in human colon cancer cells. *Chemical Research in Toxicology*, 23(4): 733-739.

Mudunkotuwa IA, Rupasinghe T, Wu C-M and Grassian VH. 2012. Dissolution of ZnO Nanoparticles at Circumneutral pH: A study of size effects in the presence and absence of citric acid*. Langmuir* 28(1): 396–403.

Muller NC and Nowack B. 2008. Exposure modeling of engineered nanoparticles in the environment. *Environment Science and Technology*, 42(12): 4447–4453.

Musee N. 2010. Simulated environmental risk estimation of engineered nanomaterials: a case of cosmetics in Johannesburg City. *Human and Experimental Toxicology*, 30(9): 1181-1195.

Musee N, Brent AC and Ashton PJ. 2010. A South African research agenda to investigate the potential environmental, health and safety risks of nanotechnology. *South African Journal of Science*, 106 (3/4): 1-6.

Musee N, Thwala M and Nota N. 2011. The antibacterial effects of engineered nanomaterials: implications for wastewater treatment plants. *Journal of Environmental Monit*oring, 13(5): 1164-1183.

Musee N. 2011. Nanowastes and the environment: potential new waste management paradigm. *Environment International*, 37(1): 112-128.

Musee N, Zvimba JN, Schaefer LM, Nota N, Sikhwivhilu LM and Thwala M. 2014. Fate and behavior of ZnO- and Ag-engineered nanoparticles and a bacterial viability assessment in a simulated wastewater treatment plant. *Journal of Environmental Science and Health, Part A: Toxic/Hazardous Substances and Environmental Engineering*, 49(1): 59-66.

Mwaanga P, Carraway ER, van den Hurk P. 2014. The induction of biochemical changes in *Daphnia magna* by CuO and ZnO nanoparticles. *Aquatic Toxicology*, 150(2014): 201-209.

Nair S, Sasidharan A, Rani VVD, Menon D, Nair S, Manzoor K and Raina S. 2009. Role of size scale of ZnO nanoparticles and microparticles on toxicity toward bacteria and osteoblast cancer cells. *Journal of Materials Science: Materials in Medicine*, 20(1): 235–241.

National Science Foundation (NSF). 2001. *Societal Implications of Nanoscience and Nanotechnology* (eds M Roco and W Bainbridge). Kluwer: Netherlands.

Navarro E, Piccapietra F, Wagner B, Marconi F, Kaegi R, Odzak N, Sigg L and Behra R. 2008. Toxicity of silver nanoparticles to *Chlamydomonas reinhardtii*. *Environmental Science and Technology*, 42(23): 8959−8964.

Nekrasova GF, Ushakova OS, Ermakov AE, Uimin MA and Byzov IV. 2011. Effects of copper (II) ions and copper oxide nanoparticles on *Elodea densa* Planch. *Russian Journal of Ecology,* 42 (6): 458-463.

Nel A, Xia T, Madler L and Li N. 2006. Toxic potential of materials at the nanolevel. *Science*, 311: 622–627.

Nickel C, Angelstorf J, Bienert R, Burkart C, Gabsch S, Giebner S, Haase A, Hellack B, Hollert H, Hund-Rinke K, Jungmann D, Kaminski H, Luch A, Maes HM, Nogowski A, Oetken M, Schaeffer A, Schiwy A, Schlich K, Stintz M, von der Kammer F and Kuhlbusch TAJ. 2014. Dynamic light-scattering measurement comparability of nanomaterial suspensions. *Journal of Nanoparticle Research*, 16(2014): 2260-2272.

Nowack B and Bucheli TD. 2007. Occurrence, behavior and effects of nanoparticles in the environment. *Environmental Pollution*, 150(1): 5-22.

Nowack B. 2009. Environmental behaviour and effects of engineered metal and metal oxide nanoparticles. In *Heavy Metals in The Environment*, eds LK Wang, JP Chen, Y Hung, NK Shammas. CRC Press USA.

Nowack B, Ranville JF, Diamond S, Gallego-Urrea JA, Metcalfe C, Rose J, Horne N, Koelmans AA and Klaine SJ. 2012. Potential scenarios for nanomaterials release and subsequent alteration in the environment. *Environmental Toxicology and Chemistry* 31(1): 50–59.

Oberdörster E. 2004. Manufactured nanomaterials (Fullerenes, C60) induce oxidative stress in the brain of juvenile largemouth bass. *Environmental Health Perspectives,* 112(10): 1058–1062.

Oberdörster G, Oberdörster E, Oberdörster J. 2005. Nanotoxicology: an emerging discipline evolving from studies of ultrafine particles. *Environmental Health Perspectives,* 113(7): 823–839.

Oberdörster E, Zhu S, Blickley TM, McClellan-Green P and Haasch ML. 2006. Ecotoxicology of carbon-based engineered nanoparticles: effects of fullerene (C_{60}) on aquatic organisms. *Carbon,* 44(6): 1112-1120.

Odzak N, Kistler D, Behra R and Sigg L. 2014. Dissolution of metal and metal oxide nanoparticles in aqueous media. *Environmental Pollution*, 191(2014): 132-138.

Oliver JD. 1993. A review of the biology of giant Salvinia *(Salvinia molesta* Mitchell). *Journal of Aquatic Plant Management,* 31: 227-231.

Omar FM, Aziz HA, Stoll A. 2014. Stability of ZnO nanoparticles in solution. Influence of pH, dissolution, aggregation and disaggregation effects. *Journal of Colloid Science and Biotechnology*, 3(1): 1-109

Organisation for Economic Co-operation and Developemnt (OECD). 2002. Guidelines for the Testing of Chemicals. *Lemna* sp. Growth Inhibition Test, Draft Guideline 221.

Ostrowski AD, Martin T, Conti J, Hurt I and Harthorn BH. 2009. Nanotoxicology: characterizing the scientific literature, 2000–2007. *Journal of Nanoparticle Research*, 11(2): 251–257

Oukarroum A, Barhoumi L, Pirastru L and Dewez D. 2013. Silver nanoparticle toxicity effects on growth and cellular viability of the aquatic plant *Lemna gibba*. *Environmental Toxicology and Chemistry*, 32(4): 902–907.

Pal S, Tak YK and Song JM. 2007. Does the antibacterial activity of silver nanoparticles depend on the shape of the nanoparticle? A study of the gram-negative bacterium *Escherichia coli*. *Applied and Environmental Microbiology*, 73(6): 1712−1720.

Pamies R, Cifre J, Espin V, Collado-Gonzalez M, Banos FG and de la Torre JG. 2014. Aggregation behaviour of gold nanoparticles in saline aqueous media. *Journal of Nanoparticle Research*, 16(2014): 2376-2386.

Park J, Lim D, Lim H, Kwon T, Choi J, Jeong S, Choi I and Cheon J. 2011. Size dependent macrophage responses and toxicological effects of Ag nanoparticles. *Chemical Communications*, 47: 4382-4384.

Park A, Kim Y, Choi E, Brown MT and Han T. 2013. A novel bioassay using root re-growth in *Lemna*. *Aquatic Toxicology*, 140– 141: 415– 424.

Park J, Kim S, Yoo J, Lee JS, Park JW and Jung J. 2014. Effect of salinity on acute copper and zinc toxicity to *Tigriopus japonicus*: The difference between metal ions and nanoparticles. *Marine Pollution Bulletin*, http://dx.doi.org/10.1016/j.marpolbul.2014.04.038.

Parlak KU and Yilmaz DD. 2012. Response of antioxidant defences to Zn stress in three duckweed species. *Ecotoxicology and Environmental Safety,* 85(2012): 52-58.

Parlak KU and Yilmaz DD. 2013. Ecophysiological tolerance of *Lemna gibba* L. exposed to cadmium. *Ecotoxicology and Environmental Safety*, 91(2013): 79-85.

Pasquet J, Chevalier Y, Pelletier J, Couval E, Bouvier D and Bolzinger M. 2014. The contribution of zinc ions to the microbial activity of zinc oxide. *Colloids and Surfaces A: Physicochemical Engineering Aspects*, 457(2014): 263-274.

PEN (Project on Emerging Nanotechnologies). 2011. The project on emerging nanotechnologies. The Woodrow Wilson International Center for Scholars, Washington, DC.

PEN (Project on Emerging Nanotechnologies). 2014. Consumer Products Inventory. Retrieved [10 July 2014], http://www.nanotechproject.org/cpi/about/analysis/

Peralta-Videa JR, Zhao L, Lopez-Moreno ML, de la Rosa G, Hong J and Gardea-Torresdey JL. 2011. Nanomaterials and the environment: A review for the biennium 2008-2010. *Journal of Hazardous Materials*, 186 (1): 1-15.

Perreault F, Oukarroum A, Melegari SP, Matias WG and Popovic R. 2012. Polymer coating of copper oxide nanoparticles increases nanoparticles uptake and toxicity in the green alga *Chlamydomonas reinhardtii*. *Chemosphere,* 87(11): 1388-1394.

Perreault F, Popovic R and Dewez D. 2014. Different toxicity mechanisms between bare and polymer-coated copper oxide nanoparticles in *Lemna gibba*. *Environmental Pollution*, 185(2014): 219-227.

Pettitt ME and Lead JR. 2013. Minimum physicochemical characterisation requirements for nanomaterial regulation. *Environment International*, 52(2013): 41-50.

Prado C, Rodriguez-Montelongo L, Gonzalez JA, Pagano EA, Hilal M and Prado FE. 2010. Uptake of chromium by *Salvinia minima*: effect on plant growth, leaf respiration and carbohydrate metabolism. *Journal of Hazardous Materials*, 177(1-3): 546-553.

Praetorius A, Arvidsson R, Molander S and Scheringer M. 2013. Facing complexity through informed simplifications: a research agenda for aquatic exposure assessment of nanoparticles. *Environmental Science: Processes and Impacts*, 15(1): 161-170.

Ratte HT. 1999. Bioaccumulation and toxicity of silver compounds: a review. *Environmental Toxicology and Chemistry*, 18(1): 89-108.

Reed RB, Ladner DA, Higgins CP, Westerhoff P and Ranville JF. 2012. Solubility of nano-zinc oxide in environmentally and biologically important matrices. *Environmental Toxicology and Chemistry*, 31(1): 93-99.

Remedios C, Rosario F and Bastos V. 2012. Environmental nanoparticles interactions with plants: morphological, physiological, and genotoxic aspects. *Journal of Botany*, 2012: 1-8.

Reinsch BC, Levard C, Li Z, Ma R, Wise A, Gregory KB, Brown GE Jr and Lowry GV. 2012. Sulfidation of silver nanoparticles decreases *Escherichia coli* growth inhibition. *Environmental Science and Technology*, 46(13): 6992-7000.

Rico CM, Majumdar S, Duarte-Gardea M, Peralta-Videa JR and Gardea-Torresdey JL. 2011. Interaction of nanoparticles with edible plants and their possible implications in the food chain. *Journal of Agricultural Food and Chemistry*, 59(8): 3485-3498.

Roco MC. 2005. International perspective on government nanotechnology funding in 2005. *Journal of Nanoparticle Research,* 7(6): 707– 712.

Roco M. 2011. The long view of nanotechnology development: the National Nanotechnology Initiative at 10 years. *Journal of Nanoparticle Research*, 13 (2011): 427–445.

RSA (Republic of South Africa). National Water Act (Act No. 36 of 1998). *Government Gazette, South Africa* 398 (19182).

Sabo-Attwood T, Unrine JM, Stone JW, Murphy CJ, Ghoshroy S, Blom D, Bertsch PM, and Newman LA. 2011. Uptake, distribution and toxicity of gold nanoparticles in tobacco (*Nicotiana xanthi*) seedlings. *Nanotoxicology*, 6(4): 353-360.

Sal'nikov DS, Pogorelova AS, Makarov SV and Vashurina IY. 2009. Silver ion reduction with peat fulvic acid. *Russian Journal of Applied Chemistry*, 82(4): 545-548.

Schluesener JK, Schluesener HJ. 2013. Nanosilver: application and novel aspects of toxicology. *Archives of Toxicology*, 87(4): 569-576.

Schrurs F and Lison D. 2012. Focusing the research efforts. *Nature Nanotechnology,* 7(2012): 546–548.

Scientific Committee on Emerging and Newly Identified Health Risks (SCENIHR). 2007. The appropriateness of the risk assessment methodology in accordance with the Technical Guidance Documents for new and existing substances for assessing the risks of nanomaterials, 21–22 June 2007. European Commission, Brussels, Belgium.

Shahverdi AR, Fakhimi A, Shahverdi HR and Minaian S. 2007. Synthesis and effect of silver nanoparticles on the antibacterial activity of different antibiotics against *Staphylococcus aureus* and *Escherichia coli*. *Nanomedicine Nanotechnology Biology and Medicine*, 3(2): 168−171.

Sharma SS and Dietz KJ. 2009. The relationship between metal toxicity and cellular redox imbalance. *Trends Plant Science,* 14(1): 43-50.

Shaw BJ and Handy RD. 2011. Physiological effects of nanoparticles on fish: a comparison of nanometals versus metal ions. *Environment International,* 37(6): 1083-1087.

Shi J, Abid AD, Kennedy IM, Hristova KR and Silk WK. 2011. To duckweeds (*Landoltia punctata*), nanoparticulate copper oxide is more inhibitory than the soluble copper in the bulk solution. *Environmental Pollution*, 159(5): 1277-1282.

Sims JL, Grove JH and Schlotzhaver WS. 1995. Soluble calcium fertilizer effects on early growth and nutrition uptake of burley tobacco. *Journal of Plant* Nutrition, 18(5): 911-921.

Singh N, Manshian B, Jenkins GJS, Griffiths SM, Williams PM, Maffeis TGG, Wright CJ and Doak SH. 2009. Nanogenotoxicology: the DNA damaging potential of engineered nanomaterials. *Biomaterials,* 30(23-24): 3891-3914.

Smith AR, Pryer KM, Schuettpelz E, Korall P, Schneider H and Wolf PG. 2006. A classification for extant ferns. *Taxonomy*, 55(3): 705-731.

Song G, Gao Y, Wu H, Hou W, Zhang C and Ma H. 2012 . Physiological effect of anantase TiO_2 nanoparticles on *Lemna minori*. *Environmental Toxicology and Chemistry*, 31(19): 2147–2152.

Sotiriou GA, Sannomiya T, Teleki A, Krumeich F, Vörös J, Pratsinis SE. 2010. Non-toxic, Dry-coated Nanosilver for Plasmonic Biosensors. *Advanced Functional Materials*, 20(24): 4250-4257.

Stebounova LV, Guio E and Grassian VH. 2011. Silver nanoparticles in simulated biological media: a study of aggregation, sedimentation, and dissolution. *Journal of Nanoparticle Research*, 13(1): 233-244.

Stone V, Nowack B, Baun A, van den Brink N, von der Kammer F, Dusinska M, Handy R, Hankin S, Hassellöv M, Joner E and Fernandes TF. 2010. Nanomaterials for environmental studies: Classification, reference material issues, and strategies for physico-chemical characterisation. *Science of the Total Environment*, 408(7): 1745–1754.

Sune N, Sanchez G, Caffaratti S and Maine MA. 2007. Cadmium and chromium removal kinetics from solution by two aquatic macrophytes. *Environmental Pollution*, 145(2): 467-473.

Suttiponparnit K, Jiang J, Sahu J, Suvachittanont S, Charinpanitkul T and Biswas P. 2011. Role of surface area, primary particle size, and crystal phase on titanium dioxide nanoparticle dispersion properties. *Nanoscale Research Letters,* 6(27): 1-8.

Tejamaya M, Romer I, Merrifield RC and Lead JR. 2012. Stability of citrate, PVP and PEG coated silver nanoparticles in ecotoxicology media. *Environmental Science and Technology,* 46: 7011-7017.

Thwala M, Sikhwivhilu L, Wepener V and Musee N. 2013. The oxidative toxicity of Ag and ZnO nanoparticles towards the aquatic plant *Spirodela punctuta* and the role of testing media parameters*. Environmental Science: Processes Impacts*, 15(13): 1830–1843.

Toduka Y, Toyooka T and Ibuki Y. 2012. Flow cytometric evaluation of nanoparticles using side-scattered light and reactive oxygen species—mediated fluorescence—correlation with genotoxicity. *Environmental Science and Technology,* 46(14): 7629–7636.

Tolaymat TM, El Badawy AM, Genaidy A, Scheckel KG, Luxton TP and Suidan M. 2010. An evidence-based environmental perspective of manufactured silver nanoparticle in syntheses and applications: A systematic review and critical appraisal of peer reviewed scientific papers. *Science of the Total Environment*, 408 (5): 999−1006.

Turner T, Brice D and Brown MT. 2012. Interactions of silver nanoparticles with the marine macroalga *Ulva lactuta*. *Ecotoxicology*, 21(1): 148-154.

Ucuncu E, Ozkan AD, Kursungoz C, Ulger ZE, Olmez TT, Tekinay T, Ortac B and Tunca E. 2014. Effects of laser ablated silver nanoparticles on *Lemnar minor*. *Chemosphere*, Early online.

United States Environmental Protection Agency (USEPA). 1996. Aquatic Plant Toxicity Test Using *Lemna* spp. United States Environmental Protection Agency, EPA 712-C-96-156.

Unrine JM, Colman BP, Bone AJ, Gondikas AP and Matson CW. 2012. Biotic and abiotic interactions in aquatic microcosms determine fate and toxicity of Ag nanoparticles. Part 1. Aggregation and dissolution. *Environmental Science and Technology*, 46(13): 6915-6924.

Upadhyay R and Panda SK. 2010. Zinc reduces copper toxicity induced oxidative stress by promoting antioxidant defense in freshly grown aquatic duckweed *Spirodela polyrrhiza* L. *Journal of Hazard Materials,* 17(1–3): 1081–1084.

Van Hoecke K, Quik J, Mankiewicz-Boczek J, de Schamphelaere K, Elsaersser A, van der Meeren P, Barnes C, McKerr G, Howard CV, van de Meent D, Rydzynski K, Dawson KA, Salvati A, Lesniak A, Lynch I, Silversmit G, de Samber B, Vincze L and Janssen CR. 2009. Fate and effects of CeO_2 nanoparticles in aquatic ecotoxicity tests. *Environmental Science and Technology,* 43(12): 4537-4546.

Velzeboer I, Quik JTK, van de Meent D and Koelmans AA. 2014. Rapoind settling of nanoparticles due to heteroaggregation with suspended sediment. *Environmental Toxicology and Chemsitry*, 33(8): 1766-1773.

von Moos N, Bowen P and Slaveykova VI. 2014. Bioavailability of inorganic nanoparticles to planktonic bacteria and aquatic microalgae in freshwater. *Environmental Science: Nano*, 1: 214-232.

Wahab R, Mishra A, Yun SI, Kim YS and Shin HS. 2010. Antibacterial activity of ZnO nanoparticles prepared via non-hydrolytic solution route. *Applied Microbiology and Biotechnology*, 87(5): 1917-1925.

Wang Y and Herron N. 1990. Quantum size effects on the exciton energy of CdS clusters. *Physical Review B,* 42**:** 7253–7255.

Wang J and Wang W. 2014. Significance of physicochemical and uptake kinetics in controlling the toxicity of metallic nanomaterials to aquatic organisms. *Applied Physics and Engineering,* 15(8):573-59.

Wang JX, Fan YB, Gao Y, Hu QH and Wang TC. 2009. TiO_2 nanoparticles translocation and potential toxicological effect in rats after intra-articular injection. *Biomaterials*, 30(27): 4590–4600.

Wang Z, Chen J, Li X, Shao J and Peijnenburg WJGM. 2012. Aquatic toxicity of nanosilver colloids to different trophic organisms: contributions of particles and free silver ion. *Environmental Toxicology and Chemistry*, 21(10): 2408-2413.

Wang J, Koo J, Alexander A, Yang Y, Westerhoff S, Zhang Q, Schnoor JL, Colvin VL, Braam J and Alvarez PJJ. 2013. Phytostimulation of poplars and *Arabidopsis* exposed to silver nanoparticles and Ag^+ at sublethal concentrations. *Environmental Science and Technology*, 47(10): 5442-5449.

Warheit DB. 2008. How meaningful are the results of nanotoxicity studies in the absence of adequate material characterisation. *Toxicological Sciences*, 10(2): 183-185.

Westerhoff P, Song G, Hristovski K and Kiser MA. 2011. Occurrence and removal of titanium at full scale wastewater treatment plants: implications for TiO_2 nanomaterials. *Journal of Environmental Monitoring*, 13(5): 1195-1203.

Westerhoff PK, Kiser MA and Hristovski K. 2013. Nanomaterial removal and transformation during biological wastewater treatment. *Environmental Engineering Science*, 30(3): 109-117.

Whiteley CM, Valle MD, Jones KC and Sweetman AJ. 2013. Challenges in assessing release, exposure and fate of silver nanoparticles within the UK environment. *Environmental Science: Processes and Impacts*, 15: 2050-2058.

Wijnhoven SWP, Dekkers S, Kooi M, Jongeneel WP, de Jong WH. 2010. Nanomaterials in consumer products. National Institute for Public Health and the Environment, Ministry of Health, Welfare and Sport, Bilthoven, Netherlands.

Willekens H, Chamnongpol S, Davey M, Schraudner M, Langebartels C, Van-Montagu M, ,Inze´ D and Van-Camp W. 1997. Catalase is a sink for H_2O_2 and is indispensable for stress defence in C3 plants. *EMBO Journal*, 16(16): 4806–4816.

Wong SW, Leung PT, Djurisic AB, and Leung KM. 2010. Toxicities of nano zinc oxide to five marine organisms: influences of aggregate size and ion solubility. *Analytical and Bioanalytical Chemistry*, 396(2): 609–618.

Xia T, Kovochich M, Liong M, Madler L, Gilbert B, Shi H, Yeh JI, Zink JI and Nel AE. 2008. Comparison of the mechanism of toxicity of zinc oxide and cerium oxide nanoparticles based on dissolution and oxidative stress properties. *ACS Nano*, 2(10): 2121-2134.

Xia T, Li N and Nel AE. 2009. Potential health impact of nanoparticles. *Annual Reviews of Public Health*, 30 (1): 137-150.

Xiao-hong Z, Huang B, Zhou T, Liu Yand Shi H. 2015. Aggregation behavior of engineered nanoparticles and their impact on activated sludge in wastewater treatment. *Chemosphere*, 119(2015): 568–576.

Xie Y, He Y, Irwin PL, Jin T and Shi X. 2011. Antibacterial activity and mechanism of action of zinc oxide nanoparticles against *Campylobacter jejuni*. *Applied Microbiology and Biotechnology*, 77 (7): 2325-2331.

Yadav T, Mugray AA, Mungray AK. 2014. Fabricated nanoparticles: current status and potential phytotoxic threats, In DM Whitcare (ed.), *Reviews of Environmental Contamination and Toxicology*, 230, Springer International Publishing, Switzerland.

Yang Y and Westerhoff P. 2014. Presence of and release of, nanomaterials from consumer products. In: *Nanomaterial, Advances in Experimental Medicine and Biology,* 811, (Eds.) DG Capco and Chen Y, Springer. DOI 10.1007/978-94-017-8739-0-1.

Yeo M and Nam D. 2013. Influence of different types of nanomaterials on their bioaccumulation in a paddy microcosm: a comparison of TiO_2 nanoparticles and nanotubes. *Environmental Pollution*, 178(2013): 166-172.

Yin L, Cheng Y, Espinasse B, Colman BP, Auffan M, Wiesner M, Rose J, Liu J and Bernhardt ES. 2011. More than the ions: the effects of silver nanoparticles on *Lolium multiflorum*. *Environmental Science and Technology*, 45 (6): 2360-2367.

Yin L, Colman BP, McGill BM, Wright JP,Bernhardt ES. 2012. Effects of silver nanoparticle exposure on germination and early growth of eleven wetland plants. Plos One 7(10): e47674.

Yu S, Yin Y and Liu J. 2013. Silver nanoparticles in the environment. *Environmental Science: Processes and Impacts,* 15: 78-92.

Zhang Y, Chen Y, Westerhoff P, Hristovski K and Crittenden JC. 2008. Stability of commercial metal oxide nanoparticles in water. *Water Research,* 42(8-9): 2204-2212.

Zhang Y, Chen Y, Westerhoff P and Crittenden J. 2009. Impact of natural organic matter and divalent cations on the stability of aqueous nanoparticles. *Water Research,* 43(17): 4249-4257.

Zhang W, Yao Y, Li K, Huang Y and Chen Y. 2011. Influence of dissolved oxygen on aggregation kinetics of citrate-coated silver nanoparticles. *Environmental Pollution,* 159(12): 3757-3762

Zhao YJ, Xing WH, Xu NO and Wong FS. 2005. Effects of inorganic electrolytes on zeta potentials of ceramic microfiltration membranes. *Separation and Purification Technology,* 42(2): 117-121.

Zhu X, Wang J, Zhang X, Chang Y and Chen Y. 2009. The impact of ZnO nanoparticle aggregates on the embryonic development of zebrafish (*Danio rerio*). *Nanotechnology*, 20(19): 195103.